Live Cell Imaging of *Plasmodiophora brassicae* Infection and Host Interactions

A Thesis Submitted to the College of

Graduate and Postdoctoral Studies

In Partial Fulfillment of the Requirements

For the Degree of Master of Science

In the Department of Biology

University of Saskatchewan

Saskatoon

By

James Bush

PERMISSION TO USE

In presenting this thesis in partial fulfillment of the requirements for a postgraduate degree from the University of Saskatchewan, I agree that the libraries of this university may make it freely available for inspection. I further agree that permission for copying of this thesis in any manner, in whole or in part, for scholarly purposes may be granted by the professor or professors who supervised my thesis work or, in their absence, by the Head of the Department or the Dean of the College in which my thesis work was done. It is understood that any copying or publication or use of this thesis or parts thereof for financial or personal gain shall not be allowed without my written permission. It is also understood that due recognition shall be given to me and to the University of Saskatchewan in any scholarly use which may be made of any material in my thesis.

James Bush

Requests for permission to copy or to make other use of material in this thesis in whole or part should be addressed to:

Head of the Department of Biology

University of Saskatchewan

112 Science Place

Saskatoon, Saskatchewan, Canada

S7N 5E2

Or

Dean of College of Graduate and Postdoctoral Studies

University of Saskatchewan

116 Thorvaldson Building, 110 Science Place

Saskatoon, Saskatchewan, Canada

S7N 5C9

ABSTRACT

Plasmodiophora brassicae Woronin, is a soil-borne obligate biotrophic plant pathogen responsible for clubroot, one of the most devastating diseases of Brassicaceae. Previous studies into the lifecycle of *P. brassicae* have focused on fixed tissue samples for histological or transmission electron microscopic investigations due to the lack of a pathogen-specific stain for live cell/tissue study. Using the fluorophore Nile red to stain lipid droplets in all life stages of *P. brassicae* allows for live cell microscopic investigation of this pathogen. Nile red can be used to label *P. brassicae ex planta* in the soil during the resting spore and infective zoospore phases, and *in planta* during its obligate life cycle phases. This Nile red labelling technique combined with transgenic *Arabidopsis thaliana* plants expressing fluorescent protein-labelled organelle markers permits imaging of the zoospore penetration of the host cell wall, subsequent pathogen development within the intracellular environment, and further allows the investigation of pathogen-induced organelle recruitment and/or disruption during the *P. brassicae-A. thaliana* interaction. Specifically, the translocation of the nucleus to the penetration site and its subsequent envelopment by plasmodia, and the establishment of a cytoplasmic vacuole-derived encasement termed the parasitophorus vacuole. This staining technique has provided insight pertaining to the cellular interactions of *P. brassicae* and its hosts.

ACKNOWLEDGEMENTS

I would like to begin my acknowledgements by thanking all educators for the work they do. Those that I have had during primary school, high school, my undergraduate, and my graduate education have provided me with encouragement, discipline, and insight while allowing me to pursue my curiosity and interests. The work done in this project would not have been possible without these people.

The funding for the period of study that I completed this work in was courtesy of the Saskatchewan Canola Development Commission, as they awarded me the Dr. Roger Rimmer Award for Excellence in Graduate Research, and the College of Graduate and Postdoctoral Studies, who awarded me the Robert P. Knowles Scholarship. I would like to thanks both the Rimmer and Knowles estates for founding trusts to finance these awards. Furthermore, I would like to thank NSERC for funding my supervisor, Dr. Yangdou Wei, who provided me with materials, office and lab/work space that he obtained with his funding.

I would like to thank the research group headed by Drs. Chris Todd, Peta Bonham-Smith, and Yangdou Wei for allowing me to pursue independent research under the umbrella of their clubroot disease research program. Likewise, I would like to thank my supervisor, Dr. Yangdou Wei, and my committee members Drs. Chris Ambrose, Peta Bonham-Smith, Dwayne Hegedus, and Gary Peng who have provided me with insight into my work, offered encouragement in times of need, and who edited my thesis in preparation of its final form.

I would also like to take this opportunity to thank the scientists who I have had the opportunity to work with in the lab: Li Qin, Abdul Halim, Igor de Albuquerque, Anouk Hendriks, Jiangying Tu, Quiongnan Gu, Dr. Tengsheng Zhou, Dr. Tao Song, Dr. Zhuquing Zhou, Dr. Long Yang, and Dr. Yangping Fu, your cooperation and communication in the lab was immensely helpful in allowing me to complete my work. I would also like to thank departmental technicians

Dr. Guosheng Liu, for his help with microscopy, Marlynn Mireau for his assistance with IT and lending me photography materials, and Jeanine Smith for her greenhouse work.

There have been many colleagues in the department who I have also been very fortunate to work with. Scott Halpin, Dr. Jill Thomson, and Gillian Murza we absolutely delightful to work with and I thoroughly enjoyed my time in the classroom when I was a teaching assistant for them. Some of my best memories were working (and marking!) with these people. I would also like to thank Deidre Wasyliw and Joan Virgl for their work as administrative assistant and executive assistant to head and department graduate chair. I would like to thank my numerous friends on the University of Saskatchewan campus, who are too numerous to list, but all either shared a beer, a laugh, or a story, with me at some point. A special shout out to the Pear Bear's Drink and Social Team! You have made my time in the department of biology one that was formative in my character and mind. I would also like to thank William Davis (University of Saskatchewan, Department of Physics), and Jillian Kusch (University of Saskatchewan, Department of Biology), who both took time to read a draft of my thesis and made substantial recommendations to improve its quality. Lastly, I would like to thank my family: Becky, Mom, Dad, Grandma, and Grandpa who all were a source of never-ending love, encouragement, and support. Thank you.

TABLE OF CONTENTS

LIST OF TABLES

LIST OF FIGURES

SUPPLEMENTAL VIDEOS

Figure S1 Video of a FM4-64-stained *P. brassicae* plasmodium in infected *B. napus* callus. *P. brassicae* plasmodia do not stain with FM4-64. Cytoplasmic streaming can be seen inside the plasmodia indicating that the FM4-64 stain works in a live cell context.

Figure S2 Video of a FM4-64-stained *P. brassicae* zoosporangium in infected *B. napus* callus. The zoosporangia was expunged from a callus cell presumably while being mounted on the slide. Individual zoospores move rapidly at random without an apparent direction of travel.

Figure S3 Video of a Nile red-stained *P. brassicae* plasmodium in infected *B. napus* callus. The dense lipid droplets in the plasmodium cytoplasm move in patterns indicating cytoplasmic streaming is occurring and that the cell remains live during investigation by this probe. In the bottom left, a young plasmodia can be seen.

Figure S4 Video of a Nile red-stained *P. brassicae* zoosporangia. The zoosporangia were expunged from a callus cell presumably while being mounted on the slide. Individual zoospores are stained and move at random without a direction of travel.

Figure S5 Video of a Nile red-stained *P. brassicae* plasmodia 34 hpi in an *A. thaliana* root hair. Cytoplasmic streaming can be seen occurring in the host cell and within individual pathogen plasmodia.

Figure S6 Video of Nile red-stained *P. brassicae* zoospores within the zoosporangium 8 dpi in *A. thaliana*. Random directional movement can be seen by the zoospores.

Figure S7 Video of a Nile red stained *P. brassicae* plasmodia in the cortical cells of a 25 day old *A. thaliana* plant. The dense lipid droplets in the plasmodia cytoplasm move in random fashion.

Figure S8 Video of Nile red-stained *P. brassicae* zoosporangia in a root hair of an *A. thaliana* plant expressing GFP fusion to the tonoplast 8 dai (CS16257, Nelson *et al.,* 2007). Zoospores populating the zoosporangium are stained with Nile red, while the parasitophorus vacuole surrounding the zoosporangium is labelled with GFP.

Figure S9 Video of Nile red-stained *P. brassicae* zoosporangia in a root hair of an *A. thaliana* plant expressing GFP fusion to the tonoplast 8 dai (CS16257, Nelson *et al.,* 2007). Zoospores populating the zoosporangia and free swimming zoospores (in dashed box) are stained with Nile red, while the parasitophorus vacuole surrounding the zoosporangia is labelled with GFP.

*Supplemental videos may be obtained by contacting the thesis author at: James.Bush@usask.ca.

LIST OF SYMBOLS AND ABBREVIATIONS

CLSM: confocal laser scanning microscope

Col-0: Columbia ecotype

cm: centimetre

cv.: cultivar

dai: days after inoculation

ETI: effector triggered immunity

ETS: effector triggered susceptibility

g: grams

GFP: green fluorescent protein

h: hour

hpi: hours post inoculation

HR: hypersensitive response

LD: lipid droplet

LSM: laser scanning microscope

M: molar

Me: methylated

min: minute

mL: millilitre

mm: millimetre

mol: mole

MS: Murashige and Skoog

NADP(H): nicotinamide adenine dinucleotide phosphate (hydroxide)

NHR: non-host resistance

nm: nanometre

PAMP: pathogen associated molecular pattern

PM: plasma membrane

PR: pathogenesis related

PRR: pattern recognition receptor

PTI: PAMP triggered immunity

PV: parasitophorous vacuole

R-gene: resistance gene

RNA: ribonucleic acid

ROS: reactive oxygen species

SA: salicylic acid

subsp.: subspecies

t: time

TCA: tricarboxylic acid

TIP: tonoplast intrinsic protein

Tsu-0: Tsu ecotype

var.: variety

X: power

Ze-0: Ze ecotype

^{2}: squared

^{3}: cubed

%: percent

°C: degrees Celsius

γ: gamma

δ: delta

µm: micrometre

1.0 INTRODUCTION

Clubroot disease is responsible for world-wide crop losses of cultivated plants including vegetables, such as beets (*Beta vulgaris*) and cauliflower (*Brassica oleracea*), and oilseed crops including black mustard (*Brassica nigra*) and canola (*Brassica napus*) (Ludwig-Müller *et al.*, 1999; Dixon, 2009). Clubroot is caused by the infection of host plant roots by the soil-borne protist, *Plasmodiophora brassicae* (Schwelm *et al.*, 2015). The infection is initiated in the root epidermis and transmitted to the root cortex. Clubroot symptom development occurs as roots become enlarged and swollen during the cortical cell infection. In severe cases, cataplastic gall outgrowths occur in the roots. Clubroot impairs the ability of the plant to take up water and nutrients, producing above ground symptoms (Schwelm *et al.*, 2015). Plant stunting, leaf wilt/drop, as well as reduced seed oil quality and quantity occur in clubroot-infected plants (Dixon, 2009). Clubroot disease is a threat to global food and nutrition security, and agricultural economies.

1.1 Clubroot Disease in Canada

Williams (1966) first identified the races of *P. brassicae* based on their ability to infect two cultivars of cabbage (*B. oleracea*), Jersey Queen and Badger Shipper, and two cultivars of rutabaga (*B. napus* cv. *napobrassica*), Laurentian and Wilhelmsburger. This method of *P. brassicae* race characterization is referred to as Williams' differentials. Using this standard, at least nine races of *P. brassicae* were identified, of which, six have been found in Canada (Sherf and MacNab, 1986; Table 1.1).

Historically, clubroot disease affected vegetable crops in eastern Canada and British Columbia (Table 1.1). Today, *P. brassicae* stands as a threat to oilseed and vegetable crop production on the Canadian prairies (Table 1.1). The Canadian prairie's canola (*B. rapa and B. napus*) crops are of enormous importance, as canola is the most important source of vegetable oil in human food and in industrial lubricants where mineral oil use is inappropriate (Dixon, 2009).

Table 1.1 *Plasmodiophora brassicae* races found in Canada.

Race	Location	Reference
1	Nova Scotia	Hildebrand and Delbridge, 1995
	Quebec	Williams, 1966
2	Alberta	Strelkov *et al.*, 2006
	New Brunswick	Ayres, 1972
	Nova Scotia	Hildebrand and Delbridge, 1995
	Prince Edward Island	Ayres, 1972
	Ontario	Reyes, 1969; Reyes *et al.*, 1974
	Quebec	Williams, 1966
3	Alberta	Strelkov *et al.*, 2006
	Nova Scotia	Hildebrand and Delbridge, 1995
	Saskatchewan	Dokken-Bouchard *et al.*, 2010
4	Prince Edward Island	Ayres, 1972
5	Alberta	Strelkov *et al.*, 2006
	Manitoba	Cao *et al.*, 2009
	Ontario	Saude *et al.*, 2012
	Quebec	Cao *et al.*, 2009
6	British Columbia	Williams, 1966
	Ontario	Reyes, 1969

In 2003, the first officially documented western-Canadian case of canola clubroot disease occurred near Edmonton, Alberta (Strelkov *et al.*, 2006). By 2010, 566 canola fields had been infested with *P. brassicae* in Alberta (Strelkov *et al.*, 2011). A *P. brassicae* epidemic is continuing in Alberta, with 287 new records of clubroot disease being found in 2015 (Strelkov *et al.*, 2016; Figure 1.1). Especially concerning is the shifting virulence of pathogen populations, as clubroot disease is affecting canola cultivars that were previously considered to be clubroot-resistant.

Resistance breakdown is most likely a consequence of the selection pressure placed on the pathogen population by using resistant cultivars in short rotation (Strelkov *et al.*, 2016).

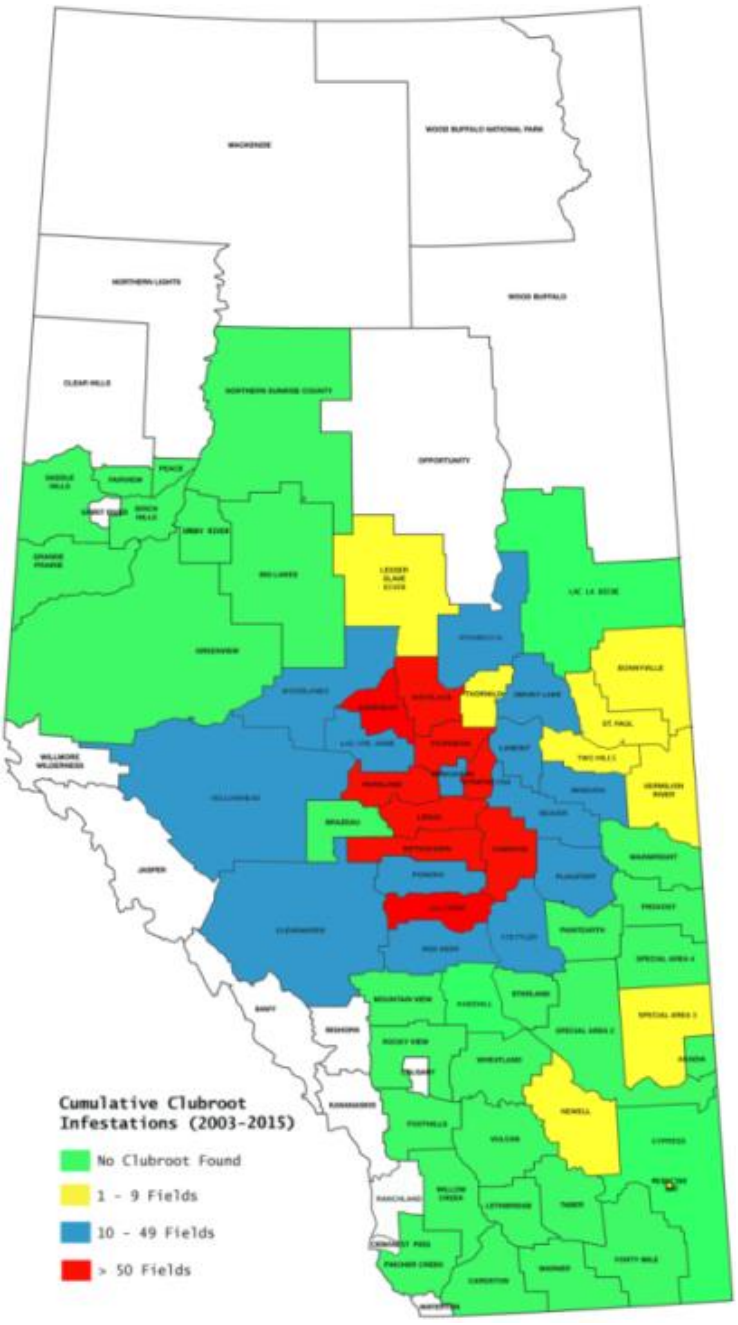

Figure 1.1 Map showing clubroot occurrence in Alberta canola fields from 2003 to 2015 (Strelkov *et al*., 2016). Green polygons had no reported clubroot disease, while yellow had 1-9 fields, blue had 10-49 fields, and red had >50 fields reported.

To date, the clubroot epidemic has been less problematic in Saskatchewan. In 2008, *P. brassicae* resting spores were detected by PCR in soil samples taken from fields near Rosthern in west-central Saskatchewan (Dokken-Bouchard *et al.*, 2008). The first documented case of clubroot disease in Saskatchewan canola occurred in the 2011 growing season (Dokken-Bouchard *et al.*, 2012). Clubroot disease has been rare since the first occurrence. The 2015 crop disease survey did not detect *P. brassicae* in soil samples from tested sites (Dokken-Bouchard *et al.*, 2016). Nevertheless, clubroot disease persists as a threat to canola production, as clubroot disease continues to be reported in isolated Saskatchewan canola crops (Strelkov *et al.*, 2011).

In 2011, the clubroot disease-impacted range again extended eastward, with *P. brassicae* infecting canola grown in Manitoba (Strelkov *et al.*, 2012). Manitoba is currently facing a clubroot threat as spore population levels are increasing in the province (MAFRD, 2016; Figure 1.2). In severely infested fields in western Canada, 30 to 100 % yield loss can occur (Strelkov *et al.*, 2007, Strelkov *et al.*, 2016; MAFRD, 2016). Similarly, the clubroot impacted area has expanded southward, with incidences of canola clubroot disease occurring in North Dakota in 2013 (Chittem et al., 2014).

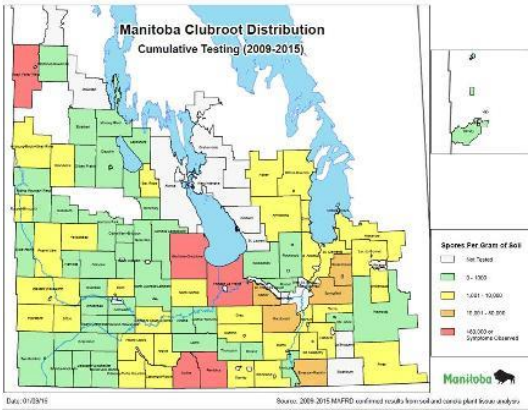

Figure 1.2 *P. brassicae* soil infestation levels in Manitoba (MAFRD, 2016). Soil from regions in white were not tested. Coloured polygons indicate resting spores were found in tested soils, with green indicating 0-1000 spores g^{-1}, yellow 1001-10000 spores g^{-1}, orange 10001-80000 spores g^{-1} and red regions >80000 spores g^{-1}.

The rapid expansion of clubroot disease on the Prairies is a consequence of human practice and natural factors. In *P. brassicae* infested areas, resting spores are generally present in large abundance within the soil. Farming and resource extraction practice dictates that machinery be moved between fields or worksites, hence, soil tag on farm or construction (*e.g.* oilfield) equipment is a source of distribution of *P. brassicae* resting spores (Strelkov *et al.,* 2006). Natural causes of *P. brassicae* geographic range expansion include anemochorous (wind) and hydrochorous (water) dispersal (Rennie *et al.,* 2015; Datnof *et al.,* 1984). On a large scale, the patchy locations of clubroot disease occurrence and its spread across the prairie to isolated locations indicates that long-range inoculum introduction by wind is likely (Rennie *et al.,* 2015). Similarly, *P. brassicae* can be spread on a smaller geographic scale with a higher degree of patch connectivity through surface water irrigation (Datnof *et al.,* 1984).

1.2 Taxonomy and Lifecycle of *P. brassicae*

P. brassicae is taxonomically classified as belonging to the Rhizaria infra-kingdom, a phylogenetic super-group originally classified as Protozoa (Cavalier-Smith and Chao, 2003; Cavalier-Smith, 2013; Dixon, 2014; Table 1.2). Plasmodiophorids have distinct features in their life history and morphology, including the ability to survive in the soil as resting spores, zoospores having two flagella of unequal length, obligate intracellular parasitism, and cruciform nuclear division (Cavalier-Smith and Chao, 2003; Aist and Williams, 1971; Braselton *et al.,* 1975). Cruciform nuclear division is a derived character state consisting of a persistent nuclear envelope and an enlarged nucleolus. During metaphase, the nucleolus divides simultaneously, with the chromatin elongating perpendicular to the equatorial chromatin plate (Braselton *et al.,* 1975). Closely related plasmodiophorid plant pathogens include the causal agent of powdery scab on potato, *Spongospora subterranea*, and the vector of beet necrotic yellow vein virus, *Polymyxa betae*, which share family Plasmodiophoraceae with *P. brassicae*.

Table 1.2 Taxonomic ranking of *Plasmodiophora brassicae* (Ruggiero *et al.* 2015; Cavalier-Smith and Chao, 2003; Cavalier-Smith, 2013, Cranmer, 2015).

Taxonomic Rank	Taxonomic Group
Domain	Eukarya
unranked group	Bikont
Kingdom	Chromista
Infra-Kingdom	Rhizaria
Phylum	Cercozoa
Subphylum	Endomyxea
Class	Phytomyxea
Order	Plasmodiophorida
Family	Plasmodiophoraceae
Genus	*Plasmodiophora*
Species	*brassicae*

A comprehensive understanding of the individual developmental stages of *P. brassicae* is necessary for the detection of the pathogen within host cells (Schuller and Ludwig-Müller, 2016). Considerable work has been done to document *P. brassicae* life forms and life stages. However, the lifecycle of *P. brassicae* has not been explained in its entirety as ambiguous and unexplained morphologies still exist (Kageyama and Asano, 2009). The three-stage life cycle documented by Ingram and Tommerup (1972) is recognized as being the most accurate. This lifecycle consists of *P. brassicae* soil survival, root hair infection, and cortical cell colonization (Kageyama and Asano, 2009; Luo *et al.*, 2013, Figure 1.3). The described morphologies that occur in this three stage lifecycle are resting spores, zoospores, plasmodia, and zoosporangia (Ingram and Tommerup

1972). Others have identified morphologies of the pathogen that are not described in this lifecycle, specifically a mobile myxamoeba phase occurring prior to the *bona fide* existence of primary plasmodia (Kunkle, 1918; Mithen and Magrath, 1992; Kobelt, 2000).

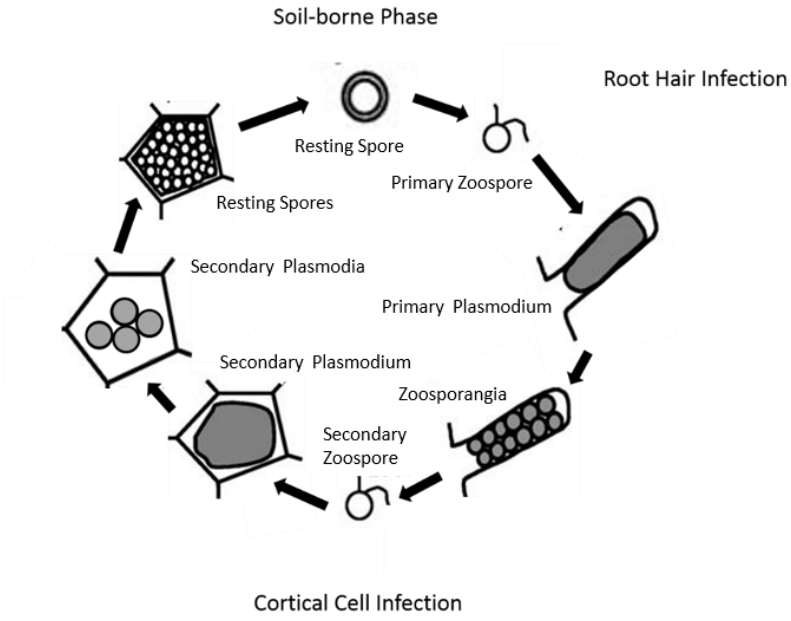

Figure 1.3 Lifecycle and life stages of *P. brassicae* (Kageyama and Asano, 2009). Life cycle stages are the soil borne state, the root hair infection, and the cortical cell infection. Stages associated with the soil borne state include resting spores and primary zoospores. The root hair infection includes the primary plasmodium zoosporangial clusters and empty zoosporangia. The cortical cell infection includes secondary plasmodia and resting spores.

P. brassicae resting spores can survive in the soil up to 20 years as the outermost layers of the resting spore are exceptionally high in protein content relative to the inner chitin-rich layers (Moxham and Bucazacki, 1983; Wallenhammar, 1996). These layers protect *P. brassicae* from chitinolytic processes occurring within the soil (Moxham and Bucazacki, 1983). It has been hypothesized that the multiple layers of the resting spore outer wall collectively contribute to the soil-hardiness of the pathogen (Moxham and Buczacki, 1983; Kageyama and Asano, 2009). Obviously, physiological adaptation must also occur.

Resting spore germination produces a zoospore that infects the host plant (Ingram and Tommerup, 1972). Resting spore germination can occur in response to host root exudates, and changes in soil pH as a consequence of dead organic matter decay in the soil, as well as calcium ion release into the soil by the host plant (Rashid *et al.*, 2013; Friberg *et al.*, 2005, Yano *et al.*, 1991). Germination of the resting spore produces a biflagellate zoospore, with a long flagellum for motility and a short flagellum (axoneme) for zoospore attachment to root hairs (Ayres, 1944; Kageyama and Asano, 2009; Aist and Williams, 1971). The primary zoospore migrates through water films in the soil matrix until it is adjacent to the cell wall of the host root hair. The mechanism of root hair penetration is limited to Aist and Williams' (1971) discussion of electron micrographs of the process (Figure 1.4). Aist and Williams (1971) describe a mechanical model of cell wall penetration where the primary zoospore attaches to the host root hair and almost immediately its flagellum coils and the axoneme retracts. This process leaves the pathogen lying parallel with the root hair in a cyst like fashion, called an encystment (Aist and Williams, 1971). First in a sequential series of steps, the adhesorium, a fibrous attachment material joining the pathogen to the root hair is formed. A statchel is pressed through the opening in the adhesorium and through the host cell wall by cyst turgor pressure developed in the parasites vacuole (Aist and Williams, 1971). After the port in the host cell wall is created, the pathogen is injected into the root hair lumen. The subsequent root hair infection is the primary infection of the disease cycle (Ingram and Tommerup, 1972; Figure 1.3).

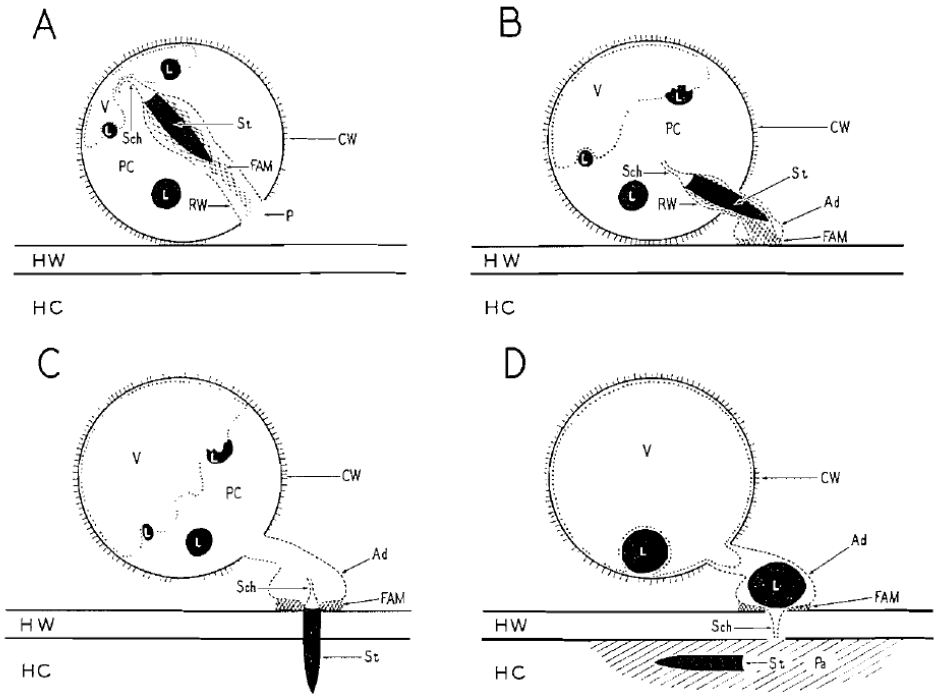

Figure 1.4 Diagrammatic summary of the *P. brassicae* root hair penetration process (Aist and Williams, 1971). Detailed are the cyst vacuole prior to enlargement (A). The cyst vacuole expansion and attachment of the adhesorium (B). The statchel puncturing the host cell wall (C). Finally, penetration has occurred and the host has deposited a papilla at the penetration site (D). HW: host cell wall, HC: host cytosol, CW: resting spore cell wall, V: vacuole, AD: adhesorium, FAM: fibrillary adhesive material, PC: parasite cytoplasm, RW: rohr wall, St: statchel, Pa: papilla, Sch: schlauch, L: lipid body P: rohr plug.

Upon infection, the primary zoospore injects its protoplasm into the root where it appears as a small, spherical amoebae (Aist and Williams, 1971). Terminology of early stages in the literature often use amoebae and plasmodium interchangeably (*eg*. Aist and Williams, 1971; Kageyama and Asano, 2009). However, results of some researchers have shown that a distinct, mobile myxamoebae exists prior to plasmodium existence (Kunkle, 1918; Mithen and Magrath, 1992; Kobelt *et al*, 2000). It has not been discussed in recent literature. However, Kunkle (1918) hypothesized that the myxameboid stage resulted from the penetration of the root hair by a single zoospore, and that the plasmodial stage of *P. brassicae* development is the result of the fusion of

one or more *P. brassicae* myxameboid's. Some authors hypothesize that motile myxamoebae or spherical amoebae must fuse with another to produce a plasmodium (Kunkle, 1918; Mithen and Magrath, 1992; Aist and Williams, 1971). Once mature, and mitotic divisions occur, a multi-nucleate plasmodium will cleave, forming zoosporangia (Kageyama and Asano, 2009). Zoosporangia form clusters in the root hair and each divide to produce 4-16 secondary zoospores (Kageyama and Asano, 2009). Interestingly, primary zoospores may achieve root hair infection in non-host species including perennial ryegrass (*Lolium perenne*), and common mignonette (*Reseda odorata*) but fail to proceed to the secondary infection (Macfarlane, 1952; Friberg *et al.*, 2005; Kageyama and Asano, 2009). The secondary infection initiates when cortical cells are targeted by secondary zoospores.

The final phase of the pathogen's lifecycle is the secondary infection of the plant (Ingram and Tommerup, 1972; Figure 1.3). The mechanism of cortical cell penetration is unknown. Although a flaw in the currently accepted life-cycle model of *P. brassicae*, this understanding is integral to understanding the epidemiology and management of clubroot disease. Two forms of cortical cell penetration have been suggested in the literature, passive and active forms (Mithen and Magrath, 1992; Moxham and Buczacki, 1983). The model of the passive form of cortical cell infection is based upon pathogen proliferation as *P. brassicae* plasmodia are seemingly "split-in-two" as a host cell divides. This fission occurs in the meristematic root tip of young plants (Kunkle, 1918; Moxham and Buczacki, 1983). Alternately, active forms of pathogen spread have been hypothesized by many groups for almost 100 years, although confirmation has yet to be reported. Kunkle (1918) noted intercellular transmission by a mobile myxameboid phase void of lipid droplets. However, Mithen and Magrath (1992) and Kobelt *et al.* (2000) noted that occasionally myxamoebae contain lipid droplets. Intercellular motility of the myxameboid morphology is aided

by cell wall breaks that the pathogen can navigate through by cytoplasmic streaming. Aist and Williams (1971) hypothesized cortical cell penetration occurred via the same mechanism as root hair penetration, with zoospore adhesion and subsequent injection of the pathogen into the cortical cell from the infected epidermal cell. While the passive forms of cortical penetration are possible only within meristematic tissues, active forms of transmission are likely to occur throughout the whole root, and therefore, if not favoured, at least conserved through natural selection. Whether passive transmission, active transmission or if both forms are indeed present and contribute to clubroot development, our understanding of pathogenesis is incomplete.

Upon infection of the host cortical cell, the secondary zoospore produces a secondary plasmodium (Garber and Aist, 1970). Following a series of mitotic divisions, this plasmodium becomes multi-nucleate (Garber and Aist, 1970). During the cessation of host vegetative growth, plasmodial nuclei undergo fusion, immediately followed by plasmodial meiosis which produces resting spores (Tommerup and Ingram, 1972). The production of resting spores in the host root cortex is the completion of the *P. brassicae* lifecycle (Tommerup and Ingram, 1972). Resting spores are released to the soil upon disintegration of the host root (Kageyama and Asano, 2009).

Primary (produced from resting spores) and secondary (produced from a zoosporangium) zoospores cannot be visually distinguished from each other. Analysis of zoospores using transmission electron microscopy has shown evidence for nucleate and binucleate forms of primary zoospores, with secondary zoospores always being nucleate (Kageyama and Asano, 2009; Aist and Williams, 1971). In their study, Moxham and Buczacki (1983) postulated that one nucleus of the binucleate primary zoospore disintegrates, or breaks down, and does not serve biological function.

1.3 Clubroot Disease Symptoms

Symptoms of clubroot disease are not obvious until *P. brassicae* has established the secondary infection (Ingram and Tommerup, 1972; Ludwig-Muller *et al.*, 2009). Above-ground symptoms can include swelling of hypocotyl tissues, wilting of epicotyl tissues, stunted growth, chlorosis, yellowing and reddening of leaves, and leaf abscission. Below ground disease symptoms include the thickening of main and lateral roots, and cataplastic galls on the roots of host plants (Woronin, 1878; Figure 1.5). The secondary infection promotes extensive cell division and enlargement and a disorganization of host vascular tissue structures (Kobelt *et al.*, 2000; Sharma *et al.*, 2011). With disease development, the host exhibits above and below-ground disease symptoms (Dixon, 2009; Figure 1.5). As a consequence of the symptoms, plants may fail to meet reproductive maturity (Strelkov *et al.*, 2011). In less severe cases, the infected host plants may fail to fill siliques with high quality oilseeds, or in the case of vegetables, yield a harvestable and marketable crop.

Figure 1.5 Symptoms of clubroot disease on *Brassica napus* cv. Westar plants. *B. napus* plants infected with *Plasmodiophora brassicae* exhibit wilting leaves and stunted plant height compared to the uninfected plant on the right (A). The main and lateral roots of infected plants (C) are hypertrophied relative to the control (B). Cataplastic tumor outgrowths can be seen on the periphery of the hypertrophied roots (C).

While the visual diagnostic symptoms of clubroot disease may seem obvious, their severity is dependent upon environmental conditions during plant growth. Environmental symptoms that exacerbate symptom development include temperature, soil moisture content, soil pH, and *P. brassicae* spore load and half-life (Gossen *et al.*, 2013; Gossen *et al.*, 2016; Donald and Porter, 2009).

Temperature influences rates of *P. brassicae* root hair infections and clubroot disease symptom progression (Sharma *et al.*, 2011a; Sharma *et al.*, 2011b; McDonald and Westerveld, 2008). *P. brassicae* resting spores germinate optimally within the temperature range of 20 °C to 25 °C (Dixon, 2009). Sharma *et al.* (2011a) found the primary phase of the *P. brassicae* lifecycle could occur at any temperature tested (10 °C, 15 °C, 20 °C, 25 °C, 30 °C), but infection occurred within 2 days after inoculation (dai) in plants grown at 25 °C, while it took 4 days for infection to establish in plants grown in 15 °C, 20 °C, and 30 °C. The optimum temperature for root hair infection is 26 °C (Sharma *et al.*, 2011a). Similarly, Sharma *et al.* (2011b) found temperature to have a large effect upon *P. brassicae* development within the host root cortex. No cortical infection was seen at 10 °C, while cortical infection rate increased as temperature increased from 15 ° to 30 °C (Sharma *et al.*, 2011b). As temperature increases infection rate, disease severity also increases. In Shanghai pak choi (*Brassica rapa* subsp. *Chinenensis* var. *communis*) and Chinese flowering cabbage (*Brassica rapa* subsp. *chinensis* var. *utilis*) grown in *P. brassicae* infested soil, mean air temperatures during crop development ranging from 15 to 22 °C correlated strongly with clubroot incidence and severity, with r-values of 0.68 and 0.72, respectively (McDonald and Westerveld, 2008). The highest correlation between air temperature and disease severity occurs during the final ten day period before crop harvest (McDonald and Westerveld, 2008).

The soil condition can have a significant effect on disease development when *P. brassicae* is present. Soil moisture is necessary for *P. brassicae* resting spores to germinate and swim via whiplash movement of their flagella. Once germinated, zoospores swim within the soil matrix to host plant root hairs (Dixon, 2014). In mineral soils, infection can occur when the soil is 9 % water by weight, while in organic soils the soil must be 60 % water by weight for root hair infection to occur (Hamilton and Crête, 1978). In wet years, more disease incidences and more severe clubroot symptoms are expected. Much like temperature, pH influences clubroot disease severity (Dixon, 2014). *Ceteris paribus*, clubroot severity is worse in acidic soil. Limed soils have reduced resting spore germination rates compared to acidic soils (Myers and Campbell, 1985). Initially, it was thought that prairie soils would not be habitable for *P. brassicae* due to their basic pH (Strelkov *et al.*, 2006). This was a short-sighted hypothesis, which ignored the potential of *P. brassicae* to adapt to new hosts and environmental conditions where host plants grow. Given the proper environment, a virulent pathogen and susceptible host, the disease will develop (Scholthof, 2007).

1.4 Clubroot Management

The broad geographic expansion of *P. brassicae* on the prairie over a small time-period in conjunction with limited disease management options poises clubroot as an important disease of concern for crop specialists (Dixon, 2009b; Strelkov *et al.*, 2012). As with other diseases, it has been proposed that disease management be employed with therapies targeting sensitive, pathogen-specific biological processes (Feng *et al.*, 2014). For clubroot disease, this means disease management may be approached by cultural methods, biocides, biocontrol, and using genetically resistant crops.

While many management solutions are being developed, few commercially-viable options exist. Managing clubroot disease is a complex issue that does not have a *bona fide*, cost-effective solution (Dixon, 2009). Limiting the soil spore population is a popular target for clubroot disease

management. *P. brassicae* has a broad host range, hence limiting weedy species that can act as potential *P. brassicae* hosts is necessary as infection of these plants can increase the soil spore load. This is extended to removal or controlling volunteer plants from the previous season (Howard *et al.,* 2010; Feng *et al.,* 2012; Alberta Clubroot Management Committee, 2008). Similarly, non-host species that are susceptible to root hair infection may be planted to act as bait plants to reduce the soil spore load (Howard *et al.,* 2010). Crop rotation may also limit any increase in the resting spore population in the soil.

Crop rotation refers to planting different crops in the same field from year to year. For example, crop rotation can be used to supplement soil nitrogen levels by alternately planting a crop and soybeans (*Glycine max*) in consecutive years (Crookston *et al.,* 1990). Rotating crops from a clubroot host such as canola, to a non-host species like wheat (*Triticum aestivum*) can help to reduce *P. brassicae* spore population buildup in the soil (Alberta Clubroot Management Committee, 2008).

The rotation of clubroot host and non-host plants is contingent upon many factors including the field use history, resting spore half-life, and the economic sustainability of long time-period crop rotations (Dixon, 2009). If a field has grown a *P. brassicae*-susceptible crop for many years and clubroot disease has been present during this period, the soil will have a large resting spore population (Wallenhammar, 1996; Alberta Clubroot Management Committee, 2008). *P. brassicae* resting spore populations have a half-life of approximately 3.6 years, and are capable of surviving for up to 20 years in the soil (Wallenhammar, 1996; Wallenhammar *et al.,* 2012). In theory, an 18-year break from planting canola in a *P. brassicae*-infested field would reduce the soil resting spore population to 3 % of its original size, making disease epidemics unlikely as under test conditions, a *P. brassicae* resting spore concentration of 10^6-10^7 spores mL^{-1} is required for clubroot

symptoms to present themselves (Dixon, 2014, Strelkov *et al.*, 2006, Sharma *et al.*, 2011a). However, a period as long as 18 years is not economically sustainable for food producers (Strelkov and Hwang, 2014). Currently, rotating canola crops with non-hosts, such as cereal grains or alfalfa (*Medicago sativa*) is recommended (Howard *et al.*, 2010). The Alberta Clubroot Management Plan recommends a 3 year rotational period in a lightly infested and a 5 year rotational strategy for moderate to highly infested fields (Alberta Clubroot Management Committee, 2008). Research has also found that clubroot crop losses can be minimized by early spring seeding in areas where soil is infested with *P. brassicae* (McDonald and Westerveld, 2008; Hwang *et al.*, 2012). It has also been demonstrated that a 2- to 4-year break under heavy infestation will alleviate the impact of clubroot on susceptible or moderately susceptible cultivars only marginally, but increase the yield of resistant cultivars substantially. Therefore, a >2-year break from canola is recommended with use of resistant cultivars for clubroot management on canola (Peng *et al.*, 2015).

To date, there has been minimal success using biocidal disease management techniques; *P. brassicae* is resistant to commonly used pesticides and soil fumigants (Donald and Porter, 2009). Treating clubroot diseased plants with sprayed biocides has had minimal success in Canada (Hwang *et al.*, 2012). However, two types of fungicides, Fluazinam (Allegro® 500F; ISK Biosciences Corp., Concord, OH) and Cyazofamid (Ranman® 400 SC; SummitAgro, Cary, NC) have been applied to *P. brassicae*-infected canola resulting in slightly decreased disease severity (Hwang *et al.*, 2012). Although these biocides had a positive result, the net benefit was not enough to justify the economic cost of the application. When the surfactant AquaGro 2000-L (Aquatrols, Paulsboro, NJ) was applied to *P. brassicae*-infected Chinese cabbage, disease progression was diminished (Hildebrand and McRae, 1998). Despite the success of this application, the surfactant was toxic to the crop itself when a high concentration (0.5%) was used. Only when AquaGro 2000-

L was applied at a concentration of 0.2% in two separate doses 10 days apart was an appropriate reduction in clubroot disease seen without affecting the host crop (Hildebrand and McRae, 1998).

Soil fumigants are biocides applied to the soil before planting that kill soil biota by producing toxic gases (Goring, 1962). The soil type has a large influence upon the effectiveness of soil fumigants when targeting *P. brassicae* (Donald and Porter, 2014). In Australian heavy clay soils, Metam sodium (Santa Cruz Biotechnology, Inc., Santa Cruz, CA) application resulted in partial control of *P. brassicae*, as resting spores are inviable after exposure to methylisothiocyanates (Porter *et al.,* 1994). Chloropicrin (Trinity Manufacturing, Inc. Hamlet, NC) is also able to make *P. brassicae* resting spores inviable, although its efficiency is dependent upon the application method and requires covering the soil with polyethylene sheeting after application (White and Buczacki, 1977). This labour intensive process would require substantial effort and its cost would most likely make this method uneconomic for large scale canola farming.

Biocontrol is the application of enemies of a target species (*P. brassicae*) to reduce its population level. Several biocontrol agents have been tested in their efficiency against *P. brassicae.* Narisawa *et al*. (2000) dipped Chinese cabbage seedlings in *Heteroconium chaetospira,* a non-mycorrhizal endophyte of *Brassica spp.* resulting in a 52-97% reduction of clubroot severity. *H. chaetospira* colonized root cortical tissues and activated induced systemic resistance which inhibited *P. brassicae* infection and development (Lahlali *et al.,* 2014). *Bacillus subtilus* co-application with the fungus *Gliocladium catenulatum* reduced clubroot severity by more than 80% in the greenhouse, although there was no significant reduction ($p \leq 0.05$) in clubroot disease in the field (Peng *et al.*, 2011).

Screening of clubroot resistance in commonly grown canola cultivars has revealed that most cultivars grown on the prairie are susceptible to *P. brassicae* infection. This presents a challenge as traditional introgression of clubroot resistance to commonly grown varieties sacrifices their most beneficial agronomic traits, such as plant height, maturity rate, pod shattering resistance, and seed quality (Strelkov *et al.*, 2012). *P. brassicae* has also been shown to rapidly adapt to resistance when widespread mono- or oliogenic resistant varieties are used (Diederichsen *et al.*, 2009). To address the risk of sacrificing resistance sources to *P. brassicae* into commonly grown cultivars, R-gene pyramiding is being purported as the backbone of *P. brassicae* resistance in Canada due to limited control options (Rahman *et al.*, 2014). In fields highly infested with *P. brassicae*, clubroot disease management can be obtained via genetic resistance (Cao *et al.*, 2009). Sources of clubroot resistance have been reported in the major Brassica crops including *B. rapa, B. oleracea,* and *B. napus* (Diederichsen *et al.*, 2009; Crisp *et al.*, 1989; Hwang *et al.*, 2011).

Sources of genetic resistance to clubroot disease include cabbage (*B. oleracea*), turnip (*B. rapa* var. *rapifera*), black mustard (*B. nigra*), and rutabagas (*B. napus* cv. *napobrassica*). Peng *et al.* (2014) evaluated 955 Brassica accessions against races of *P. brassicae* in Canada and found a broad range of clubroot resistant candidates from the diploid species *B. rapa*, *B. nigra* and *B. oleracea*.

In *Arabidopsis thaliana*, clubroot disease resistance is quantitative, meaning that resistant plants have reduced disease symptoms, but those symptoms are not eliminated as would be characteristic of qualitative disease resistance, where infection of the root cortex is stopped. Fuchs and Sacristan (1995) characterized the clubroot resistance response in *A. thaliana* ecotypes Tsu-0 and Ze-0, which displayed a lack of typical clubroot swelling after infection. Light microscopy of the incompatible interaction revealed that in contrast to susceptible interactions, the general root

anatomy remained unchanged with no hypertrophy or heteroplasia in the root cortex (Fuchs and Sacristan, 1995). Similarly, the incompatible interaction had visual symptoms of the hypersensitive response occurring within root cortical cells (Fuchs and Sacristan, 1995). Fluorescent microscopy of those unstained roots showing hypersensitive response symptoms revealed strong autofluorescence relative to control when an excitation wavelength of 420 nm-490 nm was used, suggesting an increase in phenolic compounds in cell walls. Increased fluorescence was especially evident in cell-walls of cortical cells adjacent to infected cells displaying the visual hypersensitive response symptoms (Fuchs and Sacristan, 1995).

1.5 Plant Immunity

Evolution by natural selection has manifested an effective plant immune system. Plant-pathogens must be specialized to infect their hosts (Jones and Dangl, 2006). Unlike animals, whose immune systems have mobile defender cells and somatic adaptive immunity, plants rely upon individual cells to possess innate immunity and initiate immune response (Jones and Dangl, 2006). Plant immunity considered in context of the co-evolution of hosts and pathogens indicates reciprocal adaptive genetic changes resulting in fundamentally altered interaction mechanisms between hosts and microbes (Kareiva, 1999). This has necessitated the integration of multiple defense response pathways to allow plants to fine-tune their response to microbial infection.

Plant immunity is divided into two categories: pre-existing defense and active defense (Jones and Dangl, 2006). Pre-existing defense structures or basal defense structures include anatomical form, physiological adaptation, and molecular level defense. For example, leaf surface structures, including trichomes and a waxy cuticle, have evolved to provide a difficult surface for fungal pathogens to adhere to and penetrate. Physiological adaptations to pathogen attack include the cell wall and its strengthening components, such as lignin, calcium, and silicon. These components all serve to reinforce the rebar-like cellulose structure of the cell wall, providing a

barrier to pathogen penetration (Cosgrove, 2005). On a molecular level, enzyme or toxin inhibitors, including a class of antibiotics known as phytoanticipins, are present in plant tissues, and preclude pathogen attack (VanEtten *et al.*, 1994; Dixon, 2001; Haralampidis *et al.*, 2001). Together the pre-existing defense structures form effective barriers to pathogenic attack.

Pre-existing defense structures may not be sufficient to prevent pathogen infection and colonization. Hence, plants initiate active defense responses. Active defense responses occur in separate phases (Jones and Dangl, 2006). Upon pathogen inoculation to the host, the pathogen elicits a basal host immune response by activating host trans-membrane pattern recognition receptor (PRR) proteins that detect slowly evolving, commonly occurring components of microbe anatomy, termed pathogen associated molecular patterns (PAMPs) (Jones and Dangl, 2006). If successful PRR detection of PAMPs defeats the pathogen, PAMP triggered immunity (PTI) occurs. Once PTI occurs, no further immune responses are activated (Jones and Dangl, 2006). This disease resistance model is referred to as type-1 non-host resistance (NHR) (Mysore and Ryu, 2004; Lipka *et al.*, 2005).

Plant pathogens facilitate infection by secreting effectors to overcome PTI initiated by host detection of microbial elicitors (Dodds and Rathjen, 2010). Effectors are secreted by the pathogen to the host apoplast and/or cytosol to suppress host defense responses by targeting specific host defense mechanisms. Additionally, effectors may alter the host physiology enabling pathogen nutrient uptake and pathogen survival. Hence, effectors may overcome PTI and cause effector-triggered susceptibility (ETS). If the effector action is defeated by the host plant, effector triggered immunity (ETI) occurs (Jones and Dangl, 2006; Figure 1.6). Effector triggered immunity is characterized by the production and release of reactive oxygen species, cytoskeletal rearrangement, trafficking of cellular organelles and pathogenesis related (PR) proteins to the

infection site, and phytoalexin production (Dodds and Rathgen, 2010). Lastly, a hypersensitive response (HR) occurs in cells bordering and nearby the infected area. This can be described as type 2 NHR. The differences between mechanisms inducing cell death in type 1 and type 2 NHR are not understood well (Mysore and Ryu, 2004).

The hypersensitive response is a complex form of rapidly induced localized programmed cell death (Mur, 2007). Although a comprehensive molecular model remains to be described, the hypersensitive response is a classical feature of plant disease resistance, as a sharp delineation exists between dead tissue that has undergone the hypersensitive response and the healthy adjacent tissue (Mur *et al.,* 2008). This resistance mechanism involves a co-ordinated initiation of cell death associated signals including calcium, reactive oxygen species, nitric oxide, salicylic acid, and sphingolipids coinciding with proteolytic events and cellular reorganization and degradation (Mur *et al.,* 2008). During the hypersensitive response, cytoplasmic streaming initially occurs at an accelerated rate then ceases and the cells also undergo vacuolization which is thought to package cytoplasmic contents prior to degradation (Liu *et al.,* 2005). The cytoplasm becomes granular and collapses (Mur, 2007). Coincident with cytoplasmic collapse, the host nucleus enlarges and chromatin is digested. In leaf cells undergoing hypersensitive response, thylakoid membrane stacks are disrupted and lose photosynthetic capacity, and mitochondria rapidly swell, leading to a disruption in ATP synthesis (Lam *et al.,* 2001).

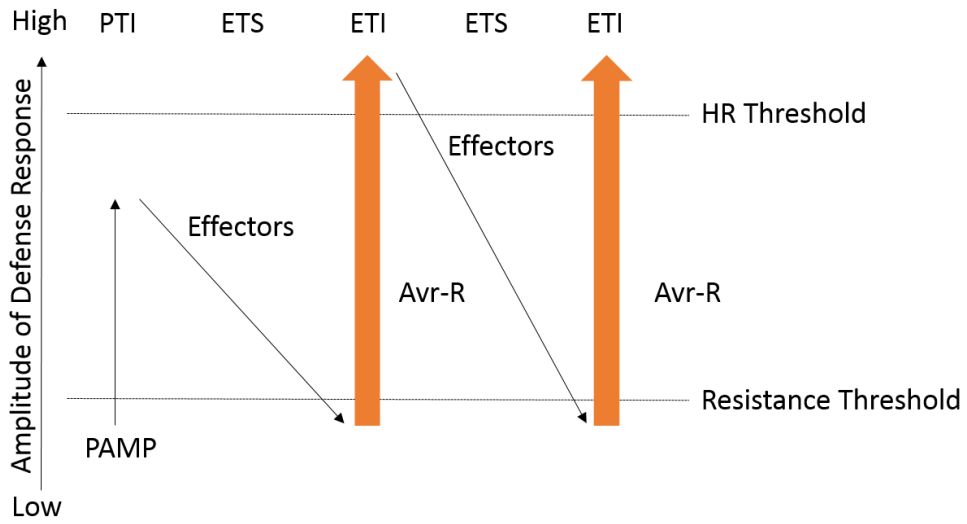

Figure 1.6 The zig-zag model of plant immunity (Jones and Dangl, 2006). Pathogen associated molecular patterns (PAMP) are detected by host plant pattern recognition receptors (PRR) which elicits the first host response, which if successful is termed PAMP-triggered immunity (PTI). Pathogens secrete effectors, low molecular weight compounds that interfere with PTI and enable nutrient uptake and pathogen establishment within the host, if this process goes undetected it is termed effector triggered susceptibility (ETS). Effectors may alternatively be detected by host avirulence gene products and triggers a signal cascade leading to the hypersensitive response, if this halts the pathogen it is termed effector triggered immunity (ETI). This mechanism of non-host detection may be overcome through pathogen-host coevolution which can result in continued ETS/ETI interaction in subsequent generations over an evolutionary time-scale.

1.6 Pathogenesis

P. brassicae is a soil borne obligate biotroph occupying the intracellular space of the host cell, one of few plant-pathogens to do so. *P. brassicae* is not unique in the fact that it occupies the intracellular space of host cells, an example of this being the causative agent of powdery scab of potato, *Spongospora subterranea* (Merz and Falloon, 2009). However, this model of host-pathogen interaction is not fully understood when compared to fungal plant pathogens.

Clubroot symptoms are a product of a variety of changes in plant metabolism, hormone ratios, and a redirection of carbon assimilates from shoot meristematic tissues to the roots (Ludwig-Muller *et al.*, 2009). Changes associated with host transcription and protein expression are induced upon *P. brassicae* infection in the *A. thaliana* root epidermis. Microarray expression studies by

Siemens *et al.* (2006), Agarwal *et al.* (2011), and Schuller *et al.* (2013) found over 1000 genes were differentially-regulated in *P. brassicae* infected plants relative to uninfected control plants. *P. brassicae* infection correlates with higher expression of genes involved in metabolic activities such as carbohydrate synthesis, sucrose synthesis, glycolysis, and the TCA cycle (Schuller *et al.*, 2013; Siemens *et al.,* 2006). Mitochondrial associated transcripts related to starch and metabolism are up-regulated (Siemens *et al.,* 2006). Genes involved in plant defense including signal transduction genes such as a calcium-dependent protein kinase, a mitogen activated protein kinase kinase, a serine-threonine protein kinase and leucine rich repeat protein kinase are up-regulated (Agarwal *et al.,* 2011). Genes down-regulated upon *P. brassicae* infection include genes involved in the oxidative burst pathway including those encoding peroxidise, NADP- dependent oxidoreductase, heat-shock protein and glutathione S-transferase (Agarwal *et al.,* 2011).

During infection of the cortical cells, the secondary life cycle phase, the pathogen is dependent upon host metabolites for survival (Siemens *et al*., 2006). Characteristic large galls centralized on the root begin to form as the cortical cell infection progresses (Kageyama and Asano, 2009). The cortical infection induces further transcriptional and proteomic regulation changes, as well as interference in host signal transduction pathways (Siemens *et al.,* 2006; Agarwal *et al.,* 2011). Cell cycle regulatory and cell expansion genes are up-regulated in relation to gall morphology and timing of cell division and subsequent cell enlargement (Siemens *et al.,* 2006). Genes associated with fermentative processes and lipid synthesis are up-regulated in plasmodia-containing cells (Schuller *et al.*, 2013). Four ion transport genes are up-regulated during cortical infection, indicating high reserve accumulation in the roots (Agarwal *et al.,* 2011; Siemens *et al.,* 2006). Plasmodia containing cortical cells had mevalonate pathway genes up-regulated, while the non-mevalonate pathway was down-regulated (Siemens *et al.,* 2006; Schuller *et al.,*

2013). Few resistance response transcriptional changes have been observed in clubbed tissues (Schuller *et al.,* 2013).

Proteome level changes associated with *P. brassicae* infection in *A. thaliana* include differential changes of proteins associated with host hormone signal transduction, defense, and metabolism (Devos *et al.,* 2005; Cao *et al.,* 2008). Devos *et al.* (2005) found cyclin-B1-1, a cyclin dependent protein kinase, is expressed in infected roots four dai. A β-glucuronidase (GUS) reporter gene fusion to cyclin-B1-1 (*CYCB1;*1::GUS) showed activation in the root meristems and in infected cells (Devos *et al.,* 2005). This consecutive re-initiation of cell division at the infection site fully supports *de novo* meristem development in infected cells. The pathogen induced meristem development becomes a metabolic sink and thus is the foundation of gall development. Both Devos *et al.* (2005) and Cao *et al.* (2008) found isopentyl-type cytokinins accumulate during the onset of *P. brassicae* infection four dai. This coincides with the down-regulation of host cytokinin synthesis genes and supports the hypothesis that cytokinins are produced by the pathogen (Ludwig-Müller *et al.,* 2015). Supporting previous results, cytokinins are intrinsically involved in meristem development, again supporting the hypothesis of meristem-like development in infected regions of roots. Auxin responses can be seen six dai, concurrent with the development of clubbed roots (Devos *et al.,* 2005). Plant defense proteins and metabolism proteins are differentially-regulated between *P. brassicae*-infected plants and control plants. Results from Cao *et al.* (2008) indicate that proteins directly and indirectly involved in the detoxification of reactive oxygen species were expressed more in *P. brassicae* infected roots than in uninfected roots. Additionally an *A. thaliana* chitinase protein was induced, suggesting that PTI defenses are activated upon *P. brassicae* infection. Host metabolism changes included limiting lignin biosynthesis and cytokinin degradation, while cellular energy metabolism was up-regulated. Changes to defense related

proteins includes down-regulation of a protein relating to defense lignin synthesis, and up-regulation of a reactive oxygen species scavenger (Devos *et al.,* 2005; Cao *et al,* 2008).

The involvement of hormonal signaling in clubroot development has been well-studied (Dekhuijzen and Overeem, 1971; Siemens *et al.*, 2006; Ludwig-Müller *et al.,* 2015). The changes in auxin and cytokinin equilibrium in infected plants indicates that host hormonal signalling is a virulence target (Siemens *et al.,* 2006). Cytokinin biosynthetic genes, cytokinin oxidases, and cytokinin dehydrogenases one and six were down-regulated throughout disease progression (Siemens *et al.,* 2006). Cytokinin signalling genes and cytokinin receptor genes are up-regulated (Siemens *et al.,* 2006). Host auxin synthesis is upregulated via the nitrilase pathway (Schuller *et al.,* 2013). The up-regulation of cytokinins and auxins produces the extensive cell division and hypertrophied roots associated with galls that characterize *P. brassicae* infection. Experiments where mutants had enhanced degradation of cytokinins induced pathogen resistance (Siemens *et al.,* 2006). *A. thaliana* mutants with dysfunctional Nitrilase1 (*nit1*) had reduced gall size (Schuller *et al.,* 2013). Hormonal imbalances are responsible for the impaired root function and morphology characterizing clubroot disease.

Pathogen involvement in hormonal defense signalling networks exists as well. During the cortical cell infection, giberellin synthesis related genes are up-regulated (Siemens *et al.,* 2006). Genes annotated in brassinosteroid synthesis and signaling are also up-regulated during cortical cell colonization (Schuller, 2013). Ethylene synthesis genes were differentially-regulated during the epidermal and cortical cell infections; older cells with large plasmodia have elevated ethylene transcription factors (Schuller *et al.,* 2013; Ludwig-Müller *et al.,* 2015). Upon infection, *LOX4,* a lipoxegenase involved in jasmonic acid synthesis, was up-regulated almost four fold (Agarwal *et al.,* 2011). The jasmonic acid signaling pathway is differentially-regulated upon *P. brassicae*

infection with receptor ligand synthesis and receptor synthesis being down-regulated. Salicylic acid (SA) is a crucial signalling molecule in activating defense responses in local and distal tissues. The SA pool is inactivated in *P. brassicae* infected cells via conjugation to glucose forming SA beta-glucoside, or by methylation forming methyl salicylate (Ludwig-Müller *et al.*, 2015). When in methylated form, SA it is more volatile and membrane permeable, and thus transmits throughout plant tissues at a faster rate. *P. brassicae* methylated (Me) SA is converted back to SA by a host MeSA esterase. The roles of MeSA in plant defence are not well understood, although evidence supports that MeSA functions as an activator of SAR in tobacco. In the *P. brassicae-A. thaliana* pathosystem, the pathogen secretes a novel effector that methylates SA. MeSA is translocated from the roots to the leaves (Ludwig-Müller *et al.*, 2015).

1.7 Microscopy of the *P. brassicae*-host Interaction

Work on understanding the cytology of *P. brassicae* and host has been limited from a technological point-of-view (Feng *et al*., 2014; Schuller and Ludwig-Müller, 2016). Difficulty in increasing clubroot disease resistance amongst host species may be the consequence of insufficient understanding of host/pathogen interaction at the molecular level (Cao *et al.*, 2008). Similarly, understanding of plant-pathogen interaction at the cellular level is limited and hinders our understanding of disease resistance. The multi-faceted virulence strategies used by *P. brassicae* indicate that there is a complex, intimate, pathogen-host interaction. Physiological, genetic, and proteomic evidence support the pathogen interfering with plant hormonal networks, host metabolism, and host defense responses. On a cellular level, no microscopy of the *in vivo* host-pathogen interaction has been completed, although many studies have focused on fixed tissues. As a consequence, details of the pathogen's life history have been ignored contributing to an insufficient understanding of *P. brassicae* (Kunkle, 1918; Mithen and Magrath, 1992; Kobelt *et al.*, 2000; Schuller and Ludwig-Müller, 2016).

The interaction of *P. brassicae* and hosts has been studied extensively by transmission electron microscopy (Aist and Williams, 1971; Dekhuijzen, 1978; Mithen and Magrath, 1992; Kobelt *et al.,* 2000). Cortical cell infection takes place before visible symptom development occurs. Multiple reports have shown that the pathogen structure initially infecting cortical cells differs drastically from the morphology of the secondary plasmodia (Dekhuijzen, 1978; Mithen and Magrath, 1992; Kobelt *et al.,* 2000). The early amoeba-like structure contains only one nucleus and few lipid droplets, while secondary plasmodia are multinucleate and have multiple lipid droplets (Dekhuijzen, 1978). The early amoeba-like structures are smaller than the smallest plasmodia, ranging from 1 to 5 µm, while the smallest plasmodia are larger than 5 µm and contain multiple lipid bodies (Aist and Williams, 1971). These amoeboid structures are seen in association with cell wall perforations, hypertrophied host cell nuclei and nucleoli (Dekhuijzen, 1978; Mithen and Magrath, 1992). Conflicting evidence surrounds the spatial location of the ameboid pathogen within the host cell. *P. brassicae* encasement within the host tonoplast as well as plasmodia associated with small protrusions of host cytoplasm into the vacuole have both been observed (Dekhuijzen, 1978; Mithen and Magrath, 1992). It has been suggested that the plasmodial protrusions would expand until the vacuole was full of plasmodia, although evidence supporting this was not published (Mithen and Magrath, 1992). Tonoplast disruption has been observed during development of the amoeba-like pathogen structure (Dekhuijzen, 1978; Mithen and Magrath, 1992). Often the amoeba-like pathogen structures were seen with pseudopod-like extensions, strand-like tubules appeared to be connected with the protrusions and lobes of the amoeba (Mithen and Magrath, 1992; Kobelt *et al.,* 2000). The tubules were hypothesized to be involved in phagocytosis or contractile movement of the amoebae (Mithen and Magrath, 1992; Kobelt *et al.,* 2000).

Analysis of cellular interaction between *P. brassicae* and a host using a light microscope has received considerable attention by clubroot researchers. Staining methods have been applied to identify pathogen and host structures, and changes to the host cell upon infection (Schuller and Ludwig-Müller, 2016). Differential staining of plant pathogen and host tissue is demanding. Selective staining of *P. brassicae* has not yet been achieved in a live cell context (Schuller and Ludwig-Müller, 2016). In the early years of clubroot research a dual-staining technique was developed using Magdala red and Lichtgrün, staining *P. brassicae* spores and plasmodia red while the host tissue was differentially stained green (Dickson, 1920) . Multiple researchers (Belánger, 1961; Humphrey and Pittman, 1974; and Buczacki and Moxham, 1979) developed and refined a triple staining method using methylene blue, azure II, and basic fuchsin that stained the host cytoplasm pale blue, lipids blueish-green, starches pink, and the plasmodial envelope, nucleoli, chromosomes and resting spore cell walls dark blue. Aniline blue has been used to stain *P. brassicae* life stages during root hair infection (Sharma *et al.,* 2011a). While methylene blue has been used to stain pathogen structures deep blue against the light-blue stained host cytoplasm during cortical cell colonization (Sharma *et al.,* 2011b).

Using fluorescence microscopy the incompatible interaction between *A. thaliana* ecotypes *Ze-0* and *Tsu-0* and *P. brassicae* isolate e could be characterized by the autofluorescence of necrotic cells in fixed tissue thin sections (Kobelt *et al.,* 2000). When studying the compatible interaction between *P. brassicae* isolate e and *A. thaliana* ecotype *Col-0* using a 450-490 nm exciation filter, a 510 nm dichoric mirror, and a 515 nm barrier filter, autofluorescence of the host cell wall, and *P. brassicae* cytoplasm, and *P. brassicae* lipid droplets could be seen (Kobelt *et al.,* 2000). *P. brassicae* lipid droplets fluoresced yellow in contrast to the green stained cytoplasm,

while the host cytoplasm had no fluorescence and the cell wall fluoresced yellow (Kobelt *et al.*, 2000).

Fluorescence stains have also been used in whole, unfixed tissues to study *P. brassicae*, primarily to assess the viability of resting spores. Resting spores stained with 4′,6-diamidino-2-phenylindole (DAPI) were analyzed by flow cytometry to assess germination rate as germinated resting spores did not fluoresce (Niwa *et al.*, 2008; Jäschke *et al.*, 2010). A double fluorescence staining approach was used by Takahashi and Yamaguchi (1988) who used ethidium bromide and calcofluor white, where viable and non-viable spores could be classified based on the staining of the cytoplasm, as the cytoplasm of inactive spores had red fluorescence.

In the closely related plasmodiophorid, *Polymyxea graminis,* fluorescence microscopy was used to study plasmodia, sporosori, and resting spores in the roots of *Sorghum bicolor* using Nile red (Littlefield *et al.*, 1997). Likewise, Nile red has been used to study post-infection development of *P. graminis* in *Triticum aestivum* (Littlefield *et al.*, 1998). In both studies, lipid droplets fluoresced in sharp contrast to the host cell under excitation from a 514 nm laser using confocal microscopy. Littlefield *et al*. (1997; 1998) were able to track the development of resting spores from sporosori; however, they did not apply this technique to samples under extended observation.

1.8 Objectives of M.Sc. Research Program

The overriding objectives of this proposed research were to understand the host-pathogen interactions between *A. thaliana* and *P. brassicae* using live cell imaging. This study examined clubroot disease which infects and causes yield loss in Brassicaceae crops worldwide. In this research, I examined the pathogenesis of *P. brassicae* by specifically examining the cellular basis of infection and disease progression. In the broad sense, this investigation attempted to increase the scientific understanding of host-pathogen interactions, especially the model of protist obligate biotroph pathogen interaction with a host on a cellular level. Specifically, I aimed to identify

unique infection strategies as plant infection by phytomyxids which requires a sophisticated subversion of host cells. In detail, my study aimed to understand the *P. brassicae* life cycle using live cell staining, and to study infective mechanisms and their contribution to pathogen establishment within the host. To achieve the general program target, I completed three objectives:

1. To develop an *in planta* staining technique for visualization of the clubroot pathogen, *Plasmodiophora brassicae.*
2. To investigate infection processes of *P. brassicae* using *A. thaliana* and established staining protocols, emphasizing root hair infection, epidermal/cortical cell infections, as well as pathogen proliferation and possible transmission within the host tissues.
3. To study the cellular responses in *A. thaliana* upon infection by *P. brassicae* using transgenic *A. thaliana* lines expressing fluorescent protein tagged host cellular components, thereby examining organelle movement and membrane partitioning in response to infection.

2.0 MATERIALS AND METHODS

2.1 Resting Spore Isolation and *P. brassicae* Infested Soil Preparation

Clubroot materials were provided by Dr. Gary Peng (AAFC, Saskatoon) who collected canola roots infected with *P. brassicae* pathotype 3 near Leduc, Alberta. Inoculum for the experiments was obtained by surface-sterilizing *P. brassicae*-infected canola roots with 30 % bleach (sodium hypochlorite, NaOCl) for five minutes. Roots were then cut into segments one cm^3 or smaller. The root segments were macerated in sterile conditions by grinding them with a mortar and pestel. *P. brassicae* resting spore concentration was determined using a haemocytometer. The root slurry was adjusted to a resting spore concentration of 10^6-10^7 resting spores mL^{-1} using water. The resting spore solution was blended with Sunshine® Mix #3 (SunGro Horticulture, Vancouver, BC) in a sterile plastic container using a ratio of one mL resting spore solution to two g of dry potting mix, as consistent symptom development occurs when *P. brassicae* resting spore concentrations are greater than 10^3 spores g^{-1} of dry soil (Donald and Porter, 2009; Faggian and Strelkov, 2009).

2.2 Amplification of *P. brassicae* Infested Soil and Production of Canola Clubroot Tissue

Canola (*Brassica napus* cv. Westar) seeds were surface-sterilized using 70 % ethanol for three min followed by 1 % bleach for five min. Canola seeds were washed with sterile water and germinated on moist paper towel in a sterile Petri dish in an incubation chamber at 22 °C under a 16 h/8 h light/dark cycle. After germination, seeds were planted with the radicle facing down, two cm below the soil surface in 15 cm wide by 23.5 cm tall plastic plant pots (Kord Products, Toronto, ON) containing the prepared *P. brassicae* infested Sunshine Mix #3. These potted plants were placed in a plant growth chamber under 16 h/8 h light/dark cycle, at 20 °C and 65 % relative humidity. Plants were grown for about eight weeks before being uprooted. The galls from the

uprooted plants were used to produce more *P. brassicae*-infested soil and for the establishment of an axenic, *P. brassicae*-infected *B. napus* callus, dual-culture system.

2.3 Establishment of an Axenic Dual-Culture System

Jiangying Tu previously used a modified method of Bulman *et al.* (2011) to produce *P. brassicae* infected callus. Using this method and with her assistance, cataplastic gall outgrowths were isolated from clubbed roots of *B. napus* cv. Westar plants grown in *P. brassicae*-infested Sunshine Mix #3 (Figure 2.1). Gall outgrowths were surface-sterilized in 70 % ethanol for one min and 30 % bleach for 20 min, followed by three washes in sterile distilled water. The galls were cut into three mm cross segments. Segments were surface-sterilized using 1 % ethanol, followed by a 20 min immersion in 2 % chloramine-T. Lastly, the segments were rinsed three times in sterile distilled water and were plated on Murashige and Skoog (MS) media containing 3 % sucrose, 300 mgL^{-1} timentin, and 1.2 % agar. The plates containing the *P. brassicae*-infected *B. napus* cv. Westar cells were then placed inside an opaque box in an incubator at 22 °C. Plates were checked daily for contamination. If contaminated pieces were found, the remaining uncontaminated pieces were transferred to a new plate using sterile forceps in a laminar flow hood. Consistent callus growth was obtained after serial re-isolations.

Figure 2.1 Cataplastic outgrowths on *B. napus* cv. Westar root infected with *P. brassicae*. The root of this canola plant shows typical clubroot symptoms of severe *P. brassicae* infection including the swelling (hypertrophy and heteroplasia) of primary and lateral roots as well as cataplastic gall outgrowths (highlighted by arrows).

2.4 Observation of Infected Callus Cells

Callus was harvested from plated tissues and placed onto microscope slides containing a droplet of water and covered with a coverslip. Slides were examined using a light microscope at 25 X or 40 X magnification. Samples that yielded *P. brassicae* infected living host cells were stained and observed using confocal laser scanning microscopy (CLSM).

2.5 Planting and Growth of *A. thaliana* Plants Grown on Murashige and Skoog Media

The *Arabidopsis thaliana* lines used in this thesis are described in Table 2.1. All lines, including those expressing fluorescence protein-tagged cellular components were of the *A. thaliana* Col-0 ecotype susceptible to *P. brassicae* (Fuchs and Sacristan, 1995). *A. thaliana* seeds were surface sterilized with 70 % ethanol for one min, 1 % bleach (sodium hypochlorite, NaOCl) for five min, then rinsed five times with sterile distilled water. Seeds were placed on ½ strength MS media containing 1 % sucrose and 1 % agar. The plated *A. thaliana* seeds were stratified at 4

°C for 2 days to break dormancy and to synchronize seed germination (Weigel and Glazebrook, 2002). Plated seeds were incubated under a 16 h/8 h light/dark cycle at 22 °C for a minimum of five days until inoculation.

Table 2.1 List of transgenic *A. thaliana* plant materials used.

Structure Labelled	Seed Stock/ Donor	TAIR annotation of Corresponding Gene/Locus	Reference
Actin	E. Blancaflor	GFP fusions to C and N terminus of fimbrin 1 actin binding domain	Wang et al., 2004
Nucleus	CS84731	cDNA sequence homology to ankyrin like protein	Cutler *et al*., 2000
Tonoplast	CS16257	γ-TIP water channel	Nelson *et al*., 2007
Tonoplast	CS84727	δ-TIP water channel	Cutler *et al*., 2000

2.6 Inoculation of Petri Dish-Grown *A. thaliana* Seedlings

Enlarged cells of callus tissue containing resting spores were used as the inoculum source for infection of *A. thaliana* plants grown in Petri dishes. A small sample of callus was collected and placed in a sterile 1.5 mL Eppendorf tube in 500 μL of sterile water and ground using a sterile plastic pestle. The ground solution was vortexed and debris allowed to settle for 10 min. The top phase of the solution containing resting spores was collected and placed into a second 1.5 mL Eppendorf tube. Resting spore concentration was measured using a haemocytometer and adjusted to 10^6-10^7 spores mL^{-1}. The adjusted spore suspension was directly inoculated onto the roots of 5-day-old *A. thaliana* plants. Inoculated plants were grown on ½ strength MS under a 16 h/8 h light/dark cycle at 22 °C.

2.7 Preparation of Staining Solutions & Staining

A Nile red 1 mg mL^{-1} stock solution (318.369 g mol^{-1}, Sigma-Aldrich) prepared in methanol was diluted to a working solution concentration in water. Infected and control *A. thaliana* roots or callus culture cells were placed on slides containing 2 drops of 15 μM Nile red staining

solution. Tissues were incubated in these solutions at room temperature for at least 15 min and then covered with a coverslip. The staining solution was washed from prepared slides by placing a paper towel on one end of the slide to act as a wick, while sterile distilled water was injected opposite to the paper towel, washing the staining solution from the slide. The samples were then viewed using CLSM. FM4-64 (607.514 g mol^{-1}, Invitrogen) stained samples were prepared in the same fashion, except for using a working concentration of 50 μM.

2.8 Confocal microscopy

CLSM was used to observe the Nile red- and FM4-64-stained callus culture samples. For Nile red staining, an excitation wavelength of a 488 nm from an argon laser, or 535 nm from a helium-neon laser was used (Figure 2.2). Fluorophore emission spectra were captured using a 585-615 nm band pass filter or a 650 nm long pass filter. Observation of FM4-64-stained samples used an excitation wavelength of 488 nm from an argon laser and fluorophore emission spectra was captured using the 650 nm long pass filter. Confocal microscopy of *A. thaliana* green fluorescence protein (GFP)-tagged lines stained with Nile red was performed using dual channel microscopy. Nile red used the same excitation wavelength and emission spectra filter as described above. For GFP an excitation wavelength of 488 nm from an Argon laser was used with the band pass emission spectra filter capturing light in the 505 – 530 nm range. All confocal microscopy was done using a Zeiss LSM510 Meta confocal microscope with image processing preformed using Zeiss LSM Image Browser, ImageJ, or Adobe Photoshop.

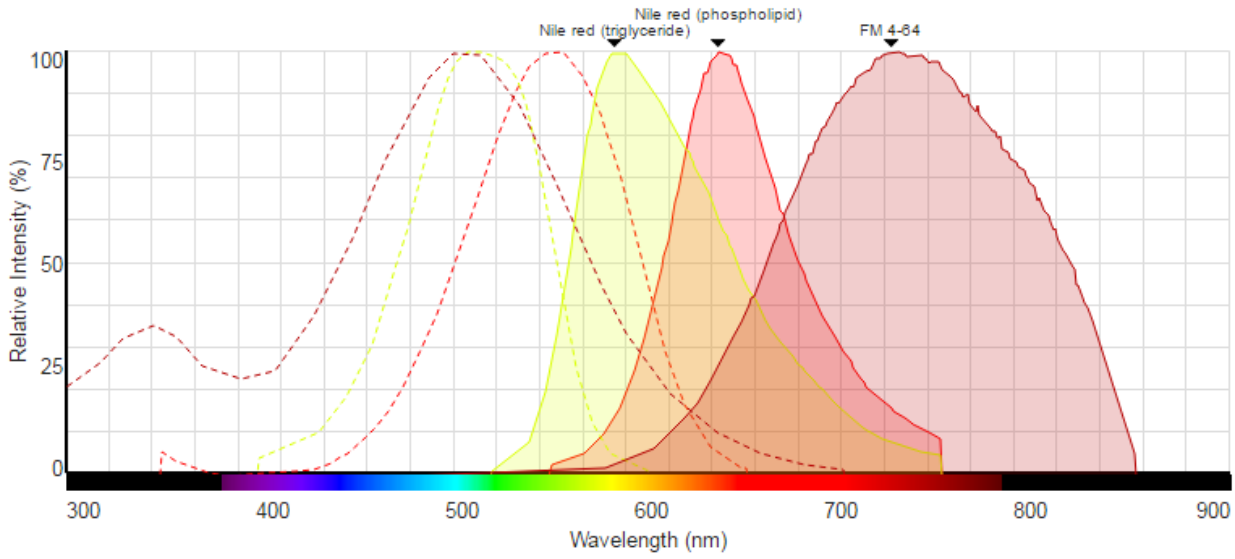

Figure 2.2 Excitation and emission spectra of Nile Red and FM4-64. Nile red triglyceride (yellow) has an excitation curve (dotted line) ranging from 400 nm to 600 nm with a peak excitation at 514 nm. Nile red triglyceride emission spectra (solid line, shaded area) ranges from 514 nm to 751 nm with peak emission at 585 nm. Nile red phospholipid (red) has an excitation curve (dotted line) ranging from 400 nm to 700 nm with peak excitation at 555 nm. Nile red phospholipid (solid line with shaded area) has an emission spectra ranging from 565 nm to 750 nm with peak emission wavelength of 636 nm. FM4-64 (burgundy) has an excitation curve (dotted line) ranging from 300 nm to 700 nm with a peak excitation at 505 nm. FM4-64 emission spectra (solid line, shaded area) ranges from 524 nm to 850 nm with peak emission at 728 nm. Image created using ThemoFisher Scientific Fluorescence SpectraViewer software.

3.0 RESULTS

3.1 Establishment of an Axenic Dual Culture System

P. brassicae was successfully amplified by producing callus culture using *Brassica napus* cv. Westar roots infected with *P. brassicae* (Figure 2.1). Callus growth was distinguishable by eye within two weeks, when disorganized tissue growth could be seen protruding from the outer edges of the cultured root segment. The majority of cultured gall segments (>70 %) became contaminated with bacteria or fungi after their initial plating. When established, uncontaminated *P. brassicae*-infected calli were re-cultured on fresh medium and continued to grow producing large, disorganized masses of off-white coloured callus tissue (Figure 3.1). This growth was continued for greater than 200 days, eventually the growing tissue necrotized resulting in dark, dehydrated callus.

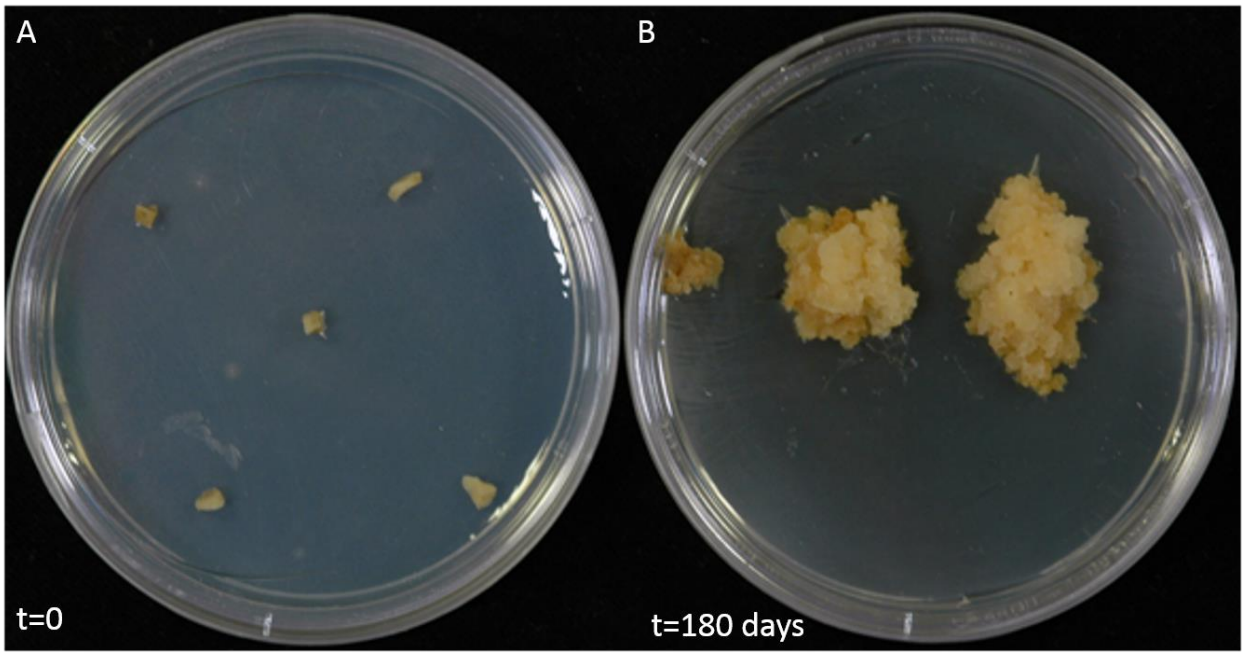

Figure 3.3 Tissue culture of *P. brassicae*-infected *B. napus* roots. Initially, the galls were sectioned and incubated on MS plates (A). After repeat plating and at 180 days of growth the callus mass was large and harbored various stages of the *P. brassicae* lifecycle (B).

3.2 Development of a Pathogen Staining Protocol

Cells harvested from *P. brassicae*-infected *B. napus* callus served as a platform to screen fluorophores for suitability as live cell stains. *P. brassicae* plasmodia, zoosporangia, and resting spores were identified concurrently within the *B. napus* callus throughout the callus incubation period. Initially, polar lipids found in cell membranes were targeted for staining with fluorescence probes. However, selectively staining non-polar lipids in droplets that are characteristic of the *P. brassicae* cellular architecture allowed for discreet observation of *P. brassicae* in callus culture.

Confocal microscopy of *P. brassicae*-infected *B. napus* calli stained with FM4-64 revealed that the host plasma membrane (PM) and the outer membranes of *P. brassicae* plasmodia and zoosporangia stained with FM4-64 (Figure 3.2 A, B and C). The host PM remained intact in infected callus (Figure 3.2 B). FM4-64 uptake by infected cells resulted in staining of membrane bound structures within those cells (Figure 3.2 B). Theses compartments included *P. brassicae* plasmodia and zoosporangia. However, if cells were damaged and the functionality of the PM was lost, FM4-64 leaked past the PM into the cell and resulted in extensive staining of cellular components (Figure 3.2 A and C).

P. brassicae plasmodia and zoosporangia both contained rapidly moving components within their cytosol, indicating that FM4-64 was not toxic to *P. brassicae* during the observation timeframe (Figure S1, Figure S2). Within a plasmodium, rapidly moving cytoplasm could be seen surrounding an enveloped starch granule (Figure S1). The envelopment of the starch granule suggested that the *P. brassicae* plasmodium fed via phagocytosis of host cellular components (Figure 3.2 A). Within the FM4-64-stained zoosporangia membrane, zoospores were too small and moved to quickly in order to observe their cellular structure by CLSM (Figure S2). The definite FM4-64-stained membranes surrounding zoospores indicated that recently produced zoospores remained within the zoosporangium membrane (Figure 3.2, Figure S2). FM4-64 was adequate in

staining the outermost membranes of plasmodia and zoosporangia in a live cell context, but was unable to stain cellular components of *P. brassicae* (Figure 3.2).

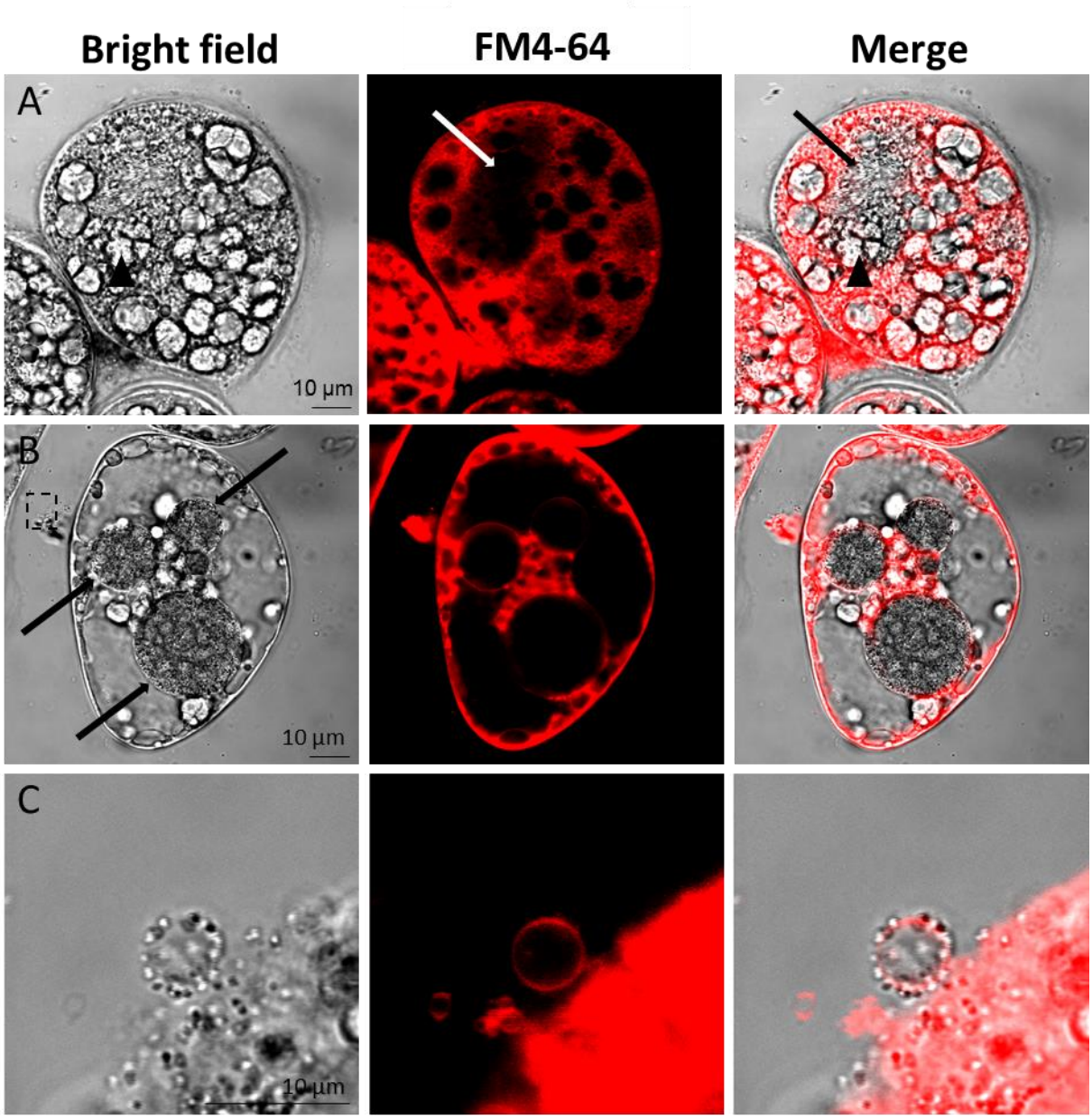

Figure 3.4 FM4-64 staining of *P. brassicae*-infected *B. napus* callus. Bright field, fluorescence and merged CLSM images indicated FM4-64 staining labeled the host cell plasma membrane (PM) and PM-derived internal cell structures. FM4-64 stained the membranes surrounding plasmodia (A) and zoosporangia (B). An expelled zoosporangia indicated by the dashed box in (B) is detailed in (C). Video of plasmodia and zoosporangia available in Figures S1 and S2. Arrows indicate plasmodia (A and B), while a black triangle indicates a starch granule (A).

CLSM of callus stained with Nile red, a membrane-diffusible hydrophobic lipid probe, revealed it to be an adequate stain for observing *P. brassicae* plasmodia, zoosporangia, and resting spores (Figure 3.3). Nile red staining worked best when lipid droplets in plasmodia, zoosporangia and resting spores were imaged using 488 nm excitation wavelength. Plasmodia stained with Nile red had extensive lipid content distributed throughout the cytosol and were found in close association with, adjacent to, or enveloping starch granules in the callus cells, again suggesting phagocytosis (Figure 3.3 A). Likewise, zoosporangia had extensive, Nile red-stained lipid components, but zoosporangia were not associated as closely with starch granules as plasmodia (Figure 3.3). Lipid droplets in plasmodia moved quickly and in stream-like patterns suggesting that organized intercellular trafficking is occurring, indicating live cell imaging of Nile red stained *P. brassicae* infected *B. napus* callus is possible (Figure S3). After maturation and plasmodia development ceased, zoosporangia were produced. A zoosporangium expelled from a cell of the callus stained with Nile red clearly indicated zoospores are positively stained by Nile red (Figure 3.3 C, Figure S4). Again, these zoospores remained bound within a membrane, as seen with the expunged zoosporangia stained with FM4-64; however, Nile red definitively stains the individual zoospores (Figure 3.3, Figure S4). Zoospores were too small to observe their cellular structure by CLSM, though the zoospores were clearly labelled by Nile red and they appeared to move randomly within the zoosporangia membrane (Figure S4). Nile red staining of older callus tissue harvested from the zone adjacent to necrotized callus tissue revealed the callus cells to be populated with resting spores with lipid droplets clearly labelled (Figure 3.4 D). Likewise, resting spores expunged from callus cells had distinct lipid droplets stained with Nile red (Figure 3.4 E).

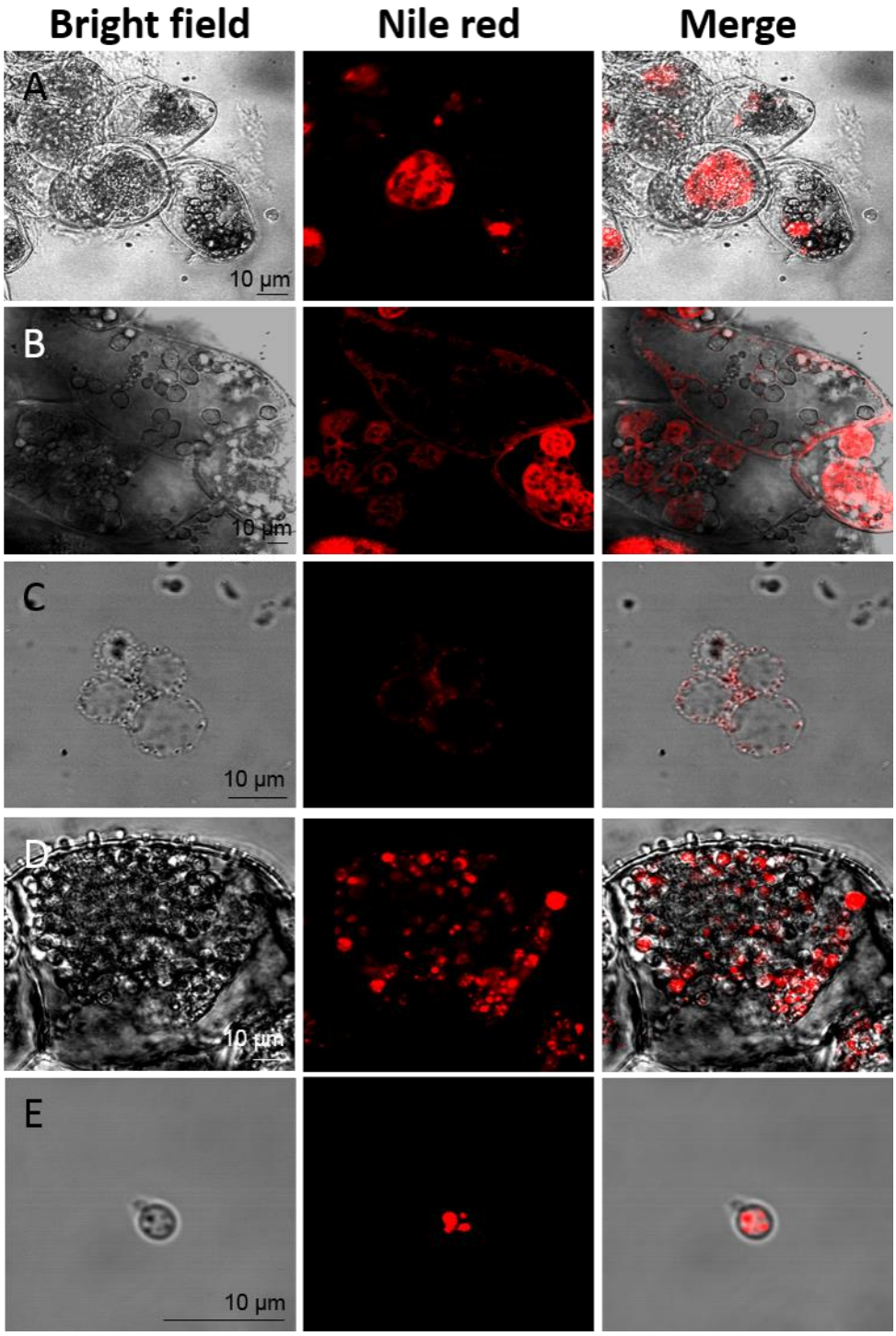

Figure 3.5 Nile red staining of *P. brassicae* infected *B. napus* callus. Bright field, fluorescence CLSM and merged images indicated that Nile red stain specifically labels *P. brassicae* in contrast to the host cell. Using 488 nm light as excitation, lipid droplets were seen in plasmodia (A), zoosporangia (B, and S3), expelled zoosporangia (C and S4), and resting spores (D and E).

Testing dilutions of Nile red stock solution indicated that 15 µM Nile red was able to stain resting spores within 15 min using a concentration greater than 15 µM (Figure 3.4). Using 15 µM Nile red to stain samples for 15 min was the best for this study as it exercised economy and also provided the ability to prepare samples in a short amount of time before observation.

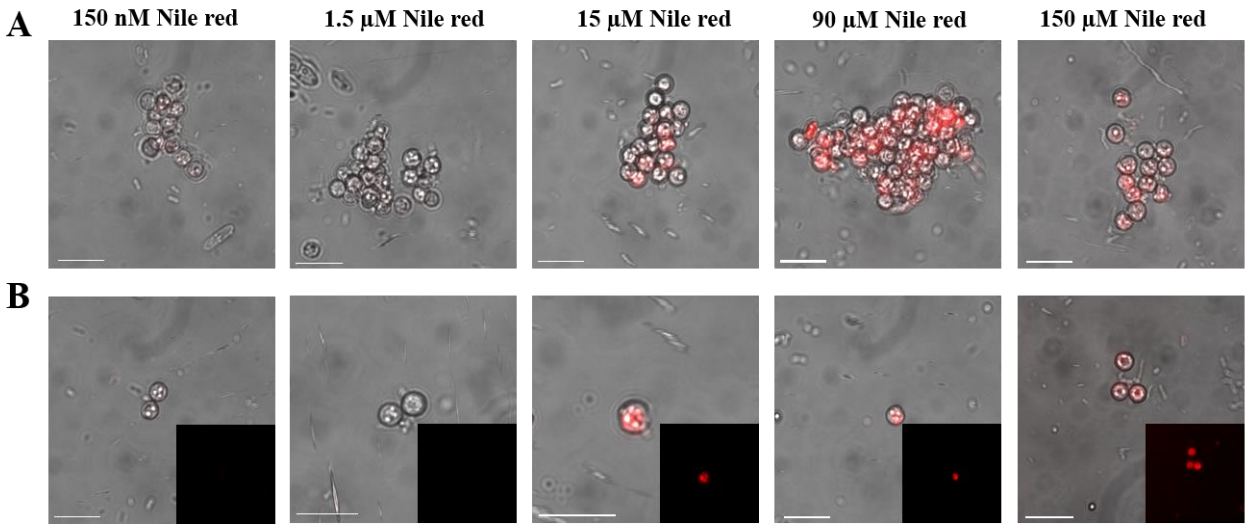

Figure 3.6 A Nile red concentration of 15 µM is sufficient to stain *P. brassicae* resting spores. Resting spores stained with 150 nM, 1.5 µM, 15 µM, 90 µM or 150 µM were examined using CLSM. Groups of resting spores could be stained with concentrations of Nile red ≥ 15 µM (A). Individual resting spores are stained using the same concentrations, with the detail in the lower right showing the fluorescence produced by lipid droplets in the resting spore (B). Scale bars represent 10 µm.

3.3 *In planta* Staining of *P. brassicae* Using the Lipid Probe Nile Red

Inoculation of wild-type *Arabidopsis thaliana* Col-0 plants grown in a Petri dish on ½ MS media inoculated with *P. brassicae* resting spores is a suitable test for Nile red's affinity for *in planta* labelling of *P. brassicae* prior to, and following infection. Nile red successfully stained lipid droplets in *P. brassicae* resting spores adjacent to *A. thaliana* root hairs (Figure 3.5). Following infection, plasmodia and zoosporangia were labelled within the root hair lumen one and eight dpi, respectively (Figure 3.5). Plasmodia in *P. brassicae*-infected *A. thaliana* root hairs stained with Nile red had rapidly moving lipid droplets within their cytosol, indicating that Nile

red was suitable for live cell *in planta*-labelling of *P. brassicae* (Figure S5). *P. brassicae* plasmodia consistently increased in size following infection, from 1 µm post-penetration to eventually growing to a 10 to 15 µm diameter spheroidal shape during the seven days following infection (Figure 3.5 C, Figure S5). At eight dpi, Nile red-stained zoospores making up the *P. brassicae* zoosporangia could be seen inside the *A. thaliana* root hairs, indicating Nile red can successfully stain *P. brassicae* life stages associated with a root hair infection (Figure 3.5 D). Furthermore, individual zoospores originating from zoosporangia rapidly move through a much larger relative space compared to the zoospores, which remain relatively sedentary, in close spatial proximity to other zoospores in the root hair. This suggested that as zoosporangia mature, the outermost membrane breaks, releasing zoospores into the host intracellular environment (Figure S6). Collectively, these data indicated Nile red to be an adequate probe for *in planta* live cell imaging of *P. brassicae*.

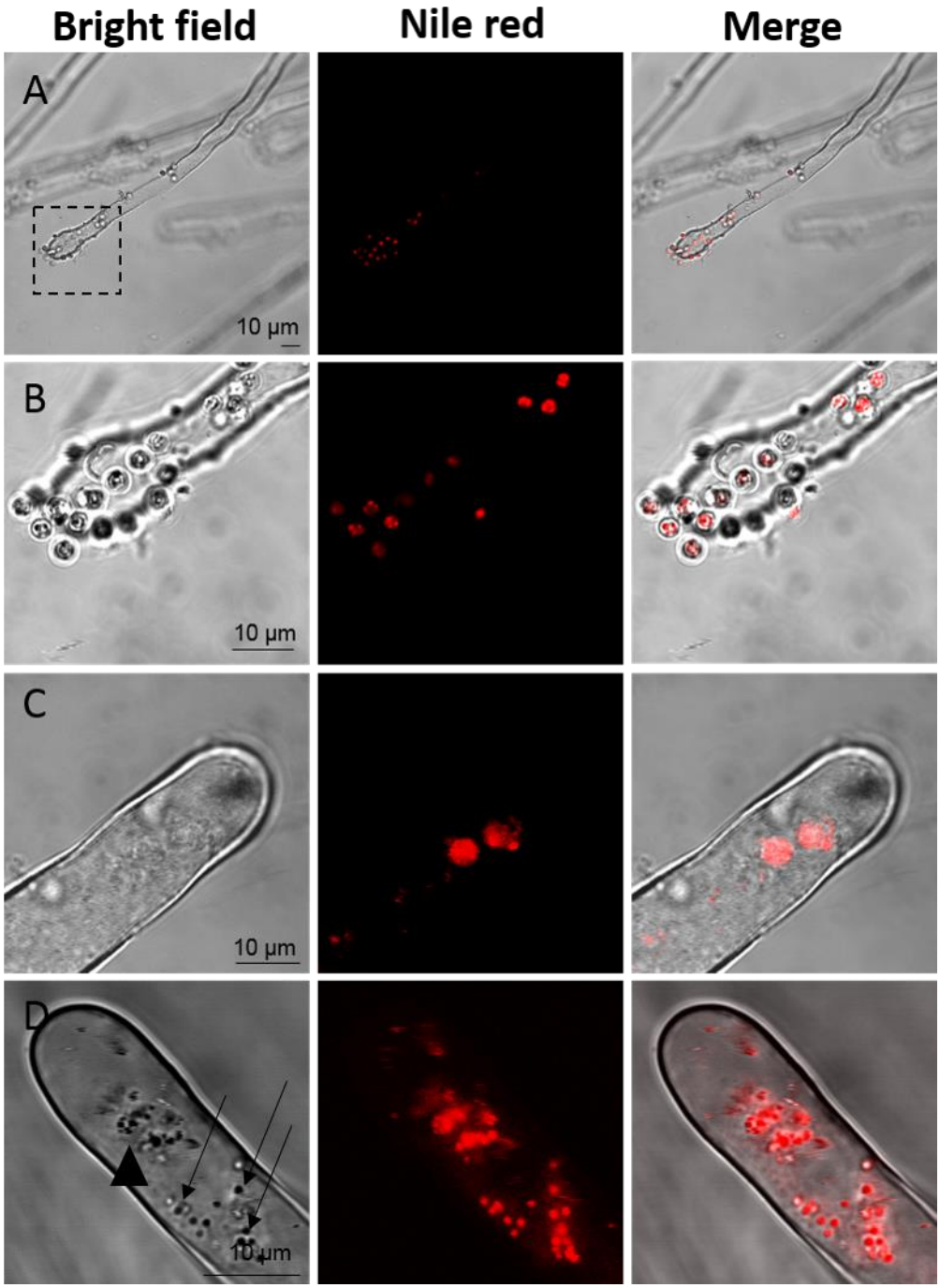

Figure 3.7 Nile red staining of root hair infection by *P. brassicae*. Resting spores (A) at eight hpi are located nearby the root hairs. The dashed box area in (A), is detailed under magnification in (B) where the resting spore lipid droplets are seen. Spheroid plasmodia at 24 hpi were located inside the host root hair (C and S5). Zoosporangia (arrowhead) and motile zoospores (arrows) at eight dpi could be seen moving in a root hair (D and S6).

Staining transverse root cross-sections of *A. thaliana* plants grown in *P. brassicae*-infested soil revealed Nile red to be adequate for staining the plasmodia and resting spore life stages (Figure 3.6, Figure S7). Sedentary secondary plasmodia were observed occupying cortical cells 20 dpi, while more active, spheroidal secondary plasmodia with rapidly moving lipid droplets were seen at 25 dpi, and resting spores were seen at 35 dpi (Figure 3.6). Beyond 40 dpi, the galls on the roots of infected *A. thaliana* plants began to rot in the soil, exposing the resting spores to the soil microcosm. Multiple secondary plasmodia showing Nile red-labelled diffuse, membrane bound, lipid content were consistently observed occupying the same host cell (Figure 3.6 A). Similarly, these secondary plasmodia cleave to produce multiple membrane bound plasmodia with rapidly moving small-sized lipid droplets within the same host cell (Figure 3.6 B; Figure S7). When root cross-sections containing resting spores were stained with Nile red, sedentary lipid droplets inside of the resting spores fluoresced (Figure 3.6 C). Collectively, Nile red served as an adequate stain to observe *P. brassicae* secondary plasmodia, zoospores, and resting spores *in vivo* during cortical cell infection (Figure 3.6).

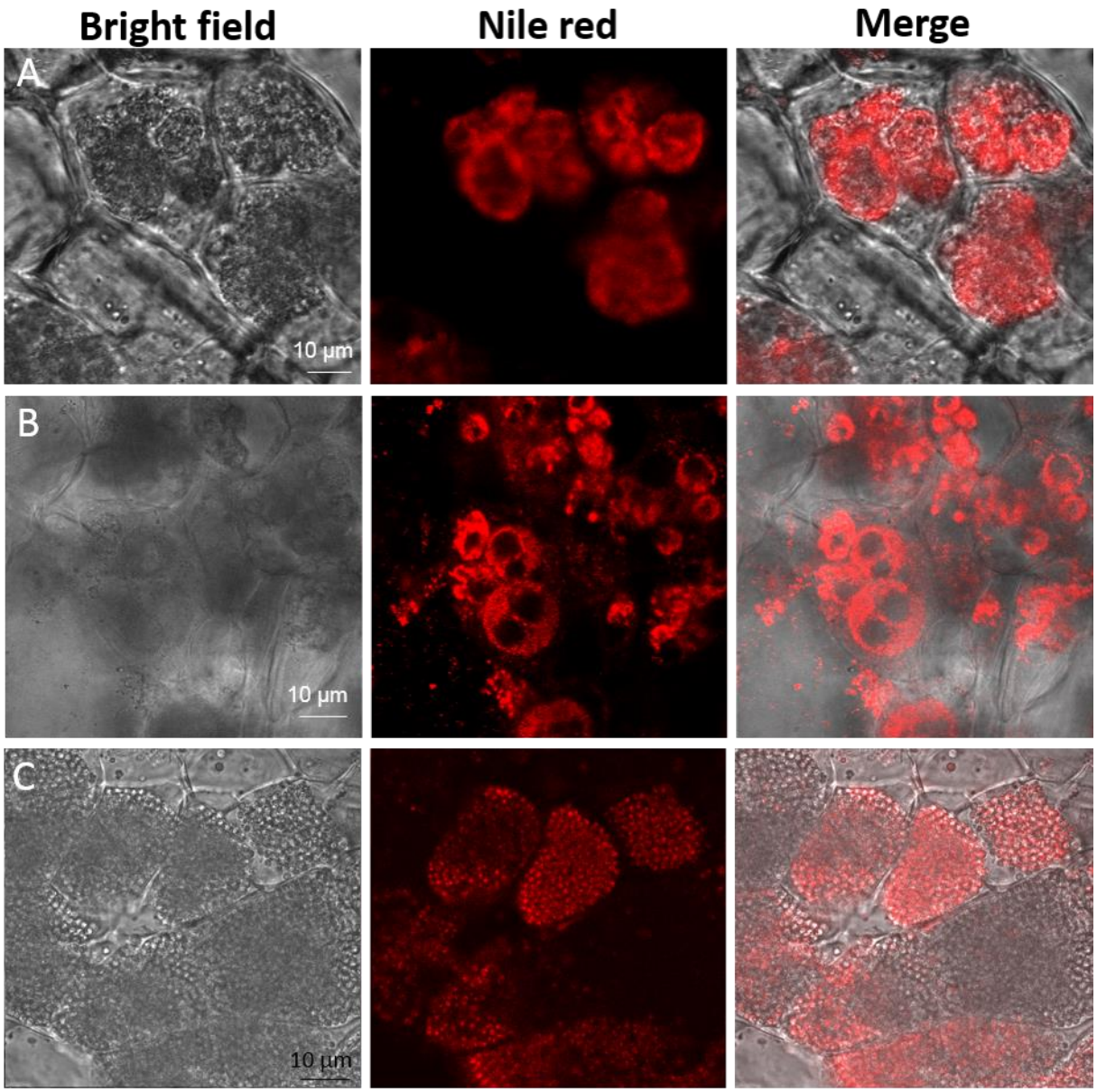

Figure 3.8 Nile red staining of *P. brassicae* in infected cortical cells**.** Roots of *A. thaliana* plants grown in *P. brassicae*-infested soil were transversely sectioned and stained with Nile red. Secondary plasmodia are seen in host cortical cells at 20 and 25 dpi (A, B and S7). Resting spores are seen in the host cortex 35 dpi (C).

3.4 Interactions Between *P. brassicae* and *A. thaliana*

Establishing a homozygous line of *A. thaliana* plants expressing an ankyrin like-GFP transgenic protein (CS84731; Cutler *et al*., 1999) allows the observation of the interactions of *P. brassicae* with the host cell nucleus (Figure 3.7). The sequence of root hair penetration begins with *P. brassicae* zoospores attaching to the outer surface of root hairs and epidermal cells, especially epidermal cells near the root tip and root extending zone (Figure 3.7). Occasionally, multiple zoospores attach to the outer surface of a single root hair (Figure 3.7). Confocal microscopy of inoculated plants revealed cytoplasmic streaming directed to the penetration site at the onset of observation. Following this, the host nucleus responded to infection and migrated to the penetration site (Figure 3.8). In control samples, the nucleus was consistently located within the root hair, remaining sedentary, approximately 30 µm and 70 µm from the tip in young and maturing root hairs, respectively (Figure 3.7 A, Figure 3.8 A, Figure 3.9 A).

Under extended incubation, root hair growth did not occur in the mock inoculated control plants (Figure 3.8). *P. brassicae* breaches the cell wall of root hairs after approximately 120 min, after this time the early-stage plasmodia occupy the intracellular space (Figure 3.8). Concurrent with *P. brassicae* to breaching the cell wall, the host nucleus could be seen translocating within the cell, in a helical fashion, from a site distant from the penetration site to its location nearby the penetration site upon penetration by the pathogen (Figure 3.8). After penetration occurred and infection established, nuclei in infected cells tended to situate either at the base of infected root hairs where they branch away from the root, or they situated in the part of the cell aligned with the root itself (Figure 3.9). Following extended incubation of *P. brassicae*-inoculated *A. thaliana* plants on MS media, observation of samples indicated that the primary plasmodia were located near the host nucleus 28 hpi (Figure 3.9). Following development of the primary plasmodia within the root hair, a close association between the primary plasmodia and host cell nucleus in both

epidermal cells and root hairs could be seen at 72 hpi (Figure 3.9 C). Nile red stained plasmodia could be seen entirely surrounding the host nucleus (Figure 3.9). In infected cells at 72 hpi the host nuclei were larger in size compared to the control when imaged so that the focal plane of the fluorescence was at its maximum spatial extent (Figure 3.9).

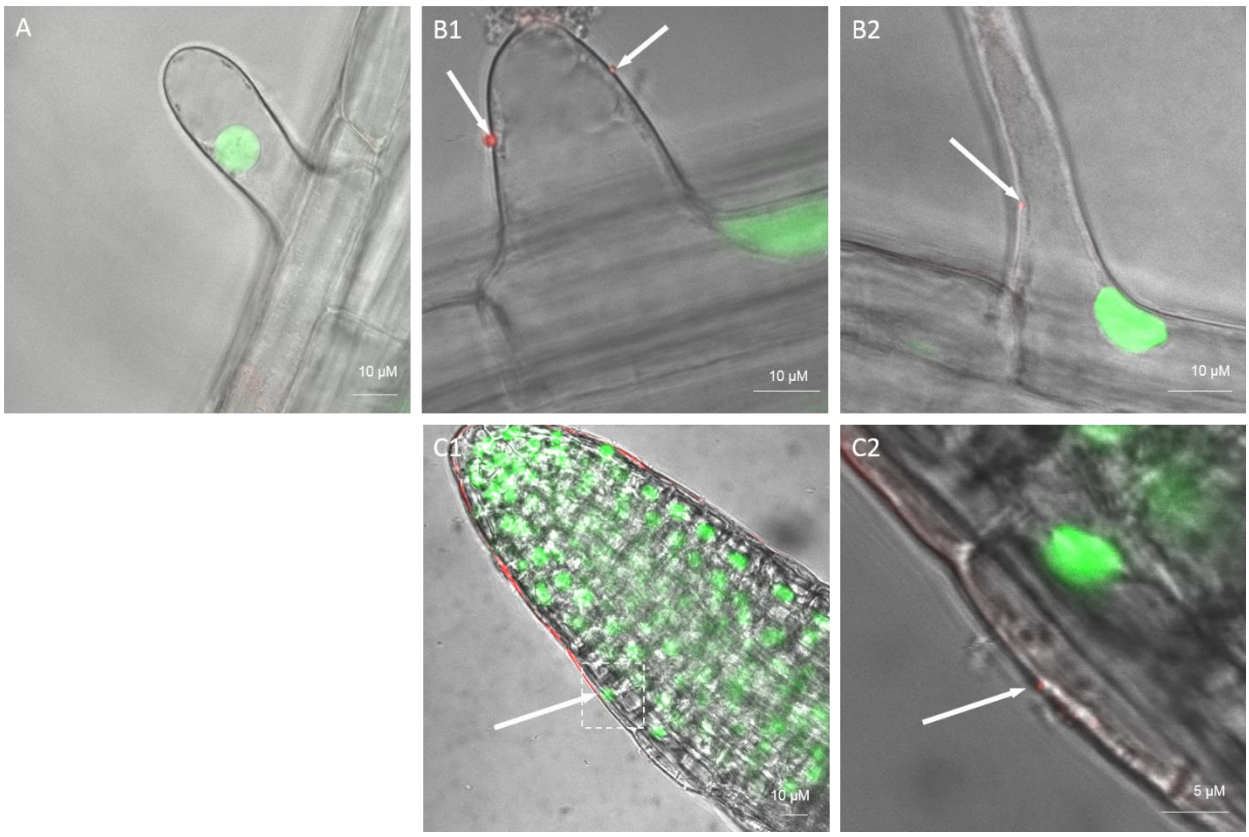

Figure 3.9 Attachment of *P. brassicae* zoospores to the cell wall of *A. thaliana* root hairs and epidermal cells at 24 hpi. There is no Nile red fluorescence signal detected in the control (A). On *P. brassicae*-inoculated *A. thaliana* roots, zoospores indicated by arrows may attach to the base or near the tip of root hairs (B1 and B2). Zoospore attachment to an epidermal cell near the root extending zone can be seen in (C1 and C2).

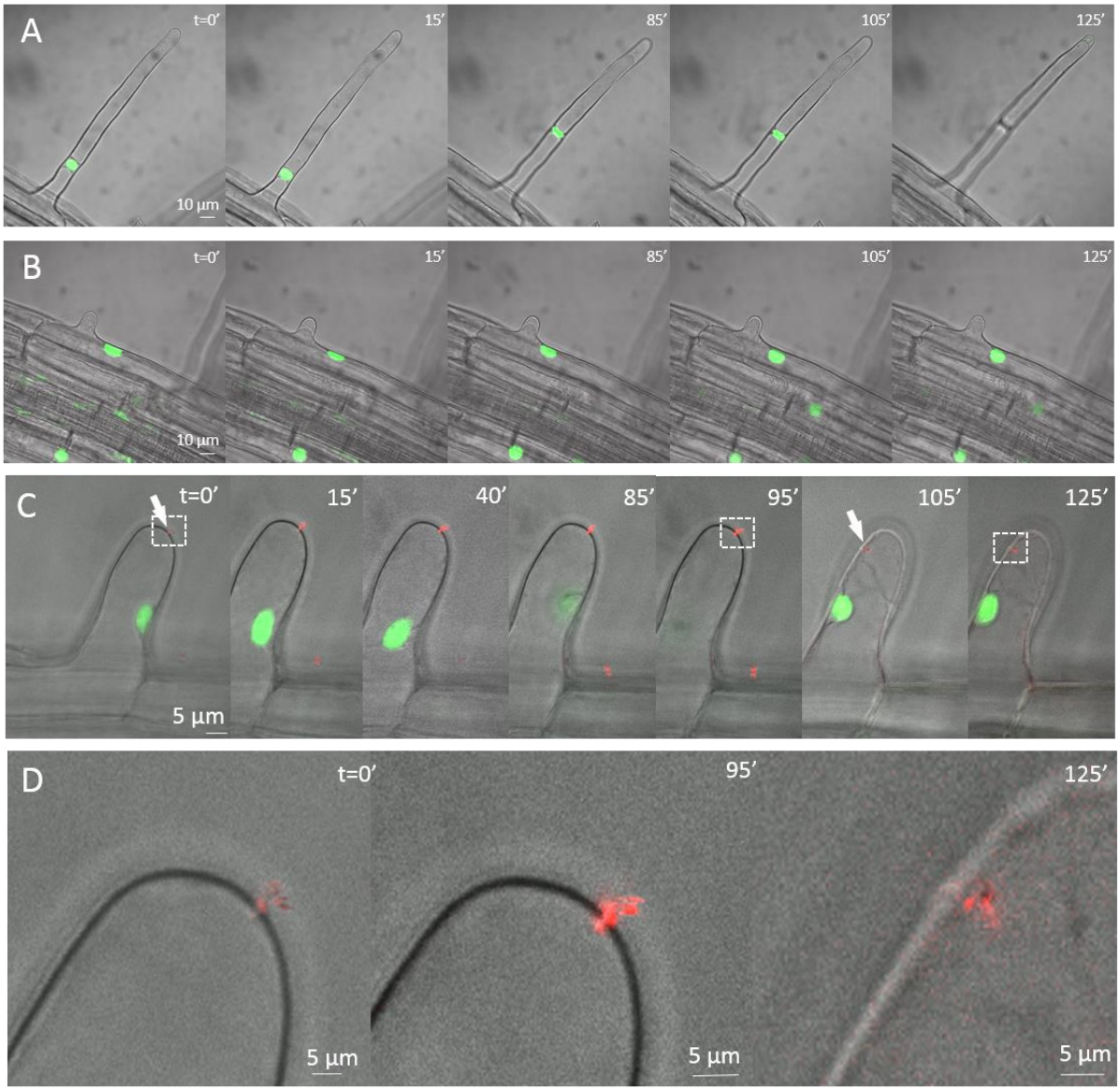

Figure 3.10 *P. brassicae* zoospore penetration of an *A. thaliana* root hair. In the mock inoculated control, the plant nucleus remains approximately 70 µm from the tip of the elongated root hair, but the root hair does not grow under extended observation (A). In the non-elongated control, the nucleus situates at the base of the root hair, but the root hair does not grow (B). In an inoculated plant, the progression of penetration over a two hour period can be seen, while the host nucleus can be seen moving to the penetration site as time progresses (C). Images of interest highlighting stages where the bulk of Nile red fluorescence occurs outside of the root hair, on both sides of the root hair cell wall, and when the pathogen is entirely inside the host cell are highlighted in (D).

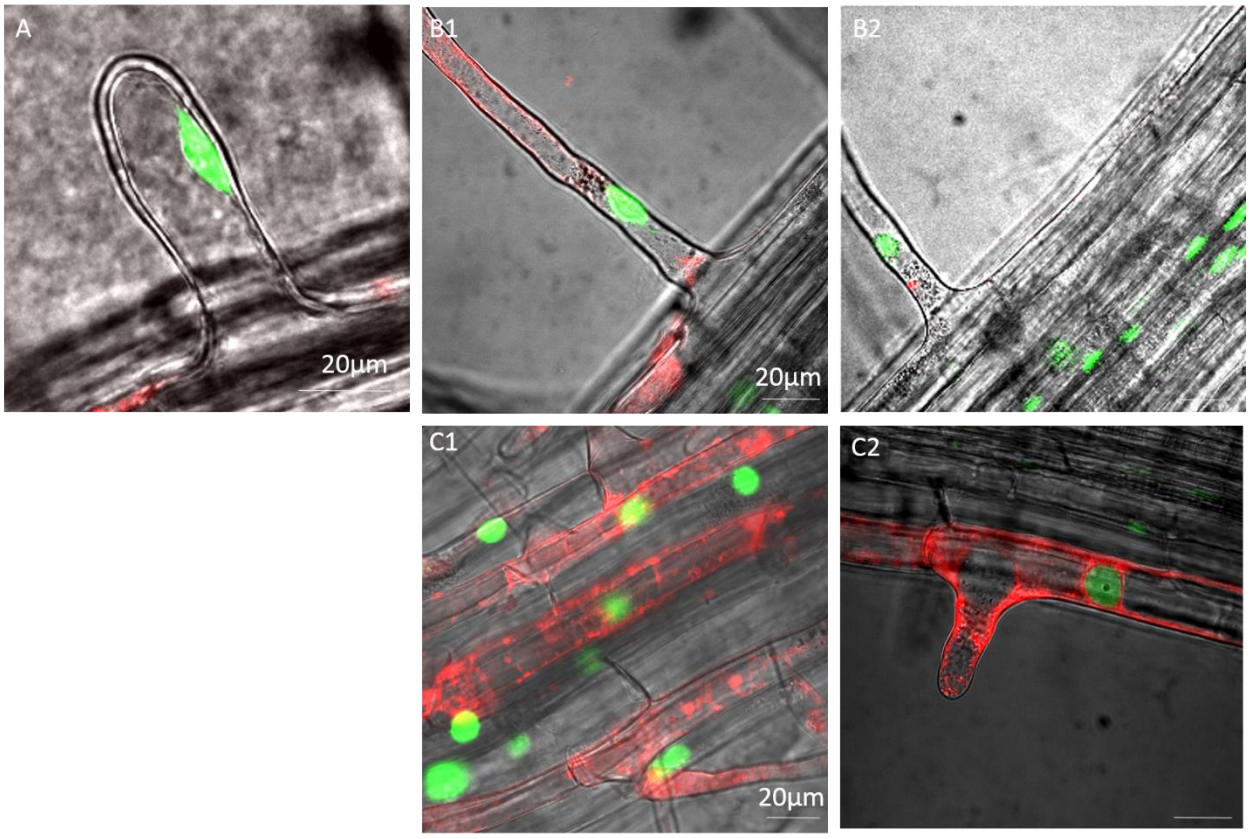

Figure 3.11 *P. brassicae* primary plasmodia association with the host cell nucleus. The control has no Nile red fluorescence, while GFP labels the nucleus (CS 84731, Cutler *et al*., 2000) (A). Plasmodia were located near the host nucleus 28 hpi (B) As they aged, a close association could be seen between plasmodia and the host nucleus 72 hpi (C). The excitation wavelength in the photo in (A), in (B1), and in (C1 and C2) were taken using 543 nm excitation for Nile red.

A. thaliana plants expressing GFP fusion to γ-TIP and δ-TIP indicating the tonoplast membrane (CS16257, Nelson *et al*., 2007; CS84727, Cutler *et al*., 2000) were inoculated with *P. brassicae* to observe the dynamics of the vacuole membrane upon infection. When *P. brassicae*-infected *A. thaliana* plants expressing the γ-TIP GFP fusion were stained with Nile red, small vacuole-derived compartments encasing *P. brassicae* lipid droplets could be seen as early as 3 hpi, and continued to be observable until between 8 and 16 hpi (Figure 3.10). These GFP-labelled compartments, termed parasitophorous vacuoles, each had a distinguishable membrane that was disjoined from the main vacuole compared to the control (Figure 3.10). Individual parasitophorous

vacuoles appeared to coalesce until they locally clustered within the root hair lumen (Figure 3.10). Once the individual parasitophorous vacuoles were adjacent to each other, they fused producing a distinguishable early stage plasmodium eight hpi (Figure 3.10). *A. thaliana* plants expressing the GFP fusion to δ-TIP were examined 16 hpi with results similar to the results of the γ-TIP GFP fusion line. At 16 hpi, a single early stage spherical plasmodium could be seen surrounded by a vacuole-derived membrane (Figure 3.10). The GFP signal clearly labelled the intact tonoplast in the host at 16 hpi, similar to the control (Figure 3.10). Upon inoculation, the GFP labelling of the host tonoplast was lost in infected cells 3 hpi (Figure 3.10). At eight hpi after the parasitophorus vacuoles had formed, the host tonoplast again was marked with GFP and also stained with Nile red (Figure 3.10).

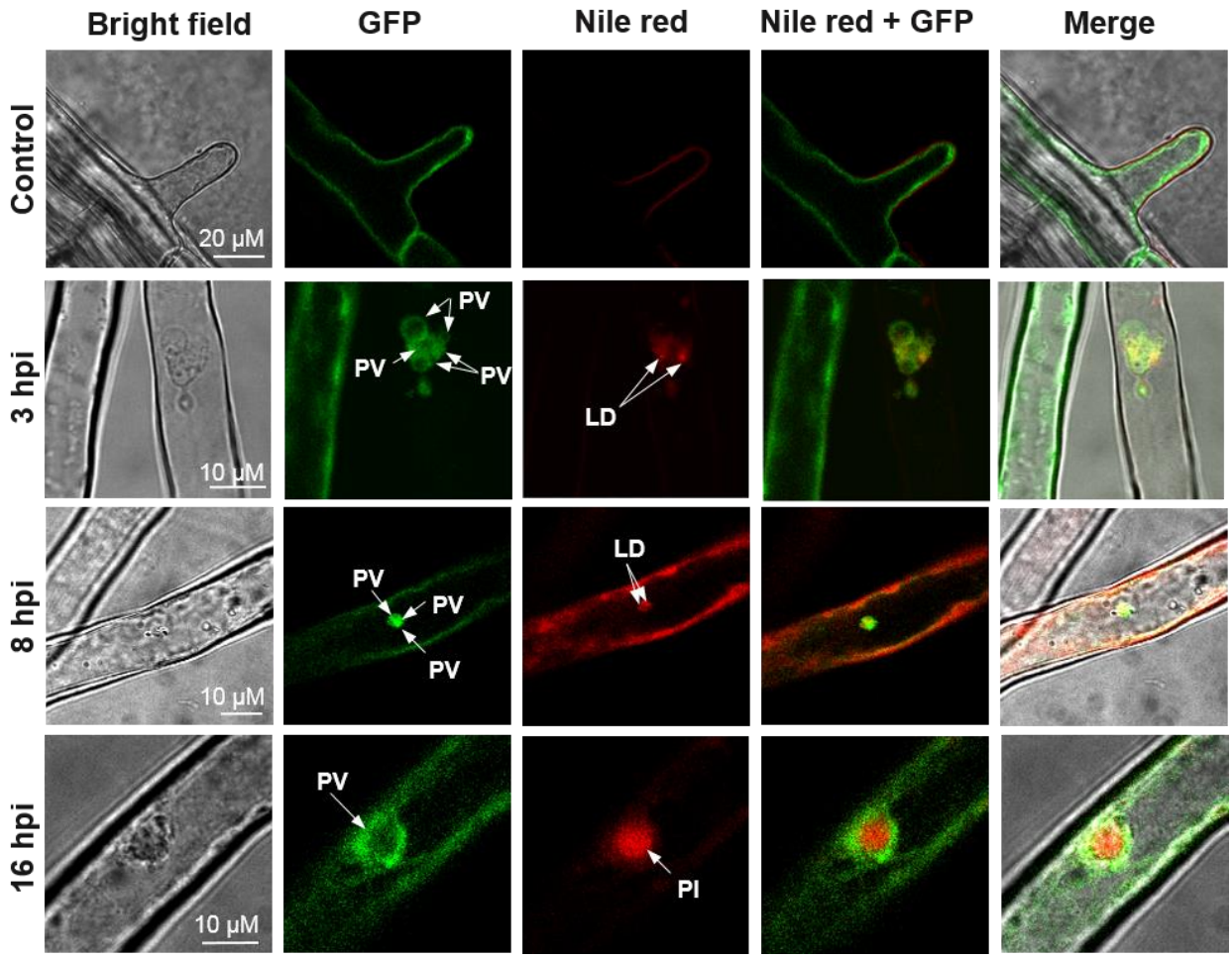

Figure 3.12 *P. brassicae* parasitophorous vacuole formation. Bright field, fluorescence and merged CLSM images indicate a vacuole-derived membrane surrounds *P. brassicae* plasmodia. The control had no Nile red fluorescence, with the main vacuole labelled with GFP [CS 16257, Nelson *et al.*, 2007; CS 84727, Cutler *et al*., 2000 (16 hpi)]. Lipid droplets (LD) stained with Nile red can be seen within individual parasitophorous vacuoles (PV) 3 hpi. As time progresses the parasitophorous vacuoles fuse to form a parasitophorus vacuole enclosing a plasmodium (Pl) as is evident at 8 and 16 hpi. The excitation wavelength used for Nile red in the photos in this figure was 543 nm.

Spherical plasmodia can be seen occupying a distinct parasitophorus vacuole at 20 hpi, while the host tonoplast does not fluoresce (Figure 3.11). At three dpi, plasmodia lost their spherical shape and increased in size while elongating in the root hair inside the host-derived parasitophorus vacuole (Figure 3.11). At 8 dai, zoosporangia could be seen forming in the root hair, or they may have matured and released their zoospores (Figure 3.11). The zoosporangium

retained the host GFP signal on its outer margin, likewise the host plant tonoplast was labelled with GFP (Figure 3.11). Finally, the empty zoosporangia membrane could be seen in root hairs indicating the end of the primary phase of the lifecycle (Figure 3.11). Host-derived GFP could be seen on the margins of the empty zoosporangia encasements (Figure 3.11).

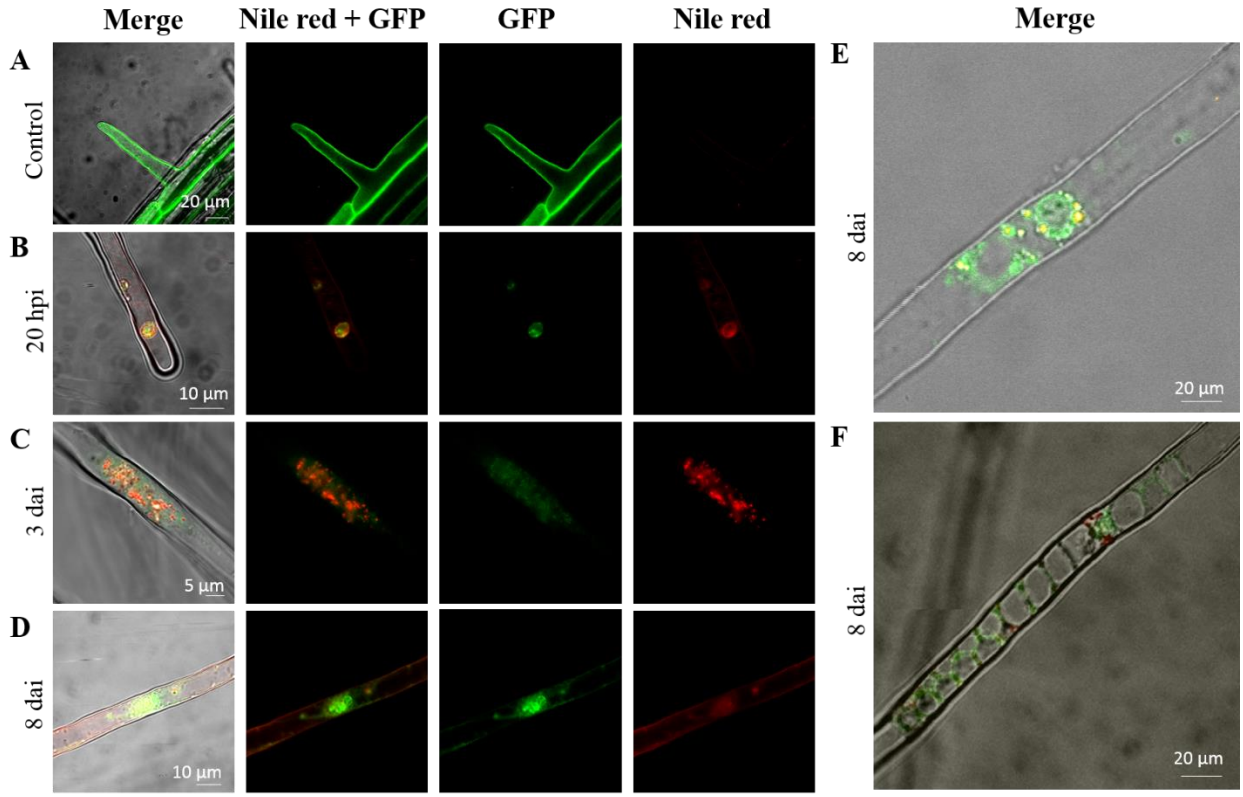

Figure 3.13 *P. brassicae* plasmodia and zoosporangia occupying a host-derived parasitophorus vacuole. Merged and fluorescence images detail *P. brassicae* labelled with Nile red and the host tonoplast labelled with GFP (CS16257, Nelson *et al.*, 2007). In the control, the host tonoplast remained intact surrounding the margin of the root hair (A). As the infection sequence progressed, the host tonoplast lost its GFP labelling, while a parasitophorus vacuole surrounding spherical plasmodia could be seen (B). 3 dai, mature plasmodia are encased in the host-derived parasitophorus vacuole (C). Maturing zoosporangia, zoospororangia releasing zoospores and evacuated zoosporangia could be seen at 8 dpi (D, E, and F). The host tonoplast was labelled with GFP while zoosporangia matured, but this signal is lost as the zoospores are released (D, E, F, Figure S8 and Figure S9). The excitation wavelength used for Nile red in the photos in this figure was 488 nm except for (B) and (D), where pictures were obtained using the 543 nm excitation wavelength.

As zoospores were released (Figure 3.12, Figure S8, Figure S9) they progressed to establish infection in the root cortex. Secondary plasmodia in the root cortex of the γ-TIP GFP fusion line

were not surrounded by a host-derived GFP labelled membrane (Figure 3.12). Likewise, the host tonoplast was not labelled with GFP (Figure 3.12). As these plants and the pathogen mature, resting spores were formed in the cortical cells of the γ-TIP GFP fusion line, again without a GFP fluorescence signature present (Figure 3.12).

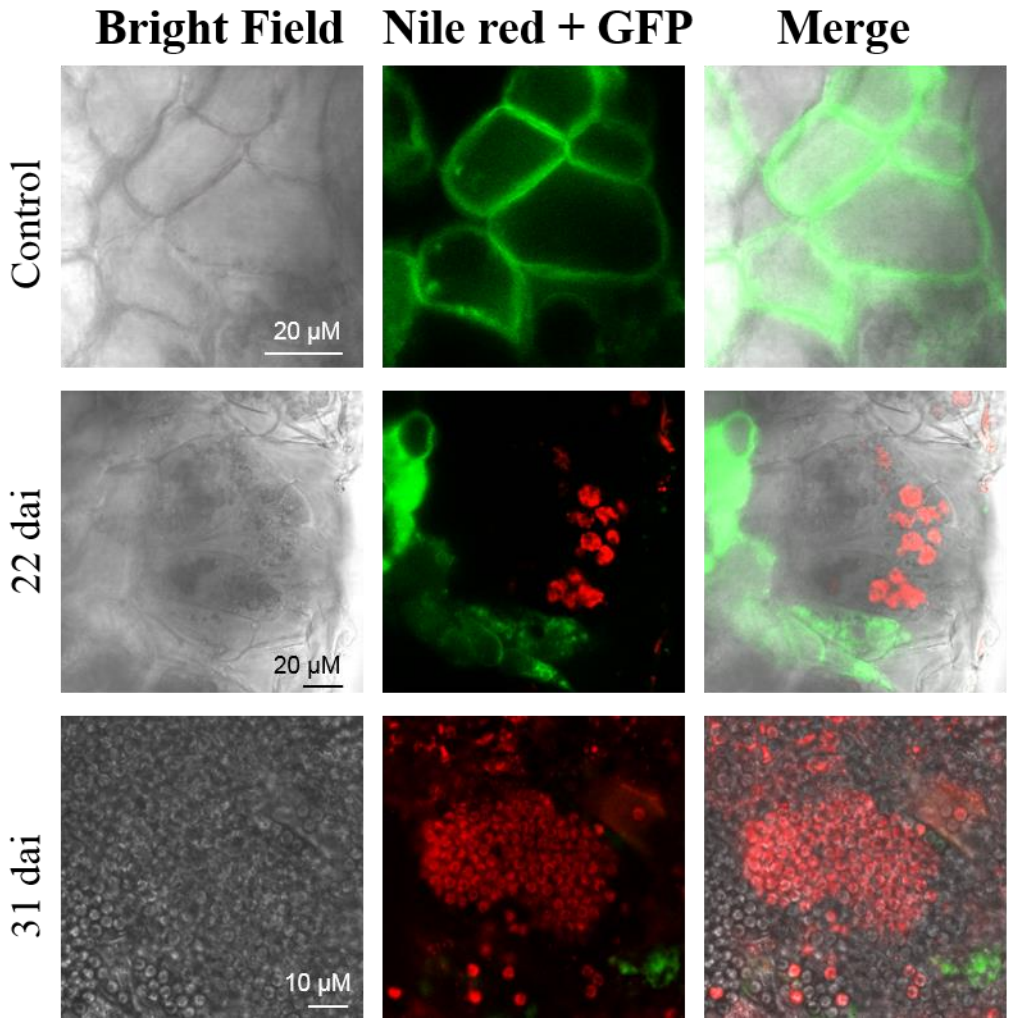

Figure 3.14 *P. brassicae* secondary plasmodia and resting spores are not encased in a parasitophous vacuole. Merged and fluorescence images detail *P. brassicae* labelled with Nile red and the host tonoplast labelled with GFP (CS 16257, Nelson *et al.*, 2007). In the control, the host tonoplast remained intact surrounding the margin of the cortical cell. In infected cells, the GFP signal was not present when secondary plasmodia or resting spores were present at 22 and 31 dai, respectively.

A. thaliana plants expressing GFP fusions to the C and N terminus of fimbrin 1 actin binding domain (GFP-ABD2-GFP) allow live cell filamentous actin dynamics to be observed using CLSM (Wang et al., 2004). Inoculation of these plants with *P. brassicae* resting spores revealed actin filament disassembly in infected cells (Figure 3.13). GFP-labelled fimbrin remained in a diffuse cytosolic state in infected cells, failing to organize into filaments in cells containing early spherical plasmodia and mature plasmodia (Figure 3.13).

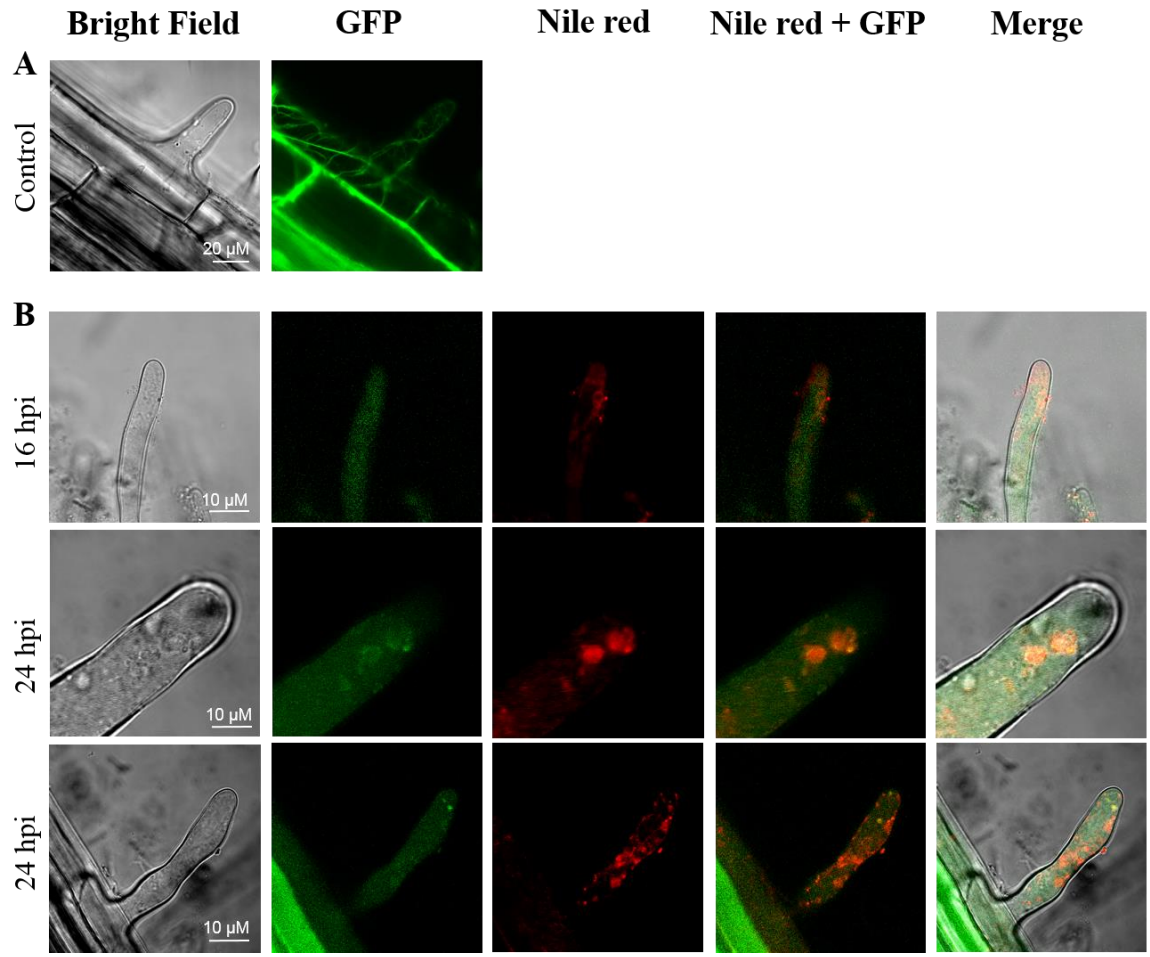

Figure 3.15 Disorganization of actin filaments in root cells of host *A. thaliana* plants upon *P. brassicae* infection. In the non-inoculated control, actin filaments labelled with GFP-ABD2-GFP form filamentous strands (A). Upon infection and subsequent pathogen development, *P. brassicae* primary plasmodia stained with Nile red were associated with host actin filament degradation (B).

4.0 DISCUSSION

The goal of the research performed was to contribute to understanding the cellular basis of host-pathogen interaction between *Arabidopsis thaliana* and *Plasmodiophora brassicae*. Specifically, my work developed a suitable stain for the *in-* and *ex-planta* life stages of *P. brassicae* which allowed *in vivo* examination of *P. brassicae* life stages using fluorescence microscopy. Through examining the cellular basis of infection and disease progression, my work elucidated and improved scientific understanding pertaining to the *P. brassicae* infection process and lifecycle. Furthermore, this work increased scientific understanding of the host nuclear localization in response to infection by *P. brassicae* and also documented the first account of parasitophorus vacuole formation during microbial pathogenesis in plants. In the broad sense, this investigation increases the understanding of host-pathogen interaction on a cellular level, especially the model of biotrophic protist interaction with a host.

4.1 An *In-* and *Ex-* planta Labelling Technique for *Plasmodiophora brassicae*

A large hindrance to previous research on clubroot disease was the lack of a suitable fluorophore for the observation of *P. brassicae* in its host. Many researchers have visualized the host-pathogen interaction using stains such as Aniline blue, Methylene blue, or FAA Phloxine (Sharma *et al*., 2011; Luo *et al*., 2013). However, these procedures were toxic to the host plant, leaving live cell imaging of the pathogen and plant-pathogen interaction impossible. I developed a *P. brassicae* positive staining technique by testing stains using a *B. napus* callus cell culture infected with *P. brassicae* as a screening platform. This provided advantages including aseptic condition, a continuous temporal availability of materials, ease of testing multiple stains, and relative ease of preparing samples for observation. Ultimately, Nile red was chosen as the best fluorophore for labelling *P. brassicae*.

P. brassicae resting spores, primary and secondary plasmodia, and zoosporangia are known to contain lipid droplets (Mithen and Magrath, 1992). Authors have also found myxamoebae containing lipid droplets, although the lipid droplets are inconsistent, and solitary when present (Mithen and Magrath, 1992; Kobelt *et al.*, 2000). After my failure of imaging polar lipids using FM4-64, and little success with Nile red, the hypothesis arose that by selectively marking lipid droplets observation of *P. brassicae* would be possible. Furthermore, using an unobtrusive approach to staining employing a non-toxic stain could permit live-cell imaging. This led to the testing of the 488 nm excitation wavelength for Nile red (Molecular Probes, Eugene, OR) of the *P. brassicae* infected callus culture.

Observation of *P. brassicae* infected callus stained using the probe FM4-64 revealed that the callus cells were able to up take FM4-64. Consistent with the literature, FM4-64 did not permeate the intact plasma membrane of the host cell (Fischer-Parton *et al*., 2000). Instead, FM4-64 was brought in by the host cell through the endocytotic pathway from the extracellular environment to intracellular membranes derived from the plasma membrane. Results indicate that in infected callus cells, FM4-64 positively stained membranes surrounding the pathogen in the cell, but labelling of *P. brassicae* itself did not occur.

Some callus cells that were prepared for observation using FM4-64 were damaged during the preparation process such that cell integrity became compromised, allowing FM4-64 leakage into the cytosol and indiscriminate membrane labelling occurring within those cells. In these cases, FM4-64 exclusively labelled cell membranes within the host cytoplasm including membranes associated with the endoplasmic reticulum, vesicles, as well as membranes enclosing *P. brassicae* plasmodia and zoosporangia, which formed the barrier between these *P. brassicae* life stages and the host cell cytoplasm. Cytoplasmic streaming within plasmodia, in cells that had FM4-64 leakage

into the cell indicated that during the period of observation (< 3 hr) the concentration of FM4-64 was non-toxic to *P. brassicae*. Callus cells that were extensively perturbed often had cytosol contents leak into the extracellular environment. This cellular leakage included *P. brassicae* zoosporangia. Although not indicative of the *in vivo* condition, the perturbed samples did provide the advantage of observing exposed zoosporangia. Observation of exposed zoosporangia indicated that FM4-64 labelled the outer membrane of zoosporangia. These zoosporangia were not fully mature as a membrane enclosed individual zoospores, thereby restricting their spatial movement. Ultimately, it was concluded that while FM4-64 staining of *P. brassicae* infected cells could provide insight into pathogen biology, it was not the appropriate stain to employ to meet the targets of the research.

Staining *P. brassicae*-infected *B. napus* callus cells with Nile red provided the ability to observe *P. brassicae* in the intracellular environment. Viewing Nile red fluorescence at excitation wavelengths of 543 nm from a Helium-Neon laser (to view phospholipids) and 488 nm from an Argon laser (to view triglycerides) indicated Nile red stained *P. brassicae* in high contrast to the host cell. Initially, observation of stained samples using the 543 nm excitation of Nile red viewed through a 650 nm long pass filter showed plasmodia and zoosporangia to stain extensively, while only the host cell plasma membrane fluoresced. This became problematic as it produced many false positives when viewing what were later determined to be dead cells (not shown), and labelling of infected host cell plasma membrane. Hence, the 488 nm excitation source was used targeting triglycerides stored within the *P. brassicae* cytoplasm for microscopy. Viewing Nile red-stained samples using the 488 nm excitation through a 585 nm to 615 nm band pass filter indicated lipid droplets in all *P. brassicae* life stages could be seen with no fluorescence from the host cell once the microscope parameters were optimized. Thus, using the 488 nm excitation wavelength was a

superior option to the 543 nm excitation wavelength when observing *P. brassicae* in high contrast to the host cell.

Nile red staining, using an excitation wavelength of 488 nm, confirmed the previously reported lifecycle stages that were most recently reviewed by Kageyama and Asano (2009). As well as producing the first time-series photographs of a zoospore penetrating the root hair cell wall. Nile red staining proved to be especially useful for tracking the earliest stages of infection and for the imaging of small spherical plasmodia 24 hpi that had previously been noted by Kunkle (1918), but which have otherwise been absent in the literature, with plasmodia being photographed in their more mature stage as a large, amoeba–like cytoplasmic mass.

A fluorophore capable of staining *P. brassicae in-* and *ex-planta* is a desired tool for studying clubroot disease (Schuller and Ludwig-Müller, 2016). By staining lipid droplets unique to *P. brassicae* with Nile red, it is possible to discreetly observe the pathogen outside of the host cell and in high contrast to the host cell during infection. Other researchers have used traditional stains and fluorescence probes to observe *P. bassicae* interaction with its host, but have struggled to overcome some barriers that using Nile red can surmount. A procedure that can differentially stain a pathogen from the host cell is a valuable tool for investigation, although this is difficult to achieve (Schuller and Ludwig-Müller, 2016). Some researchers have developed staining procedures that can either stain *P. brassicae in-* or *ex-planta*, but never both. Likewise, a stain and staining method that permits live cell investigation has not been developed (Schuller and Ludwig-Müller, 2016).

Fixed tissue staining protocols rely on imaging thin-sections of static, non-living cells. Dickson (1920) developed a dual staining technique using Magdala red and Lichtgrün, staining *P. brassicae* spores and plasmodia red, while the host tissue is differentially stained green in fixed

tissues. Researchers who developed the triple staining method to study resin-embedded sections of host tissue infected with *P. brassicae* prioritized differentiation between the parasite and host cytoplasm, and to detect cellulose, lipids, starch, membranes, nucleoli, and chromosomes (Humphrey and Pittman, 1974; Buczacki and Moxham, 1979). This technique was used to study the genesis of the resting spore wall and aspects of nuclear division in *P. brassicae.* Both the dual staining and the triple staining method provided the ability to distinguish *P. brassicae* plasmodium cytoplasm. The dual staining method stained plasmodia red against a green host cytoplasm. Using the triple staining method, plasmodia are distinguished from the host as they took a greenish tinge when examined under light microscope, due being replete with lipid droplets (Buczacki and Moxham, 1979).

Staining protocols used to view the *P. brassicae*-host interaction in whole plant roots by light microscope were successful in staining *P. brassicae,* although not in a live cell context (Sharma *et al.*, 2011a; Zhao *et al.*, 2017). The technique used by Sharma *et al.* (2011a), stained with Methylene blue to stain pathogen structures deep blue against the light-blue stained host cytoplasm. Zhao *et al.* (2017) used Trypan blue to stain *P. brassicae* infected *A. thaliana* roots during early infection. While both of these procedures allowed imaging by light microscope, presented figures often displayed dead cells with evident vacuolization, cytoplasmic aggregation, and crinkled cell walls which are not indicative of the natural state of pathogen and host. This is especially evident in the Zhao *et al*. (2017) work as Trypan blue cannot stain a living cell, hence to image the cells one would have to look at *P. brassicae* existing in an already dead cell. Furthermore, host tissues were stained in the background leaving a *bona fide* pathogen-specific dye a desired tool.

Fluorescence probes that have been used to stain *P. brassicae* have only been employed to observe resting spores, their viability, and germination (Takahashi and Yamaguchi, 1988; Niwa *et al.*, 2008; Jäschke *et al.*, 2010). A double fluorescence staining approach using ethidium bromide and Calcofluor white to differentially stain viable and inviable spores was based on the staining of the cytoplasm, as inviable resting spores had red fluorescence in their cytoplasm (Takahashi and Yamaguchi, 1988). Niwa *et al.* (2008), and Jäschke *et al.* (2010) applied DAPI, a toxic probe localizing to chromatin, to *ex planta* resting spores. Germinated resting spores did not show fluorescence, hence the germination rate could be assessed. DAPI was not applied to *P. brassicae in planta*. Nile red is superior to these fluorescence probes for observing *P. brassicae in planta*, with *ex planta* staining having competing advantages with the double fluorescence probe and DAPI techniques.

Similar to the results of Littlefield *et al.* (1997 and 1998) who used Nile red to stain lipid droplets in the plasmodiophorid *Polymyxea graminis* in wheat and sorghum roots, lipid droplets could be seen in *P. brassicae* when stained with Nile red. Littlefield *et al.* (1997 and 1998) used fluorescence microscopy to study plasmodia, sporosori, and resting spores (Littlefield *et al.* 1997, Littlefield *et al.*, 1998). In both studies, lipid droplets fluoresced in stark contrast to the host cell under excitation from a 514 nm laser. Littlefield *et al*. were able to track the development of resting spores from sporosori; however, they did not apply this technique to samples under extended observation. My study revealed Nile red to work satisfactorily under extended observation of samples. Furthermore, I was able to stain *P. brassicae* lipid droplets in much less time, with a less concentrated Nile red solution than Littlefield *et al.* (1997 and 1998), who stained their samples overnight with a 3 mM solution of Nile red.

Nile red is a near ideal lysochrome for labelling intracellular lipid droplets (Greenspan *et al*., 1985). Nile red staining of *P. brassicae* during infection overcomes the barriers present in context of its intracellular location in the host cell. Nile red must penetrate through multiple obstacles including the host cell wall, host plasma membrane, a membrane derived from the host vacuole membrane, the pathogen plasma membrane and the micelle monolayer before binding to lipid. Nile red is strongly fluorescent in a hydrophobic environment and it does not destroy the lipid structure it labels (Greenspan *et al*., 1985). Nile red serves as a suitable probe for observing pathogen morphologies in a live cell context. Using Nile red I was able to track resting spore germination until attachment to and penetration through the cell wall. Likewise, Nile red is able to label the pathogen inside the host as soon as infection occurs. Subsequently, *P. brassicae* life stages can be seen during the epidermal and cortical cell infections *in vivo*. Nile red staining is a suitable technique for visualizing the previously cryptic ontogeny of *P. brassicae*.

4.2 Infection Processes and *P. brassicae* Proliferation in Host *A. thaliana*

I set out to further understand and verified existing information pertaining to infection of epidermal and cortical cells, including *P. brassicae* transmission and proliferation within host tissues using the Nile red staining protocol developed in the first phase of the research program. Using *A. thaliana* plants grown on 1/2 MS media and inoculated with *P. brassicae* and *A. thaliana* plants grown in *P. brassicae* infested soil allowed for the observation of the immediate infection and subsequent pathogen development within host tissues. Correspondingly, *P. brassicae* was viewed from the resting spore stage through initial infection, and subsequently, through to resting spore development within the root cortex.

Using Nile red to observe samples inoculated with *P. brassicae* resting spores, the real time penetration of the host cell wall was observed. Following resting spore germination, zoospore

migration and its attachment to the host cell wall was observed. Consistent with the findings of Aist and Williams (1971), zoospore encystment was consistently observed 24 hpi. Following encystment, penetration of the host root hair occurs. Tracking the penetration of zoospores through the host cell wall also indicated that multiple zoospores could attach to the same root hair and attempt to penetrate it to establish infection within the host. Real time observation of root hair penetration indicated that penetration took at least two hours to occur. During this window of observation, Nile red-stained *P. brassicae* lipid droplets could be seen crossing the barrier of the host cell wall. Initially, *P. brassicae* was seen stained outside of the host cell wall. During penetration, *P. brassicae* slowly breached the cell wall and could be observed slowly occupying the host intracellular environment with an ever increasing amount of fluorescence occurring within the root hair immediately adjacent to the host cell wall, while the fluorescence outside of the cell wall decreasing during the same time interval. The accumulation of *P. brassicae* cytoplasm inside of the root hair occurred until the bulk of the cytoplasm was located inside the host intracellular environment, at which point *P. brassicae* rapidly completed penetration and was located totally within the host cell. After penetrating the host cell, *P. brassicae* could be seen near the penetration site; however, it did not appear to remain directly near the host penetration site.

Coincident with the penetration of the host root hair, host cytoplasmic streaming to the penetration site occurred. Cell wall appositions are known to accumulate at the point of pathogen penetration as an active, first line response to halt pathogen progress. Occasionally zoospores that were penetrating the host wall were defeated by the cell wall apposition and their penetration was halted with no fluorescence signature occurring within the intracellular environment under extended incubation. Conversely, the attempted halting of penetration was defeated by *P. brassicae* as it was successful in breaching cell walls where papillae were accumulating. While

cell wall appositions were commonly seen, usually the pathogen was successful in breaching the cell wall before the apposition could fulfill its function.

Unfortunately I was unable to definitively track the penetration of the root cortex by *P. brassicae* life stages, using the Nile red staining protocol. However, convincing evidence that the initial infection by resting spores occurs only in the root epidermis was obtained, as no primary plasmodia were seen in the root cortex during observation of the primary infection. This questions the assertion that primary zoospores may penetrate the root cortex and establish infection in the root cortex as a component of the primary infection (Mithen and Magrath 1992; and Kobelt *et al.* 2000), instead indicating that primary zoospores are not capable of penetrating the root cortex as was initially suggested (Dobson and Gabrielson, 1983). Likewise, a mobile myxameboid phase navigating to the root cortex through cell wall breaks has been reported (Mithen and Magrath 1992; and Kobelt *et al.* 2000). I observed no evidence of this occurring. *P. brassicae* life stages were only seen in the root cortex 20 dpi. During the 20 dpi observations, secondary zoospores were infrequently seen swimming in root cortical cells, lending credence to secondary zoospores migrating to the root cortex to produce secondary infection. Based upon these observations, I agree with the suggestion that the production of zoospores in the root epidermis functions to allow zoospores to penetrate through to the root cortex and establish the secondary infection (Aist and Williams 1971). However, evidence was not observed to determine if secondary zoospores use the same mechanism to breach cortical cell walls as the primary zoospores use to breach the epidermal cell walls.

Following the primary infection penetration, plasmodia and zoosporangia were only observed in the *A. thaliana* root epidermis, while there was no evidence of transmission to the root cortex. Following analysis of the primary infection, observation of the secondary infection

provided positive identification of secondary plasmodia and resting spores occupying cells of the root cortex (Figure 4.1).

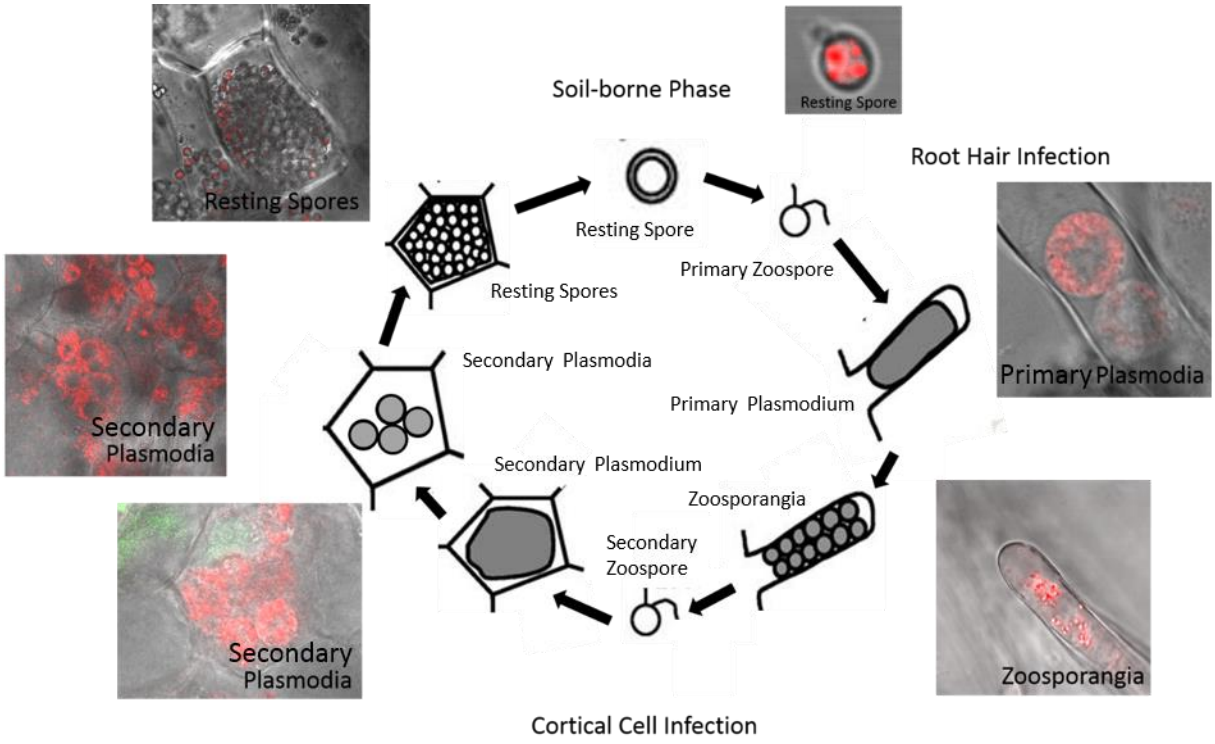

Figure 4.1 The lifecycle of *P. brassicae* imaged with Nile red. The pathogen is present as a soil borne resting spore, following germination it becomes a zoospore. Primary infection begins with penetration of the root hair producing primary plasmodia, and subsequently, zoosporangia. The secondary zoospore infects the cortex producing secondary plasmodia, that cleave prior to resting spore formation. The lifecycle concludes with the production of resting spores in cells of the root cortex. Modified from Kageyama and Asano (2009).

Secondary plasmodia were extensive in the cells of the root cortex of plants grown in *P. brassicae* infested soil. Immature plasmodia are sedentary while occupying the host cell. After time has progressed and plasmodia mature, they segregate before forming resting spores. Obviously, secondary plasmodia cleavage and resting spore production exist as a mechanism of pathogen proliferation within the host tissue, as the amount of spores would greatly increase due to extensive pathogen reproduction. This is an important fact to consider with respect to land management for clubroot disease. In Manitoba, the current management suggestion is to use crop

rotation including cultivars of canola with quantitative resistance to *P. brassicae* (MAFRD, 2016). However, those plants with quantitative resistance are still susceptible to infection especially under high inoculum density levels in soils where multiple pathotypes are found. Hence, any *P. brassicae* zoospores that infect a canola plant and successfully complete their lifecycle would in turn allow the soil spore population to persist. Furthermore, those spores that complete their lifecycle in a resistant plant could also respond to the selection pressure that is the resistance mechanism deployed against *P. brassicae*. Hence, continuing to use plants with quantitative resistance can contribute to inoculum increase in the soil, in turn making future management more troublesome. In cases where multiple pathotypes are present, a host selection pressure may be placed on an avirulent pathotype leading to a virulent pathotype becomming more common in the soil.

In conclusion, this part of the research program allowed for confirmation of the time required for zoospores to mechanically breach the epidermal cell wall. Furthermore this study confirmed the expected life-stages occurring in the root cortex. However, the ability to track secondary zoospores from the epidermis to the root cortex is still a desired target using Nile red staining.

4.3 *A. thaliana* Host Cellular Dynamics Upon *P. brassicae* Infection

Using the Nile red staining technique to observe *A. thaliana* plants expressing GFP-tagged cellular components infected with *P. brassicae* allowed for discreet live cell observation of the cellular interactions occurring during pathogenesis. In particular, the host cellular dynamics of the nucleus, tonoplast, and actin were examined in response to infection. I was able to study the movement of the host nucleus upon infection and during early stages of the root hair infection. Furthermore, I was able to observe the involvement of the host tonoplast during the epidermal and

cortical cell infections. Lastly, I was able to investigate the involvement of actin filaments during establishment of the primary infection.

Nuclear movement and positioning is an active process occurring in all living cells. Nuclear movement may occur during developmental processes or in response to an abiotic signal or during plant-microbe interactions. Nucleocytoplasmic trafficking plays an essential role in plant immunity, acting as the organizational centre of microbial recognition (Deslandes and Rivas, 2011). Stimulus-induced nuclear translocation constitutes spatial restriction of plant defense regulators by the nuclear envelope and an important level of defense-associated gene regulation (Heath *et al.*, 1997). Mutation in critical components of the nuclear envelope including nucleoporins, importins, or Ran-GTP elements impedes resistance signalling in the host (Deslandes and Rivas, 2011). Using transgenic *A. thaliana* plants expressing GFP localized to the nucleus in combination with Nile red allowed for the observation of host nuclear dynamics upon *P. brassicae* infection.

Nuclear translocation has been described in plant-microbe interactions, especially during nodule formation in leguminous plants, during establishment of intracellular symbiotic fungi, and during pathogenesis of oomycete and fungal plant pathogens (Deslandes and Rivas, 2011; Heath *et al.*, 1997; Sieberer and Emons, 2000; Genre *et al.*, 2005; Griffis *et al.*, 2014). During nodule formation of the mutualistic plant-microbe interaction between rhizobia and the legume host, the nucleus is translocated from a random position within the root hair to the expanding tip of the root hair (Sieberer and Emons, 2000). As the root hair tip swells, the nucleus sits at the base of the swelling until the swelling associated growth is 20 mm in size, at which point the host nucleus occupies the swollen tip (Sieberer and Emons, 2000). After occupation, the nucleus maintains a

position 30 µm from the tip. Once nodulation has ceased, the nucleus returns to a random position in the root hair shank (Sieberer and Emons, 2000).

In plant-oomycete pathogen interactions, such as potato (*Solanum tuberosum*) and *Phytophthora infestans*, or tobacco (*Nicotiana benthamiana*) and *Phytophthora nicotianae*, or *A. thaliana* and *Phytophthora palmivora*, nuclear translocation and dynamics depend on the compatibility of the host-pathogen interaction (Guest, 1986; Freytag *et al.*, 1994; Daniel and Guest, 2006; Griffis *et al.*, 2014). In resistant host plants, such as *S. tuberosum* inoculated with *Phytophthora infestans*, the host nucleus migration to the pathogen contact site occurs within three hpi, followed by cytoplasmic aggregation and localized cell wall strengthening and thickening (Daniel and Guest, 2006; Freytag *et al.*, 1994). Following successful defeat of the penetration attempt, the nucleus moves elsewhere in the cell away from the area of penetration. If the pathogen successfully penetrates the resistant host cell and haustoria are produced, nuclear and cytoplasmic aggregation surround the haustoria followed by triggering of the hypersensitive response. In susceptible host plants, such as *A. thaliana* inoculated with *Phytophthora palmivora*, the host nucleus does not initially translocate to the penetration site following inoculation; however 12 hpi, nuclear migration and cytoplasmic aggregation occur (Daniel and Guest, 2006). In *N. benthamiana* inoculated with *Phytophthora nicotianae*, infected cell autonomous nuclear migration was not observed; however, at 24 hpi neighbouring cell nuclei could be seen positioning nearby the infected cell (Guest, 1986). As the pathogen breaches the cell wall and forms haustoria, nuclear and cytoplasmic association may occur, though this is not a requirement for pathogenesis (Griffis *et al.*, 2014).

Fungal plant pathogen attack consistently results in nuclear translocation to the penetration site regardless of host compatibility (Heath *et al.*, 1997). Working with resistant and susceptible

cowpea (*Vigna unguiculata*) plants challenged with the cowpea rust fungus *Uromyces vignae*, it has been demonstrated that, similar to nuclear translocation during nodule formation in root hairs, the nucleus translocates to the penetration site (Heath *el al.* 1997). In a compatible interaction, the host nucleus migrates to the region underneath the appressorium where the nucleus remains for one hour. If a papilla forms at the fungal penetration site, the host nucleus remains near the attempted infection site until the papilla is no longer expanding. However, if the more likely penetration occurs, the nucleus migrates away from the penetration location, coincident with the time that the penetration peg contacts the host plasma membrane (Heath *et al.*, 1997). After hyphal development and the hyphae measured 10 µm long, cytoplasmic strands focused on the hyphae and the nucleus migrated to this location. At 48 hpi, the nucleus could be seen in the center of the hyphal mass (Heath *et al.*, 1997). In resistant plants challenged with *U. vignae*, an initial nuclear migration to the penetration site followed by retreat was observed (Heath *et al.*, 1997). Following this, the nucleus failed to return to the penetration site as the hypersensitive response occurred rendering the host cell dead (Heath *et al.*, 1997). However, it could not be concluded if the lack of migration was an early indicator of the hypersensitive response or if it was due to necrosis occurring preceding triggering of nuclear migration (Heath *et al.*, 1997).

In plants that are not challenged by pathogen attack, nuclear translocation occurs in response to mechanical stimuli simulating microbial penetration. In tobacco (*N. benthamiana*) leaf epidermal cells that were sequentially perturbed using a syringe, the host nucleus could be seen sequentially translocating to the wounding points without a lag time or change in velocity (Qu and Sun, 2007). Initially the nucleus is tethered to the stimulation site by a cytoplasmic strand followed by cytoskeletal organization and nuclear migration suggesting the host nucleus is an organization centre for responding to mechanical stimuli (Qu and Sun, 2007).

It is well understood that *P. brassicae* has a strong association with the host cell nucleus during secondary plasmodium development (Ingram, 1969; Mithen and Magrath, 1992; Kobelt *et al*. 2000). In infected callus culture, secondary plasmodia were found in association with enlarged host (*B. oleracea* cv. Badger Shipper) cell nuclei and nucleoli (Ingram, 1969). *In planta*, secondary plasmodia were described to be grouped closely or clustered around the host nucleus (Mithen and Magrath, 1992; Kobelt *et al*. 2000). As pathogenesis occurs, plasmodia envelop the host nucleus and it becomes large and distorted (Mithen and Magrath, 1992). However, the relationship of the host nucleus and *P. brassicae* during the early stages of infection has not been described. This study indicated the pattern of nuclear migration to protist penetration sites and the relationship of *P. brassicae* primary plasmodia during the early stages of root hair infection. The host cell nucleus exhibits a similar pattern of movement when responding to *P. brassicae* infection compared to host nucleus response to oomycete and fungal pathogen challenge. As mechanical perturbation is detected, the host nucleus moves to the penetration site and focuses cytoplasmic streaming towards the area under the adhesorium. Following successful penetration of the pathogen, the host nucleus remains in close proximity to the developing plasmodia in the root hair, but they are not associated with it. At 72 hpi, the host nucleus is surrounded by a primary plasmodium.

Plants are sessile and are continually exposed to conditions that threaten survival and competitiveness. Hence, the balance of growth and survival are paramount to ensure reproductive success. While conditions for growth may not be ideal, plants must muster a dynamic response to stressors, such as pathogen challenge. The stressed conditions required for microscopy inhibited the growth of root hairs. However, nuclei could be seen maintaining a position consistent with what has been seen in growing root hairs (Ketelaar *et al*., 2002). During time-lapse microscopy the host nuclei are positioned 70 µm from the leading tip. However, no root hair growth was seen.

Despite the root hairs inability to grow under the conditions of microscopy the root hair itself was able to respond to pathogen penetration. This suggests that conditions for root hair growth are more strict than conditions for responding to pathogen attack.

Studying infection in *A. thaliana* plants expressing GFP localized to the tonoplast revealed the pathogen to enter individual vacuolar encasements containing early stage *P. brassicae.* In human liver tissue infected with *Plasmodium falciparum* (malaria) or *Toxoplasma gondii* (toxoplasmosis), developing sporozites occupy a tonoplast or plasma-membrane derived membrane termed the parasitophorous vacuole (Ward *et al*. 1993; Beckers *et al.*, 1994). With respect to *P. brassicae* infection, the parasitophorus vacuole describes a unique tonoplast-derived membrane bound cytoplasmic compartment within the host cell. Parasitophorus vacuoles have not been acknowledged in other intracellular plant pathogens, such as *Spongospora subterranea*, and they are distinct from structures associated with extracellular plant pathogens, *e.g*. *Blumeria gramminis*. Likewise, the membranes associated with *P. brassicae* did not have their origin determined, but were postulated to be the host tonoplast (Dekhuijzen 1978; and Mithen and Magrath, 1992). Hence my observations of the *P. brassicae* parasitophorus vacuole derived from the tonoplast furthers understanding of a previously undescribed interface of microbial pathogenesis in plants.

Parasitophorus vacuole formation occurs during root hair infection following successful penetration and occupation of the host cell, with individual *P. brassicae* primary plasmodia each being surrounded with their own individual tonoplast-derived membrane. As the pathogen matured, individual parasitophorus vacuoles containing *P. brassicae* coalesce synchronously producing a plasmodium. Other authors have also described a membrane surrounding *P. brassicae* life stages from TEM images of *P. brassicae* infected plants. Dekhuijzen (1978) observed the

pathogen fully encased within the host tonoplast, while Mithen and Magrath (1992) observed myxamoebae associated with small protrusions of host cytoplasm into the vacuole. Mithen and Magrath (1992) hypothesised that the protrusion would expand until the vacuole was full of plasmodia, although evidence supporting this was not published. Consistent with my observations, both Dekhuijzen (1978) and Mithen and Magrath (1992) observed tonoplast disruption during development of the amoeba-like pathogen structure. It is important to distinguish that these authors did not go so far as to suggest a unique tonoplast derived membrane surrounding the pathogen. However, the collective evidence suggests that *P. brassicae* is encased within a vacuole-derived compartment in the host cell.

During cortical cell infection, both secondary plasmodia and resting spores were not surrounded by a parasitophorus vacuole, despite uninfected host cells still expressing the γ-TIP-GFP. This is consistent with the observations of Mithen and Magrath (1992) who recognized that secondary plasmodia were directly associated with the host cytoplasm, without a double membrane surrounding them. Hence, from my work, and the TEM work of others, it seems likely that the parasitophorus vacuole surrounds early stage *P. brassicae* amoeba which fuse to produce plasmodia (Moxham and Buczacki, 1983; Mithen and Magrath, 1992). While my work stands alone in suggesting that the parasitophorus vacuole exists surrounding mature plasmodia and zoosporangia during the latter primary infection.

As the root hair infection establishes, it was noted that host filamentous actin degrades. Hence, the host cytoskeleton is disorganized as the parasitophorus vacuole forms, suggesting that it is dysfunctional. A similar phenomena has been observed during merozite invasion of ethrocytes during *T. gondii* infection. An indentation develops at the contact point of two cells and continues to deepen until the merozite is completely surrounded by the parasitophorous vacuole membrane

(Ward *et al*., 1993). The model of parasitophorus vacuole formation for this pathosystem describes the initial invagination of the ethrocycte lipid bilayer, concomitant with a localized restructuring of the host cell cytoskeleton (Ward *et al*., 1993). Hence, the results from my study suggest similar conditions occur during parasitophorus vacuole formation during *P. brassicae* infection when compared to *T. gondii* infection.

Utilizing Nile red staining to image *A. thaliana* plants expressing GFP labelled cellular components allowed for the live cell imaging and investigation of the role of the nucleus and tonoplast membranes during pathogenesis. The establishment of the parasitophorus vacuole is a novel mechanism of host cell infection amongst plant pathogens, especially amongst rhizarian biotrophic plant pathogens, as this mechanism is influential in describing how *P. brassicae* evades host immunity and colonizes the intracellular environment. Kobelt *et al*. (2000), and Siemens *et al*. (2006) hypothesized that upon infection, plant immune responses favour pathogen death, followed by an equilibrium between pathogen attack, finally with host defense shifted in favour to the pathogen. The establishment of host compatibility by biotrophic plant pathogens involves sophisticated mechanisms enabling pathogen suppression or evasion of the host immune response and pathogen induced manipulation of metabolism.

In fungal plant pathogens, controlled secretory activity and distinct interface layers enable pathogens to establish host compatibility (Schulze-Lefert and Panstruga, 2003). I hypothesize that it is likely the parasitophorus vacuole membrane allows the early stage *P. brassicae* primary plasmodium to avoid host detection, which may be why *P. brassicae* can establish primary infection in non-host plants. It is likely that the parasitophorus vacuole membrane must exchange proteins, nutrients, and metabolites between *P. brassicae* and the host cell. The fact that this membrane permitted Nile red to cross its boundary when staining occurred suggests that this

tonoplast-derived membrane is a site of molecular exchange. However, it is interesting that the parasitophorus vacuole encasement does not occur in the cortical cell infection.

Clubroot disease symptoms are not distinguishable by eye until the cortical cell infection has established. Obligate biotrophic pathogens must secrete effector proteins to ensure host compatibility. With respect to *P. brassicae*, this indicates that the majority of effectors or effector families that produce clubroot disease symptoms may only be synthesized and secreted to the host during the cortical cell infection. Collectively, the parasitophorus vacuole may impede effector secretion to the host. Thus, its presence would not be evolutionarily conserved or selected for, rather, there exists a greater selection pressure on effector gene function to suppress host defence and promote pathogen growth during the cortical cell infection.

4.4 Future research, directions, and considerations

While my work has led to the discovery of new phenomena and clarification of existing hypotheses, thereby increasing understanding of *P. brassicae* biology and infection strategies, it most certainly asks further questions that remain unanswered. As a reliable *in vivo* staining procedure has been pioneered that works in conjunction with fluorescence protein-tagged cellular components, the obvious extension of this is to study the relationship of *P. brassicae* with other cellular components, especially those relating to protein trafficking in the host cell. There is evidence suggesting that *P. brassicae* shares infection strategies with *P. falciparum* (malaria) and *T. gondii* (toxoplasmosis) parasites, and modification of the host cytoskeleton may be necessary for synthesis of the parasitophorus vacuole. Furthermore, the relationship of components of protein trafficking in the *P. brassicae*/host interaction should be examined as this may indicate a subversion of host protein trafficking favouring pathogen survival.

Further investigation into the establishment of the parasitophorus vacuole in *A. thaliana* plants should be completed using hosts expressing different fluorescent proteins labelling the PM and tonoplast, respectively. Obviously, *P. brassicae* must modify or breach the host PM before it encounters the tonoplast and the integrity of the PM remains a gap in understanding the establishment of the parasitophorus vacuole. The model of parasitophorus vacuole formation in plants would complement current plant-pathogen interaction research regarding haustorial membrane establishment. Not only would this be an obvious examination of convergent or divergent evolution amongst plant pathogen infection strategies, but it would further foundational understanding of molecular exchange between pathogen and host. This work could also be extended to work with the *Spongospora subterranea – Solanum tuberosum* pathosystem to explore the potential development of parasitophorus vacuoles in this phylogenetically-related clade.

Nile red staining also provides imaging capabilities for identifying resistant cultivars to use in disease management. Resting spores may be easily identified in plants that have grown in *P. brassicae* infected soil, hence easing screening of resistance, and potentially validating or improving or understanding of associated molecular or spectrographic data pertaining to host resistance mechanisms. Currently, this methodology is being applied at the Agriculture and Agrifood Canada Saskatoon Research and Development Centre to understand the role that lignin plays in clubroot disease resistance. RNA sequencing and analysis of plants using a synchrotron have indicated that certain enzymes of phenylpropanoid pathway are up-regulated and that lignin is in higher abundance in the cell walls of *P. brassicae* resistant plants. Preliminary analysis using light microscopy has validated one *B. napus* cultivar as resistant, as no resting spores have been identified in the host, and further work indicates that *P. brassicae* susceptible plants have less lignin autofluorescence than this resistant cultivar.

In summary, my project has established an *in*- and *ex- planta* staining protocol for the live cell labelling of *P. brassicae.* This protocol has allowed for the live cell imaging of zoosporangia in the root cortex, a previously unidentified aspect of the pathogen life cycle. Furthermore, Nile red staining has allowed for the elucidation of host nuclear dynamics in response to protist infection in root hairs. Finally, this protocol has allowed discovery of the parasitophorous vacuole establishment during the early phases of the root hair infection, a novel mechanism of microbial pathogenesis in plants.

5.0 REFERENCES

Agarwal, A., Kaul, V., Faggian, R., Rookes, J. E., Ludwig-Müller, J., and Cahill, D. M. 2011. Analysis of Global Host Gene Expression During the Primary Phase of the *Arabidopsis thaliana-Plasmodiophora brassicae* Interaction. *Functional Plant Biology* **38**: 462-478.

Aist, J. R., and Williams, P. H. 1971. The Cytology and Kinetics of Cabbage Root Hair Penetration by *Plasmodiophora brassicae*. *Canadian Journal of Botany* **49**: 2023-2034.

Alberta Clubroot Management Committee. 2010. *Alberta Clubroot Management Plan: Agriculture and Rural Development.* http://www1.agric.gov.ab.ca/$Department/deptdocs.nsf/all/agdex11519.

Ayers, G. W. 1944. Studies on the Life History of the Clubroot Organism, *Plasmodiophora brassicae*. *Canadian Journal of Research* **22**:143-149.

Ayres, G. W. 1972. Races of *Plasmodiophora brassicae* Infecting Crucifer Crops in Canada. *Canadian Plant Disease Survey* **72:** 77-81.

Beckers, C. J. M., Dubremetz, J-F., Mercereau-Puijalon, O., and Joiner, K. A. 1994. The *Toxoplasma gondii* Rhoptry Protein ROP2 is Inserted into the Parasitophorous Vacuole Membrane, Surrounding the Intracellular Parasite, and Is Exposed to the Host Cell Cytoplasm. *The Journal of Cell Biology* **127**: 947-961.

Belánger, L. F. 1961. Staining Processed Radioautographs. *Stain Technology* **36**: 313-317.

Braselton, J. P., Miller, C. E., and Pechak, D. G. 1975. Ultrastructure of Cruciform Nuclear Division in *Sorosphaera veronicae* (Plasmodiophoromycete). *American Journal of Botany* **62**: 349-358.

Buczacki, S. T., and Moxham, S. E. 1979. A Triple Stain for Differentiating Resin Embedded Sections of *Plasmodiophora brassicae* in Host Tissues Under the Light Microscope. *Transactions of the British Mycological Society* **72**: 311-347.

Bulman, S., Candy, J. M., Fiers, M., Lister, R., Conner, A. J., and Eady, C. C. 2011. Genomics of Biotrophic, Plant-infecting Plasmodiophorids Using In Vitro Dual Cultures. *Protist* **162**: 449-461.

Cao, T., Manolii, V. P., Hwang, S. F., Howard, R. J., and Strelkov, S. E. 2009. Virulence and Spread of *Plasmodiophora brassicae* (Clubroot) in Alberta, Canada. *Epidemiology* **3**: 321-329.

Cao, T., Srivastava, S., Rahman, M. H., Kav, N. N. V., Hotte, N., Deyholos, M. K., and Strelkov, S. E. 2008. Proteoome-level Changes in the Roots of *Brassica napus* as a Result of *Plasmodiophora brassicae* Infection. *Plant Science* **174**: 97-115.

Cavalier-Smith, T. 2013. Symbiogenesis: Mechanisms, Evolutionary Consequences, and Systematic Implications. *Annual Review of Ecology, Evolution, and Systematics* **44**: 145-172.

Cavalier-Smith, T., and Chao, E. E. 2003. Phylogeny and Classification of Phylum Cercozoa (Protozoa). *Protist* **154**: 341-358.

Cosgrove, D. J. 2005. Growth of the Plant Cell Wall. *Nature Reviews Molecular Cell Biology* **6:** 850-861.

Chiang, M. S., and Crête, R. 1972. Screening Crucifers for Germplasm Resistance to Clubroot (*Plasmodiophora brassicae*). *Canadian Plant Disease Survey* **2:** 45-50.

Chittem, K., Mansouripour, S., and del Rio Mendoza, L. E. 2014. First Report of Clubroot on Canola Caused by *Plasmodiophora brassicae* in North Dakota. *Plant Disease*. **10:** 1438.

Cranmer, T. J. 2015. Vertical Distribution of *Plasmodiophora brassicae* Resting Spores in Soil and the Effect of Weather Conditions on Clubroot Development. Masters Thesis. University of Guelph. Guelph, Canada.

Crisp, P., Crute, I. R., Sutherland, R. A., Angell, S. M., Bloor, K., Burgess, H., and Gordon, P. L. 1989. The exploitation of Genetic Resources of *Brassica oleracea* in Breeding for Resistance to Clubroot (*Plasmodiophora brassicae*). *Euphytica* **42**: 215-226.

Crookston, R. K., Kurle, J. E., Copeland, P. J., Ford, J. H., and Lueschen, W. E. 1990. Rotational Cropping Sequence Affects Yeild of Corn and Soybean. *Agronomy Journal* **83**: 108-113.

Cutler, S. R., Ehrhardt, D. W., Griffiths, J. S., and Somerville, C. R. 1999. Random GFP::cDNA Fusions Enable Visualization of Subcellular Structures in Cells of *Arabidopsis* at a high frequency. *Proceedings of the National Academy of Sciences of the USA* **97**: 3718-3723.

Daniel, R., and Guest, D. 2006. Defense Responses Induced by Potassium Phosphate in *Phytopthora palmivora*- Challenged *Arabidopsis thaliana*. *Physiological and Molecular Plant Pathology* **67**: 194-201.

Datnof, L. E., Kroll, T. K., and Fox, J. A. 1984. Occurrence and Population of *Plasmodiophora brassicae* in Sediments of Irrigation Water Sources. *Plant Disease* **68**: 200-203.

Dekhuijzen, H. M., and Overeem, J. C. 1971. The Role of Cytokinins in Clubroot Formation. *Physiological Plant Pathology* **1**: 151-161.

Dekhuijzen, H. M. 1978. Electron Microscopic Studies on the Root Hairs and Cortex of a Susceptible and a Resistant Variety of *Brassica campestris* Infected with *Plasmodiophora brassicae. Netherlands Journal of Plant Pathology* **85**: 1-17.

Deslandes, L., and Rivas, S. 2011. The Plant Cell Nucleus A True Arena for the Fight Between Plants and Pathogens. *Plant Signalling and Behaviour* **6**: 42-48.

Dettmer, J., Hong-Hermesdorf, A., Stierhof, Y. D., and Schumacher, K. 2006. Vacuolar H^+-ATPase Activity Is required for Endocytic and Secretory Trafficking in *Arabidopsis*. *The Plant Cell* **18**: 715-730.

Devos, S., Laukens, K., Deckers, P., Van Der Straeten, D., Beeckman, T., Inzé, D., Van Onckelen, H., Witters, E., and Prinsen, E. 2006. A Hormone and Proteome Approach to Picturing the Initial Metabolic Events During *Plasmodiophora brassicae* Infection on *Arabidopsis*. *Molecular Plant Microbe Interactions* **19**: 1431-1443.

Dickson, B. T. 1920. The Differential Staining of Plant Pathogen and Host. *Science* **52**: 63-64.

Diederichsen E., Frauen, M., Linders, E. G. A., Hatakeyama, K., Hirai, M. 2009. Status and Perspectives of Clubroot Resistance Breeding in Crucifer Crops. *Journal of Plant Growth Regulation* **28**: 265-281.

Dixon, G. R. 2009a. The Occurrence and Economic Impact of *Plasmodiophora brassicae* and Clubroot Disease. *Journal of Plant Growth Regulation* **28**: 194-202.

Dixon, G. R. 2009b. *Plasmodiophora brassicae* in its Environment. *Journal of Plant Growth Regulation* **28**: 212-228.

Dixon, G. R. 2014. Clubroot (*Plasmodiophora brassicae* Woronin) – an Agricultural and Biological Challenge Worldwide. *Canadian Journal of Plant Pathology* **36**(S1): 5-18.

Dixon, R. A. 2001. Natural Products and Plant Disease Resistance. *Nature* **411:** 843-847.

Dobson, R. L., and Gabrielson, R. L. 1983. Role of Primary and Secondary Zoospores of *Plasmodiophora brassicae* in the Development of Clubroot in Chinese Cabbage. *Phytopathology* **73**: 559-561.

Dodds, P. N., and Rathjen, J. P. 2010. Plant Immunity: Towards an Integrated View of Plant-Pathogen Interactions. *Nature Reviews Genetics* **11**: 539-548.

Dokken-Bouchard, F. L., Anderson, K., Bassendowski, K. A., Bouchard, A., Brown, B., and Cranston, R. 2012. Survey of Canola Diseases in Saskatchewan. *Canadian Plant Disease Survey* **92**: 125-129.

Dokken-Bouchard, F. L., Baugh, F., Blackmore, B., Campbell, E., Chant, S., Cowell, L. E., Cubbon, D., Friesen, S., Gilrolyd, J., Gray, K., Haddow, C., Hertz, S., Hicks, L., Holba, K., Ippolito, J., Jacob, C., Jurke, C., Kindrachuk, K., Kirkham, C. L., Kowalski, J., Borhan, M. H., Larkan, N. J., Leppa, N., Loverin, J., Lustig, M., Pettit, M., Peru, J., Philip, N., Platford, R. G., Roberts, S., Scott, C., Senko, S., Stephens, D. T., Stonehouse, K., Voth, B., Wagman, B., Ward, W., Wuchner, A., and Ziesman, B. 2016. Survey of Canola Diseases in Saskatchewan. *Canadian Plant Disease Survey* **96**: 163-169.

Dokken-Bouchard, F.L., Bouchard, A.J., Ippolito, J., Peng, G., Strelkov, S., Kirkham, C.L., and Kutcher, H. R. 2010. Detection of *Plasmodiophora brassicae* in Saskatchewan, 2008. *Canadian Plant Disease Survey* **90**: 126

Donald, E. C., and Porter, I. J. 2009. Integrated Control of Clubroot. *Journal of Plant Growth Regulation* **28**: 289-303.

Donald, E. C., and Porter, I. J. 2014. Clubroot in Australia: The History and Impact of *Plasmodiophora brassicae* in Brassica Crops and Research Efforts Directed Toward its Control. *Canadian Journal of Plant Pathology* **36(**S1): 66-84.

Faggian, R., and Strelkov, S. E. 2009. Detection and Measurement of *Plasmodiophora brassicae. Journal of Plant Growth Regulation* **28**: 282-288.

Feng, J., Hwang, S. F., and Strelkov, S. E. 2014. Genetic Transformation of the Obligate Parasite *Plasmodiophora brassicae*. *Phytopathology* **103**: 1052-1057.

Feng, J., Xiao, Q., Hwang, S. F., Strelkov, S. E., and Gossen, B. D. 2012. Infection of Canola By Secondary Zoospores of *Plasmodiophora brassicae* Produced on a Nonhost. *European Journal of Plant Pathology* **132**: 309-315.

Fischer-Parton, S., Parton, R. M., Hickey, P. C., Dijksterhuis, J., Atkinson, H. A., and Read, N. D. 2000. Confocal Microscopy of FM4-64 as a Tool for Analysing Endocytosis and Vesicle Trafficking in Living Fungal Hyphae. *Journal of Microscopy* **198**: 246-259.

Freytag, S., Arabatzis, N., Hahlbrock, K., and Schmelzer, E. 1994. Reversible Cytoplasmic Rearrangements Precede Wall Aposition, Hypersensitive Cell Death, and Defense-Related Gene Activation in Potato/*Phytopthora infestans* Interactions. *Planta* **194**: 123-135.

Friberg, H. 2005. Persistence of *Plasmodiophora brassicae*- Influence of Non-host Plants, Soil Fauna, and Organic Material. Doctoral Thesis. Swedish University of Agricultural Sciences, Uppsala, Sweden.

Fuchs, H., and Sacristan, M. D. 1995. Identification of a Gene in *Arabidopsis thaliana* Controlling Resistance to Clubroot (*Plasmodiophora brassicae*) and Characterization of the Resistance Response. *Molecular Plant Microbe Interaction* **9**: 91-97.

Garber, R. C., and Aist, J. R. 1970. The Ultrastructure of Meiosis in *Plasmodiophora brassicae* (Plasmodiophorales). *Canadian Journal of Botany* **57**: 2509-2518.

Genre, A., Chabaud, M., Timmers, T., Bonfante, P., and Barker, D. G. 2005. Arbuscular Mycorrhizal Fungi Elicit a Novel Intracellular Apparatus in *Medicago truncatula* Root Epidermal Cells before Infection. *The Plant Cell* **17:** 3489-3499.

Goring, C. A. I. 1962. Theory and Principals of Soil Fumigation. *Advances in Pest Control Research* **5**: 47-84.

Gossen, B. D., Kasinathan, H., Cao, T., Manolii, V. P., Strelkov, S. E., Hwang, S. F., and McDonald, M. R. 2013. Interaction of pH and Temperature Affect Infection and Symptom Development of *Plasmodiophora brassicae* in Canola. *Canadian Journal of Plant Pathology* **35**: 294-303.

Gossen B. D., Kasinathan, H., Deora, A., Peng, G., and McDonald, M. R. 2016. Effect of Soil Type, Organic Matter Content, Bulk Density and Saturation on Clubroot Severity and Biofungicide Efficacy. *Plant Pathology* **68:** 1238-1245.

Greenspan, P., Mayer, E. P., and Fowler, S. D. 1985. Nile Red: A Selective Fluorescent Stain for Intracellular Lipid Droplets. *The Journal of Cell Biology* **100**: 965-973.

Griffis, A. H. N., Groves, N. R., Zhou, X. J., and Meier, I. 2014. Nuclei in Motion: Movement and Positioning of Plant Nuclei in Development, Signaling, Symbiosis, and Disease. *Frontiers in Plant Science* **5**: 129-136.

Guest, D. I. 1986. Evidence From Light Microscopy of Living Tissues That Fosetyl-Al Modifies the Defense Response in Tobacco Seedlings Following Inoculation by *Phytopthora nicotianae* var. *nicotianae*. *Physiological and Molecular Plant Pathology* **29**: 251-261.

Hamilton, H. A., and Crête, R. 1978. Influence of Soil Moisture, Soil pH and Liming Sources on the Incidence of Clubroot, the Germination and Growth of Cabbage Produced in Mineral and Organic Soils Under Controlled Conditions. *Canadian Journal of Plant Science* **58**: 45-53.

Hara-Nishimura, I., and Hatsugai, N. 2011. The Role of Vacuole in Plant Cell Death. *Cell Death and Differentiation* **18**: 1298-1304.

Haralampidis, K., Bryan, G., Qi, X., Papadopoulou, K., Bakht, S., Melton, R., and Osbourn, A. 2001. A New Class of Oxidosqualene Cyclase Directs Synthesis of Antimicrobial Phytoprotectants in Monocots. *Proceedings of the National Academy of Sciences of the United States of America* **98:** 13431-13436.

Hasan, M. J., Strelkov, S. E., Howard, R. J., and Rahman, H. 2012. Screening of *Brassica* Germplasm for Resistance to *Plasmodiophora brassicae* Pathotypes Prevalent in Canada for Broadening Diversity in Clubroot Resistance. *Canadian Journal of Plant Science* **92**: 501-515.

Heath, M. C., Nimchuck, Z. L., and Xu, H. 1997. Plant Nuclear Migrations as Indicators of Critical Interactions Between Resistant or Susceptible Cowpea Epidermal Cells and Invasion Hyphae of the Cowpea Rust Fungus. *The New Phytologist* **135**: 689-700.

Hildebrand, P. D., and Delbridge, R. W. 1995. Race survey of *Plasmodiophora brassicae* in Nova Scotia. *Canadian Plant Disease Survey*, **75**: 170.

Hildebrand, P. D., and McRae, K. B. 1998. Control of Clubroot Caused by *Plasmodiophora brassicae* With Nonionic Surfactants. *Canadian Journal of Plant Pathology* **20**: 1-11.

Howard, R. J., Strelkov, S. E., and Harding, M. W. 2010. Clubroot of Cruciferous Crops – New Perspectives on an Old Disease. *Canadian Journal of Plant Pathology* **32**: 43-57.

Humphrey, C. D., and Pittman, A. 1974. Simple Methylene Blue - Azure II – Basic Fuchsin Stain for Epoxy-Embedded Tissue Sections. *Stain Technology* **40**: 9-14.

Hwang, S. F., Cao, T., Xiao, Q., Ahmed, H. U., Manolii, V. P., Turnbull, G. D., Gossen, B. D., Peng, G., and Strelkov, S. E. 2012. Effects of Fungicide, Seeding Date, and Seedling Age on Clubroot Severity, Seedling Emergence, and Yield of Canola. *Canadian Journal of Plant Science* **92**: 1175-1186.

Hwang, S. F., Strelkov, S. E., Feng, J., Gossen, B. D., and Howard, R. J. 2011. *Plasmodiophora brassicae*: a Review of an Emerging Pathogen of the Canadian Canola (*Brassica napus*) Crop. *Molecular Plant Pathology* **13**: 105-113.

Ingram, D. S. 1969. Growth of *Plasmodiophora brassicae* in Host Callus. *Microbiology* **55**: 9-18.

Ingram, D. S., and Tommerup, I. C. 1972. The Life History of *Plasmodiophora brassicae* Woron. *Proceedings of The Royal Society of London B* **180**: 103-112.

Jäschke, D., Gugassa-Gobena, D., Karlovsky, P., Vidal, S., and Ludwig-Müller, J. 2010. Supression of Clubroot Development in *Arabidopsis thaliana* by the Endophytic Fungus *Acremonium alternatum*. *Plant Pathology* **59**: 100-111.

Jones, J. D. G., and Dangl, J. L. 2006. The Plant Immune System. *Nature* **444**: 323-329.

Kareiva, P. 1999. Co-evolutionary Arms Races: Is Victory Possible. *Proceedings of the National Academy of Sciences of the USA* **96**: 8-10.

Kageyama, K., and Asano, T. 2009. Life Cycle of *Plasmodiophora brassicae*. *Journal of Plant Growth Regulation* **28**: 203-211.

Ketelaar, T., Faivre-Moskalenko, C., Esseling, J. J., de Ruijter, N. C. A., Grierson, C. S., Dogterom, M., and Emons, A. M. C. 2002. Positioning of Nuclei in Arabidopsis Root Hairs An Actin-Regulated Process of Tip Growth. *The Plant Cell* **14**: 2941-2955.

Kobelt, P., Siemens, J., and Sacristan, M. D. 2000. Histological Characterization of the incompatible interaction between *Arabidopsis thaliana* and the obligate biotrophic pathogen *Plasmodiophora brassicae*. *Mycological Research* **104**: 220-225.

Koh, S., André, A., Edwards, H., Ehrhardt, D., and Somerville, S. 2005. *Arabidopsis thaliana* subcellular responses to compatible *Erysiphe cichoracearum* infections. *The Plant Journal* **44**: 516-529.

Kunkle, L. O. 1918. Tissue invasion by *Plasmodiophora brassicae*. Journal of Agricultural Research **14**: 543-572.

Lam, E., Kato, N., and Lawton, M. 2001. Programmed Cell Death, Mitochondria and The Plant Hypersensitive Response. *Nature* **411**: 848-853.

Lipka, V., Dittgen, J., Bednarek, P., Bhat, R., Wiermer, M., Stein, M., Landtag, J., Brandt, W., Roshal, S., Scheel, D., Llorente, F., Molina, A., Parker, J., Somerville, S., and Schulze-Lefert, P. 2005. Pre- and Postinvasion Defenses Both Contribute to Nonhost Resistance in *Arabidopsis. Science* **310:** 1180-1183.

Littlefield, L. J., Delfosse, P., Whallon, J. H., Hassan, Z. M., Sherwood, J. L., and Reddy, D. V. R. 1997. Anatomy of Sporosori of *Polymyxa graminis*, the Vector of Indian Peanut Clump Virus, in Roots of *Sorghum bicolor*. *Canadian Journal of Plant Pathology* **19**: 281-288.

Littlefield, L. J., Whallon, J. H., Doss, P. J., and Hassan, Z. M. 1998. Postinfection Development of *Polymyxa graminis* in roots of *Triticum aestivum*. *Mycologia* **90**: 869-882.

Liu, Y., Schiff, M., Czymmek, K., Talloczy, Z., Levine, B., and Dinish-Kumar, S. P. 2005. Autophagy Regulates Programmed Cell Death During the Plant Innate Immune Response. *Cell* **121:** 567-577.

Ludwig-Müller, J., Bennett, R. N., Kiddle, G., Ihmig, S., Ruppel, M., and Hilgenberg, W. 1999. The Host Range of *Plasmodiophora brassicae* and its Relationship to Endogenous Glucosinolate Content. *The New Phytologist* **141**: 443-458.

Ludwig-Müller, J., Jülke, S., Geiß, K., Richter, F., Mithöfer, A., Šola, I., Rusak, G., Keenan, S., and Bulman, S. 2015. A Novel Methyltransferase From The Intracellular Pathogen *Plasmodiophora brassicae* Methylates Salicylic Acid. *Molecular Plant Pathology* **16**: 349-364.

Ludwig-Müller, J., Prinsen, E., Rolfe, S. A., and Scholes, J. D. 2009. Metabolism and Plant Hormone Action During Clubroot Disease. *Journal of Plant Growth Regulation* **28**: 229-244.

Luo, H. C., Chen, G. K., Liu, C. P., Huang, Y., and Xiao, C. G. 2014. An Improved Culture Solution Technique for *Plasmodiophora brassicae* Infection and the Dynamic Infection in the Root Hair. *Australasian Plant Pathology* **43**: 53-60.

Macfarlane, I. 1952. Factors Affecting the Survival of *Plasmodiophora brassicae* Wor. In the Soil and Its Assessment by a Host Test. *Annals of Applied Biology* **39**: 239-256.

Manitoba Agriculture, Food and Rural Development. 2016. Retrieved from https://www.gov.mb.ca/agriculture/crops/plant-diseases/clubroot-distribution-in-manitoba.html

McDonald, M. R., and Westerveld, S. M. 2008. Temperature Prior to Harvest Influences the Incidence and Severity of Clubroot on Two Asian Brassica Vegetables. *HortScience* **43**: 1509-1513.

Merz, U., and Falloon, R. E. 2009. Review: Powdery Scab of Potato – Increased Knowledge of Pathogen Biology and Disease Epidemiology for Effective Disease Management. *Potato Research* **52**: 17-37.

Moulder, J. W. 1985. Comparative Biology of Intracellular Parasitism. *Microbiology Reviews* **49**: 298-337.

Moxham, S. E., and Buczacki, S. T. 1983. Structure of the Resting Spore Wall of *Plasmodiophora brassicae* Revealed by Electron Microscopy and Chemical Digestion. *Transactions of the British Mycological Society* **81**: 221-231.

Mithen, R., and Magrath, R. 1992. A Contribution to the Life History of *Plasmodiophora brassicae*: Secondary Plasmodia development in Root Galls of *Arabidopsis thaliana*. *Mycological Research* **96**: 877-885.

Mur, L. A. 2007. Hypersensitive Response in Plants. *eLS*.

Mur, L. A., Kenton, P., Lloyd, A. J., Ougham, H., and Prats, E. 2008. The Hypersensitive Response; The Centenary is Upon Us But How Much Do We Know? *Journal of Experimental Botany* **59**: 501-520.

Myers, D. F., and Campbell, R. N. 1985. Lime and the Control of Clubroot of Crucifers: Effects of pH, Calcium, Magnesium and Their Interactions. *Phytopathology* **75**: 670-673.

Mysore, K. S., and Ryu, C-M. 2004. Non-Host Resistance: How Much Do We Know? *Trends in Plant Science* **9:** 98-103.

Narisawa, K., Ohki, K. T., and Hashiba, T. 2000. Suppression of Clubroot and Verticillium Yellows in Chinese Cabbage in the Field by the Root Endophytic Fungus, *Heteroconium chaetospira. Plant Pathology* **49**: 141-146.

Nelson, B. K., Cai, X., and Nebenführ, A. 2007. A Multicolored Set of *in vivo* Organelle Markers for Co-localization Studies in Arabidopsis and Other Plants. *The Plant Journal* **51**: 1126-1136.

Niwa, R., Nomura, Y., Osaki, M., Wzawa, T. 2008. Suppression of Clubroot Disease Under Neutral pH Caused By Inhibition of Spore Germination of *Plasmodiophora brassicae* in the Rhizosphere. *Plant Pathology* **57**: 445-452.

Peng, G., McGregor, L., Lahlali, R., Gossen, B. D., Hwang, S. F., Adhikari, K. K., Strelkov, S. E., and McDonald, M. R. 2011. Potential Biological Control of Clubroot on Canola and Crucifer Vegetable Crops. *Plant Pathology* **60**: 566-574.

Peng, G., Pageau, D., Strelkov, S. E., Gossen, B. D., Hwang, S. F., and Lahlali, R. 2015. A >2-Year Crop Rotation Reduces Resting Spores of *Plasmodiophora brassicae* in Soil and the Impact of Clubroot on Canola. *European Journal of Agronomy* **70**: 78-84.

Porter, I. J., Cross, S. J., Asirifi, N., and Morgan, W. 1994. Integrated Management of Clubroot of Crucifers: Surveys and Plot Studies. Final Report for Project VG306. *Sydney: Horticultural Research and Development Corporation.*

Qu, L-H., and Sun, M-X. 2007. The Plant Cell Nucleus is Constantly Alert and Highly Sensitive to Repetitive Local Mechanical Stimulations. *Plant Cell Reports* **26**: 1187-1193.

Rahman, H., Peng, G., Yu, F., Falk, K. C., Kulkarni, M., and Selvaraj, G. 2014. Genetics and Breeding for Clubroot resistance in Canadian Spring Canola (*Brassica napus* L.). *Canadian Journal of Plant Pathology* **36(**S1): 122-134.

Rashid, A., Ahmed, H. U., Xiao, Q., Hwang, S. F., and Strelkov, S. E. 2013. Effects of Root Exudates and pH on *Plasmodiophora brassicae* Resting Spore Germination and Infection of Canola (*Brassica napus* L.) Root Hairs. *Crop Protection* **48**: 16-23.

Rennie, D. C., Holtz, M. D., Turkington, T. K., Leboldus, J. M., Hwang, S. F., Howard, R. J., and Strelkov, S. E. 2015. Movement of *Plasmodiophora brassicae* Resting Spores in Windblown Dust. *Canadian Journal of Plant Pathology* **37**: 188-196.

Reyes, A. A. 1969. Detection of *Plasmodiophora brassicae* races 2 and 6 in Ontario. *Plant Disease Reports* **53**: 223-225.

Reyes, A. A., Davidson, T. R., and Marks, C. F. 1974. Races, Pathogenicity, and Chemical Control of *Plasmodiophora brassicae* in Ontario. *Phytopathology* **64**: 173-177.

Ruggiero, M. A., Gordon, D. P., Orrell, T. M., Bailly, N., Bourgoin, T., Brusca, R. C., Cavalier-Smith, T., Guiry, M. D., and Kirk, P. M. 2015. A Higher Level Classification of All Living Organisms. *PLoS One* **10:** e0119248.

Saude, C., Mckeown, A., Gossen, B. D., and McDonald, M. R. 2012. Effect of Host Resistance and Fungicide Application on Clubroot Pathotype 6 in Green Cabbage and Napa Cabbage. *HortTechnology* **22**: 311-319.

Scholthof, K. B. G. 2007. The Disease Triangle: Pathogens, the Environment and Society. *Nature Reviews Microbiology* **5**: 152-156.

Schuller, A., Kehr, J., and Ludwig-Müller, J. 2013. Laser Microdissection Coupled to Transcriptional Profiling of Arabidopsis Roots Inoculated by *Plasmodiophora brassicae* Indicates a Role for Brassinosteroids in Clubroot Formation. *Plant and Cell Physiology* **174**.

Schuller, A., and Ludwig-Müller, J. 2016. Histological Methods to Detect the Clubroot Pathogen *Plasmodiophora brassicae* During Its Complex Life Cycle. *Plant Pathology* **65:** 1223-1237.

Schulze-Lefert, P., and Panstruga, R. 2003. Establishment of Biotrophy By Parasitic Fungi and Reprogramming of Host Cells for Disease Resistance. *Annual Reviews in Phytopathology* **41**: 641-667.

Schwelm, A., Fogelqvist, J., Knaust, A., Jülke, S., Lilja, T., Bonilla-Rosso, G., Karlsson, M., Shevchenko, A., Dhandapani, V., Choi, S.R., and Kim, H.G., 2015. The *Plasmodiophora brassicae* Genome Reveals Insights in its Life Cycle and Ancestry of Chitin Synthases. *Nature Scientific Reports* **5**.

Sharma, K., Gossen, B. D., and McDonald, M. R. 2011a. Effect of Temperature on Primary Infection by *Plasmodiophora brassicae* and Initiation of Clubroot Symptoms. *Plant Pathology* **60**: 830-838.

Sharma, K., Gossen, B. D., and McDonald, M. R. 2011b. Effect of Temperature on Cortical Infection by *Plasmodiophora brassicae* and Clubroot Severity. *Phytopathology* **101**: 1424-1432.

Sherf, A. F., and MacNab, A. A. 1986. Vegetable Diseases and Their Control. 2nd Edition. John Wiley and Sons. 256-260.

Sieberer, B., and Emons, A. M. C. 2000. Cytoarchitecture and Pattern of Cytoplasmic Streaming in Developing Root Hairs of *Medicago truncatula* and During Deformation by Nod Factors. Doctoral Thesis. Wageningen University, Wageningen, Netherlands.

Siemens, J., Keller, I., Sarx, J., Kunz, S., Schuller, A., Nagel, W., Schmulling, T., Parniske, M., and Ludwig-Müller, J. 2006. Transcriptome Analysis of *Arabidopsis* Clubroots Indicate a Key Role for Cytokinins in Disease Development. *Molecular Plant Microbe Interactions* **19**: 480-494.

Strelkov, S. E., and Hwang S. F. 2014. Clubroot in the Canadian Canola Crop: 10 Years Into the Outbreak. *Canadian Journal of Plant Pathology* **36**: 1-4.

Strelkov, S. E., Hwang, S. F., Howard, R. J., Hartman, M., and Turkington, T. K. 2011. Progress towards the Sustainable Management of Clubroot (*Plasmodiophora brassicae*) of Canola on the Canadian Prairies. *Prairie Soils & Crops Journal* **4**: 114-121.

Strelkov, S. E., Manolii, V. P., Cao, T., Xue, S., and Hwang, S. F. 2007. Pathotype Classification of *Plasmodiophora brassicae* and its Occurrence in *Brassica napus* in Alberta, Canada. *Journal of Phytopathology*, **155**: 706–712.

Strelkov, S. E., Manolii, V. P., Harding, M. W., Sieusahai, G., Hwang, S. F., Shi, Y., Lawson, A., Fisher, J., Cornelsen, J., Daniels, G. C., and Feindel, D. 2016. Occurrence and Spread of Clubroot on Canola in Alberta in 2015. *Canadian Plant Disease Survey* **96**: 163-169.

Strelkov, S. E., Manolii, V. P., Rennie, D. C., Manolii, E. V., Fu, H., Strelkov, I. S., Hwang, S.F., Howard, R. J., and Handing, M. W. 2012. The Occurence of Clubroot on Canola in Alberta in 2011. *Canadian Plant Disease Survey* **94:** 158-161.

Strelkov, S. E., Tewari, J. P., and Smith-Degenhardt, E. 2006. Characterization of *Plasmodiophora brassicae* populations from Alberta, Canada. *Canadian Journal of Plant Pathology* **28**: 467-474.

Takahashi, K., and Yamaguchi, T. 1988. A Method for Assessing the Pathogenic Activity of Resting Spores of *Plasmodiophora brassicae* by Fluorescence Microscopy. *Annals of the Phytopathological Society of Japan* **54**: 466-475.

Thrane, C., Olsson, S., Nielsen, T. H., and Sorensen, J. 1999. Vital Fluorescence Stains for Detection of Stress in *Pythium ultimatum* and *Rhizoctonia solani* Challenged with Viscosinamide from *Pseudomonas fluorescens* DR54. *FEMS Microbial Ecology* **30**: 11-23.

Turner, J. G., and Novacky, A. 1974. The Quantitative Relation Between Plant and Bacterial Cells Involved in the Hypersensitive Response. *Phytopathology* **64**: 885-890.

VanEtten, H. D., Mansfield, J. W., Bailey, J. A., and Farmer, E. E. 1994. Two Classes of Plant Antibiotics: Phytoalexins versus Phytoanticipins. *The Plant Cell* **6:** 1191-1192.

Wallenhammar, A. C. 1996. Prevalence of *Plasmodiophora brassicae* in a Spring Oilseed Rape Growing Area in Central Sweden and Factors Influencing Soil Infestation Levels. *Plant Pathology* **45**: 710-719.

Wallenhammar, A. C., Almquist, C., Soderstrom, M., and Jonsson, A. 2012. In-field Distribution of *Plasmodiophora brassicae* Measured Using Quantitative Real-time PCR. *Plant Pathology* **61**: 16-28.

Wang, Y.S., Motes, C. M., Mohamalawari, D. R., and Blancaflor, E. 2004. Green Fluorescent Protein Fusions to Arabidopsis Fimbrin 1 for Spatio-temporal Imaging of F-Actin Dynamics in Roots. *Cell Motility and the Cytoskeleton* **59**: 79-93.

Ward, G. E., Miller, L. H., and Dvorak, J. A. 1993. The Origin of Parasitophorus Vacuole Membrane Lipids in Malaria-infected Erythrocytes. *Journal of Cell Science* **106**: 237-248.

Weigel, D., and Glazebrook, J. 2002. Arabidopsis: A Laboratory Manual, Cold Spring Harbor Laboratory Press, Cold Spring Harbor, NY, USA.

White, J. G., and Buczacki, S. T. 1977. The Control of Clubroot by Soil Partial Sterilization: a Review. *Annals of Applied Biology* **85**: 287-300.

Williams, P. H. 1966. A System for the Determination of Races of *Plasmodiophora brassicae* that Infect Cabbage and Rutabaga. *Phytopathology* **56**: 624-626.

Woronin, M. 1878. *Plasmodiophora brassicae*, the Cause of Cabbage Hernia. Translated by C. Chupp. Phytopathological Classics, The American Phytopathological Society, 1934.

Yano, S., Tanaka, S., Kameya, M., and Katumoto, K. 1991. Relation of Ca2+ Efflux to Germination of Resting Spores of Clubroot Fungus. Bulletin of the Faculty of Agriculture-Yamaguchi University.

Zhao, Y., Bi, K., Gao, Z., Chen, T., Liu, H., Xie, J., Cheng, J., Fu, Y., and Jiang, D. 2017. Transcriptome Analysis of *Arabidopsis thaliana* in Response to *Plasmodiophora brassicae* During Early Infection. *Frontiers in Microbiology* **8**.